

Provable Robust Learning Based on Transformation-Specific Smoothing

Linyi Li[†] * Maurice Weber[‡] * Xiaojun Xu[†] * Luka Rimanic[‡] Tao Xie[§]
 Ce Zhang[‡] Bo Li[†]

[†] University of Illinois at Urbana-Champaign, USA {linyi2, xiaojun3, lbo}@illinois.edu

[‡] ETH Zurich, Switzerland {webermau, luka.rimanic, ce.zhang}@inf.ethz.ch

[§] Peking University, China {taoxie}@pku.edu.cn

Abstract

As machine learning systems become pervasive, safeguarding their security is critical. Recent work has demonstrated that motivated adversaries could manipulate the test data to mislead ML systems to make arbitrary mistakes. So far, most research has focused on providing provable robustness guarantees for a specific ℓ_p norm bounded adversarial perturbation. However, in practice there are more adversarial transformations that are realistic and of semantic meaning, requiring to be analyzed and ideally certified. In this paper we aim to provide *a unified framework for certifying ML model robustness against general adversarial transformations*. First, we leverage the function smoothing strategy to certify robustness against a series of adversarial transformations such as rotation, translation, Gaussian blur, etc. We then provide sufficient conditions and strategies for certifying certain transformations. For instance, we propose a novel sampling based interpolation approach with the estimated Lipschitz upper bound to certify the robustness against rotation transformation. In addition, we theoretically optimize the smoothing strategies for certifying the robustness of ML models against different transformations. For instance, we show that smoothing by sampling from exponential distribution provides tighter robustness bound than Gaussian. We also prove two generalization gaps for the proposed framework to understand its theoretic barrier. Extensive experiments show that our proposed unified framework significantly outperforms the state-of-the-art certified robustness approaches on several datasets including ImageNet.

1 Introduction

Recent advances in machine learning (ML) have vastly improved the capabilities of computational reasoning in complex domains, exceeding human-level performance in tasks such as image recognition (He et al., 2015) and game playing (Silver et al., 2017; Moravčík et al., 2017). Despite all of these advances, there are significant vulnerabilities inherent in these systems: image recognition systems can be easily misled (Szegedy et al., 2013; Goodfellow et al., 2014; Xiao et al., 2018a), and malware detection models can be evaded (Tong et al., 2019; Xu et al., 2016).

The current practice of security in ML has fallen into the trap that every month new attacks are identified (Xiao et al., 2018b; Goodfellow et al., 2014; Eykholt et al., 2018), followed by new countermeasures (Ma et al., 2018; Tramèr et al., 2017), which are subsequently broken (Athalye et al., 2018), and so on *ad infinitum*.

Recent investigations have been made to provide *provable or certifiable robustness* guarantees for existing learning models. Such certification usually follows the form that when the perturbation is within a certain

*The first three authors contribute equally to this work.

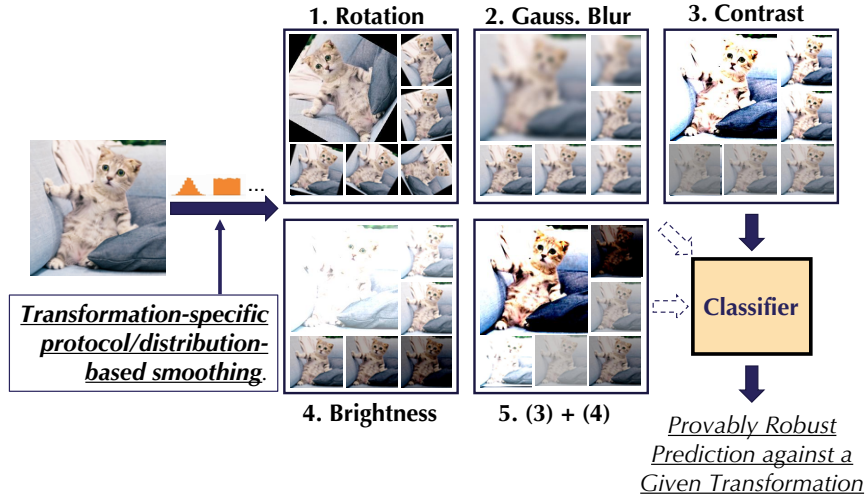


Figure 1: An illustration of the proposed general model smoothing framework against different semantic transformations. In this paper, we develop a range of different transformation-specific smoothing protocols with different smoothing distributions to provide substantially better certified robustness bound against transformations over the state-of-the-art approaches.

threshold, the ML model is provably robust against arbitrary adversarial attacks as long as the added perturbation satisfies the threshold. So far, different certifiable defenses and robustness verification approaches have provided non-trivial robust guarantees especially when the perturbation is bounded by ℓ_p norm (Kolter & Wong, 2017; Tjeng et al., 2018; Li et al., 2019; Cohen et al., 2019).

However, only certifying adversarial examples within the ℓ_p norm distance is not sufficient toward certifying learning robustness against practical attacks. For instance, it has been shown that simple rotations or other semantic transformations on image instances are able to mislead ML models (Engstrom et al., 2017; Ghiasi et al., 2020). Therefore, a natural question arises: *Can we provide provable robustness guarantees for these semantic transformations?*

In this paper, we propose a series of theoretic and empirical analysis to certify the model robustness against general semantic transformations beyond the ℓ_p norm bounded adversarial perturbation. The theoretical analysis is non-trivial and our empirical results set new state-of-the-arts for a range of different semantic transformations.

We first propose a general framework via function smoothing to provide provable robustness for ML models against a range of different adversarial transformations, including rotation, translation (brightness, contrast, and their composition), and Gaussian blur as shown in Figure 1.

However, a general framework that can be applied to all these transformations is just the very first step. Our main contribution is a series of transformation-specific techniques that improve each specific type of transformations. This requires us to *jointly* reason about (1) function smoothing under different smoothing distributions and (2) optimize it with specific properties of each transformation. To our best knowledge, this is the first time that such type of analysis has been conducted in the context of function smoothing and semantic transformations.

For *smoothing distributions* we leveraged to perform function smoothing, we analyze sampling distributions beyond the isotropic Gaussian distribution that previous work relies on (Cohen et al., 2019; Fischer et al., 2020) — We explore the non-isotropic Gaussian and other distributions such as uniform, exponential and Laplace. We show that against certain adversarial transformation such as Gaussian blur, smoothing by

sampling from the exponential distribution is better than isotropic Gaussian.

Digging deeper into each transformation also leads to a collection of interesting results that goes significantly beyond existing techniques. For example, rotation does not satisfy the transition property and introduces extra interpolation error. To certify the model robustness against rotation, we first prove the Lipschitz upper bound of rotation and then propose a novel sampling strategy accordingly to calculate the certification. Note that though we are able to provide advanced transformation-specific smoothing strategies, it is straightforward for us to perform the function smoothing on each independent transformation and therefore certify against general adversarial individual transformations. Moreover, for some composition of transformations such as brightness and contrast, we also provide provable non-isotropic Gaussian smoothing strategy based on a novel lower bound of prediction probability, and obtain non-trivial robustness guarantee.

In addition, we go beyond the provable robustness and provide theoretical analysis on the model benign accuracy tradeoff, and we prove two generalization gaps for the smoothed models to further understand the theoretic barrier of our smoothing strategies.

Empirically, we conduct extensive experiments to evaluate the proposed certification framework and show that it outperforms the state-of-the-art approaches substantially on different datasets against a series of practical semantic transformations.

This paper makes the following technical contributions:

- We propose the first *general* model smoothing framework to certify the model robustness against generic semantic transformations such as rotation, translation (e.g., brightness, contrast, their composition), and Gaussian blur.
- For specific transformations, such as rotation, we theoretically provide the upper bound of its Lipschitz constant based on which we propose a novel sampling strategy to certify the robustness. We show that such proposed transformation-specific smoothing strategy has substantially helped to improve our certified robustness bound.
- We theoretically explore different smoothing strategies by sampling from different distributions including non-isotropic Gaussian, uniform, and Laplace. We show that for specific transformations, such as Gaussian blur, smoothing with exponential distribution is better.
- We prove two generalization gaps between the smoothed and original models to further explore the theoretic barrier for the model smoothing strategies.
- We conduct extensive experiments with open-source code for reproducibility. We show that the proposed general model smoothing framework can provide substantially higher certified robustness compared with the state-of-the-art approaches, against a range of semantic transformations on MNIST, CIFAR-10, and ImageNet.

2 Related work

Certified robustness against ℓ_p norm bounded perturbation Certified adversarial robustness training and verification approaches have been proposed to demonstrate their effectiveness. In particular, semidefinite programming (SDP) framework has been leveraged to certify model robustness by formulating the properties of activation functions as constraints (Raghunathan et al., 2018). Interval bounding technique has also been applied to certify the model robustness (Gowal et al., 2018). In addition, function smoothing is shown to be scalable and effective by smoothing the model with Gaussian noise (Cohen et al., 2019). With improvements on training including pretraining and adversarial training, the performance can be further improved (Carmon et al., 2019; Salman et al., 2019a). However, these certifiable approaches are only able to provide robustness guarantees for the ℓ_p norm bounded perturbations, while in practice the semantic transformation based

perturbation would create more stealthy and realistic adversarial instances.

Robustness against semantic transformations Several efforts have been taken towards certifying the robustness against adversarial semantic transformations. The interval propagation based bounding strategy provides the first verification approach against rotation (Singh et al., 2019). The linear programming based strategy has been utilized to certify model robustness against geometry transformations (Balunovic et al., 2019). A recent work has applied the function smoothing scheme to provide provable robustness against general transformations (Fischer et al., 2020). However, Fischer et al. only consider Guassian distributions and do not consider transformation-specific properties, and we will show that our approach outperforms theirs significantly and leads to new theoretical understanding of function smoothing-based techniques.

3 Function Smoothing for Semantic Transformations

We now state the *general* theorem for certifying robustness under semantic transformations using function smoothing. This theorem is general — in the next sections we will leverage this result for smoothing strategies with different distributions against different semantic transformations.

3.1 Problem Setup

We denote the space of inputs as $\mathcal{X} \subseteq \mathbb{R}^d$ and the set of labels as $\mathcal{Y} = \{1, \dots, C\}$ where $C > 1$ is the number of classes. We denote the C -dimensional probability simplex by \mathcal{S}_C and use the notation \mathbb{P}_X to denote the probability measure induced by the random variable X . By μ_X we denote the probability mass function, in the discrete case, or the probability density function, if X admits one, in the continuous case. For a measurable set S we denote its probability by $\mathbb{P}_X[S]$. Finally, we refer to base classifiers as general deterministic functions $h: \mathcal{X} \rightarrow \mathcal{S}_C$, mapping inputs to class probabilities. Let \mathcal{Z} denote noise space where $\mathcal{Z} \subseteq \mathbb{R}^m$ for continuous and $\mathcal{Z} \subseteq \mathbb{Z}^m$ for discrete noise.

Semantic Transformations We model semantic transformations as general deterministic functions $\phi: \mathcal{X} \times \mathcal{Z} \rightarrow \mathcal{X}$, mapping data points to a transformed version with a \mathcal{Z} -valued parameter α . Examples of such transformations include rotations and translations as discussed in Section 5.

Function Smoothing is a method for constructing a new classifier from an arbitrary base classifier h by introducing randomness to input transformations. Given an input x , the smoothed classifier predicts the class which h is most likely to return when the input is perturbed by some random transformation. Using this notion of function smoothing and transformations, we can define a smoothed classifier:

Definition 1 (ε -Smoothed Classifier). Suppose we are given a transform $\phi: \mathcal{X} \times \mathcal{Z} \rightarrow \mathcal{X}$, a random variable $\varepsilon \sim \mathbb{P}_\varepsilon$ taking values in \mathcal{Z} and a base classifier $h: \mathcal{X} \rightarrow \mathcal{S}_C$. We define the ε -smoothed classifier $g_h^\varepsilon: \mathcal{X} \rightarrow \mathcal{S}_C$ as

$$g_h^\varepsilon(x) := \mathbb{E}_\varepsilon[h(\phi(x, \varepsilon))]. \quad (1)$$

The next definition allows us to quantify the confidence of a smoothed classifier in making a prediction at an input x_0 .

Definition 2 ((p_A, p_B) -Confidence at x_0). Let $x_0 \in \mathcal{X}$, $\phi: \mathcal{X} \times \mathcal{Z} \rightarrow \mathcal{X}$ an input transform, $h: \mathcal{X} \rightarrow \mathcal{S}_C$ a base classifier, $c_A \in \mathcal{Y}$ and $p_A, p_B \in [0, 1]$. We say that the ε -smoothed classifier g_h^ε is (p_A, p_B) -confident at x_0 if

$$g_h^\varepsilon(x_0)_{c_A} \geq p_A \geq p_B \geq \max_{c \neq c_A} g_h^\varepsilon(x_0)_c. \quad (2)$$

3.2 Robustness Guarantee for Transformations

Suppose that the ε -smoothed classifier predicts input x_0 to be of class c_A with probability p_A and the second most likely class with probability p_B . We hope to construct a δ -smoothed classifier that is robust for any random variable δ satisfying a condition depending only on ε , p_A and p_B — As long as δ satisfies this condition, this δ -smoothed classifier will output the same prediction as the ε -smoothed classifier at point x_0 . In the following, we provide a generic theorem to specify such a condition. This theorem itself is *not* the main contribution of this work; however, it forms the foundation for the more engaged analysis of different specific cases of this theorem in Section 4-5.

For the sequel, suppose that \mathcal{X} is endowed with Lebesgue measure on \mathbb{R}^d , and \mathcal{Z} is a measure space with Lebesgue measure, if $\mathcal{Z} \subseteq \mathbb{R}^m$, and counting measure, if $\mathcal{Z} \subseteq \mathbb{Z}^m$. We consider transforms ϕ such that the maps $\phi_x: \mathcal{Z} \rightarrow \mathcal{X}$ given by $\phi_x(z) := \phi(x, z)$ are measurable for each $x \in \mathcal{X}$.

Definition 3 (Lower Level Sets). Let $\varepsilon \sim \mathbb{P}_\varepsilon$, $\delta \sim \mathbb{P}_\delta$ be two random variables with densities μ_ε and μ_δ and values in \mathcal{Z} . For $t \geq 0$, we define lower and strict lower level sets as

$$\underline{S}_t := \left\{ z \in \mathcal{Z} \mid \frac{\mu_\delta(z)}{\mu_\varepsilon(z)} < t \right\}, \quad (3)$$

$$\overline{S}_t := \left\{ z \in \mathcal{Z} \mid \frac{\mu_\delta(z)}{\mu_\varepsilon(z)} \leq t \right\}. \quad (4)$$

Theorem 1. Let $\varepsilon \sim \mathbb{P}_\varepsilon$, $\delta \sim \mathbb{P}_\delta$ be two random variables with densities μ_ε and μ_δ . Let $\phi: \mathcal{X} \times \mathcal{Z} \rightarrow \mathcal{X}$ be a transform, h a base classifier, $x_0 \in \mathcal{X}$, and suppose that the ε -smoothed classifier g_h^ε is (p_A, p_B) -confident at x_0 for some $c_A \in \mathcal{Y}$. Let $\zeta: \mathbb{R}_{\geq 0} \rightarrow [0, 1]$ be defined by

$$\zeta(t) := \mathbb{P}_\varepsilon[\overline{S}_t]. \quad (5)$$

Denote by $\zeta^{-1}(p) := \inf\{t: \zeta(t) \geq p\}$ its generalized inverse. For $t \geq 0$ and $p \in [0, 1]$ let

$$\mathcal{S}_{t,p} := \{S \subseteq \mathcal{Z} \mid \underline{S}_t \subseteq S \subseteq \overline{S}_t \wedge \mathbb{P}_\varepsilon[S] \leq p\}$$

and define the function $\xi: \mathbb{R}_{\geq 0} \times [0, 1] \rightarrow [0, 1]$ by

$$\xi(t, p) := \sup\{\mathbb{P}_\delta[S] \mid S \in \mathcal{S}_{t,p}\}.$$

If δ satisfies

$$1 - \xi(\zeta^{-1}(1 - p_B), 1 - p_B) < \xi(\zeta^{-1}(p_A), p_A), \quad (6)$$

then

$$g_h^\delta(x_0)_{c_A} > \max_{c \neq c_A} g_h^\delta(x_0)_c \quad (7)$$

This theorem is a more general version of what is proved in [Cohen et al. \(2019\)](#), and its generality allows us to analyze cases beyond what is supported by [\(Cohen et al., 2019\)](#) in Section 4 and Section 5. A detailed proof is provided in [Appendix A](#). In the next sections we will instantiate ε and δ with specific transformations and distributions which will lead to more intuitive results.

The above theorem reasons about the condition under which the δ -smoothed classifier $g_h^\delta(x) = \mathbb{E}_\delta[h(\phi(x, \delta))]$ is going to give the same prediction as the ε -smoothed classifier $g_h^\varepsilon(x) = \mathbb{E}_\varepsilon[h(\phi(x, \varepsilon))]$. However, to use the above theorem to certify semantic transformations, we care about a slightly different target, namely the prediction of the smoothed classifier on an adversarially transformed input:

$$g_h^\varepsilon(\phi(x, \alpha)) = \mathbb{E}_\varepsilon[h(\phi(\phi(x, \alpha), \varepsilon))] \quad (8)$$

and reason about its robustness against α , which is the transformation parameter used by an attacker. In the supplementary material, we show that for transformations that are *resolvable* (which applies to all transformations we consider in this paper), one can connect the robustness over δ with robustness over parameters α . Due to space limitations, we omit this result from the main body of this paper.

Certification Process *How can we use the above theorem to certify robustness under semantic transformations?* Given an input example x , the system estimates $g_h^\varepsilon(x) = \mathbb{E}_\varepsilon[h(\phi(x, \varepsilon))]$ (see (Cohen et al., 2019)), from which it calculates p_A and p_B . Given this information, the system can certify a regime of parameters $\alpha \in A$ such that:

$$g_h^\varepsilon(\phi(x, \alpha)) \text{ predicts the same as } g_h^\varepsilon(x)$$

4 Smoothing Strategies

The theorem in the previous section is generic and leaves two questions open: (1) *How can we instantiate this general theorem with different smoothing distributions?* (2) *How can we apply it to specific semantic transformations?* In this section, we focus on the first question.

Previous work mainly provide results for cases in which this distribution is Gaussian, while extending it to other distributions are non-trivial. In this section, we conduct novel analysis and provide results for a range of distributions, and discuss their differences. As we will see, *for different scenarios, different distributions behave differently and can certify different radii*. Throughout this section we suppose that $\phi: \mathcal{X} \times \mathcal{Z} \rightarrow \mathcal{X}$ is a resolvable transform, $h: \mathcal{X} \rightarrow \mathcal{S}_C$ is a base classifier, $c_A \in \mathcal{Y}$ and $x_0 \in \mathcal{X}$ such that g_h^ε is (p_A, p_B) -confident at x_0 . We state all results here, whereas we provide detailed proofs in supplementary materials.

Corollary 1 (Gaussian Noise). *Suppose that $\mathcal{Z} = \mathbb{R}^m$, $\Sigma := \text{diag}(\sigma_1^2, \dots, \sigma_m^2)$, $\varepsilon \sim \mathcal{N}(0, \Sigma)$, and let $\delta := \alpha + \varepsilon$, for some $\alpha \in \mathbb{R}^m$. Then $g_h^\delta(x_0)_{c_A} > \max_{c \neq c_A} g_h^\delta(x_0)_c$ whenever α satisfies*

$$\sqrt{\sum_{i=1}^m \left(\frac{\alpha_i}{\sigma_i}\right)^2} < \frac{1}{2} (\Phi^{-1}(p_A) - \Phi^{-1}(p_B)). \quad (9)$$

Corollary 2 (Exponential Noise). *Suppose that $\mathcal{Z} = \mathbb{R}_{\geq 0}^m$, fix some $\lambda > 0$, and let $\varepsilon_i \sim \text{Exp}(1/\lambda)$ be independent and identically distributed. Let $\varepsilon := (\varepsilon_1, \dots, \varepsilon_m)^T$ and $\delta := \alpha + \varepsilon$, for some $\alpha \in \mathbb{R}_{\geq 0}^m$. Then $g_h^\delta(x_0)_{c_A} > \max_{c \neq c_A} g_h^\delta(x_0)_c$ whenever α satisfies*

$$\|\alpha\|_1 < -\frac{\log(1 - p_A + p_B)}{\lambda}. \quad (10)$$

Corollary 3 (Uniform Noise). *Suppose that $\mathcal{Z} = \mathbb{R}^m$ and $\varepsilon \sim \mathcal{U}([a, b]^m)$, for some $a < b$. Set $\delta := \alpha + \varepsilon$ for $\alpha \in \mathbb{R}^m$. Then $g_h^\delta(x_0)_{c_A} > \max_{c \neq c_A} g_h^\delta(x_0)_c$ if α satisfies*

$$1 - \left(\frac{p_A - p_B}{2}\right) < \prod_{i=1}^m \left(1 - \frac{|\alpha_i|}{b - a}\right)_+ \quad (11)$$

where $(x)_+ := \max\{x, 0\}$.

Corollary 4 (Laplace Noise). *Suppose that $\mathcal{Z} = \mathbb{R}$ and $\varepsilon \sim \mathcal{L}(0, b)$ follows a Laplace distribution with mean 0 and scale parameter $b > 0$. Let $\delta := \alpha + \varepsilon$ for $\alpha \in \mathbb{R}$. Then $g_h^\delta(x_0)_{c_A} > \max_{c \neq c_A} g_h^\delta(x_0)_c$ if α satisfies*

$$|\alpha| < \begin{cases} -b \log(2p_B) & p_A = \frac{1}{2}, p_B < \frac{1}{2} \\ -b \log(2(1 - p_A)) & p_A > \frac{1}{2}, p_B = \frac{1}{2} \\ -b \log(1 - p_A + p_B) & p_A > \frac{1}{2}, p_B < \frac{1}{2}. \end{cases} \quad (12)$$

Corollary 5 (Folded Gaussian Noise). *Suppose that $\mathcal{Z} = \mathbb{R}_{\geq 0}$, $\varepsilon \sim |\mathcal{N}(0, \sigma)|$, and $\delta := \alpha + \varepsilon$ for some $\alpha > 0$. Then $g_h^\delta(x_0)_{c_A} > \max_{c \neq c_A} g_h^\delta(x_0)_c$ if α satisfies*

$$\alpha < \sigma \cdot \left(\Phi^{-1} \left(\frac{1 + \min\{p_A, 1 - p_B\}}{2} \right) - \Phi^{-1} \left(\frac{3}{4} \right) \right). \quad (13)$$

Table 1: Comparison of certification radii. The variance is normalized to 1 and dimensionality of the noise space is $m = 1$. Note that for Exponential and Folded Gaussian distributions the perturbations are restricted to \mathbb{R}_+ .

Distribution	Robust Radius
$\mathcal{N}(0, 1)$	$\Phi^{-1}(p_A)$
$\mathcal{L}(0, \frac{1}{\sqrt{2}})$	$-\frac{1}{\sqrt{2}} \cdot \log(2 - 2p_A)$
$\mathcal{U}([- \sqrt{3}, - \sqrt{3}])$	$2\sqrt{3} \cdot (p_A - \frac{1}{2})$
Exp(1)	$-\log(2 - 2p_A)$
$ \mathcal{N}(0, \sqrt{\frac{\pi}{\pi-2}}) $	$\sqrt{\frac{\pi}{\pi-2}} \cdot (\Phi^{-1}(\frac{1+p_A}{2}) - \Phi^{-1}(\frac{3}{4}))$

4.1 Comparison of smoothing noise distributions

In order to compare the different radii for a fixed base classifier, we assume that *the smoothed classifier g_h^ε always has the same confidence p_A for noises with equal variance*. Corollaries 1-5 show that the certified radius for transformations varies across different noise distributions, summarized in Table 1. We leave more details to the Appendix.

1. *Exponential noise could provide larger robust radius.* We notice that smoothing with exponential noise generally allows for larger adversarial perturbations than other distributions. We also observe that, while all distributions behave similar for low confidence levels, it is only non-uniform noise distributions that converge towards $+\infty$ when $p_A \rightarrow 1$ and exponential noise converges quickest.
2. *Additional knowledge can lead to larger radius.* When we have additional information on the transformation, e.g., all perturbations in Gaussian blur are positive, we can take advantage of it to certify larger radii. For example, under this assumption, we can use folded Gaussian noise for smoothing instead of a standard Gaussian, resulting in a larger radius.

5 Adversarial Semantic Transformations

In this section, we provide approaches to certify a range of different semantic transformations. Some transformations can be certified by directly applying Theorem 1; however, many transformations need more engaged analysis and it is delicate and non-trivial to reason about which smoothing distributions fit a given transformation better. We state all results and provide proofs in supplementary materials.

5.1 Gaussian blur

Gaussian blur is a transformation which is widely used in image processing to reduce noise and image detail. Mathematically speaking, applying Gaussian blur amounts to convolving an image with a Gaussian function

$$G_\alpha(k) = \frac{1}{\sqrt{2\pi\alpha}} \exp\left(-\frac{k^2}{2\alpha}\right) \quad (14)$$

where $\alpha > 0$ is the squared kernel radius. For $x \in \mathcal{X}$, we define Gaussian blur as the transform $\phi_B: \mathcal{X} \times \mathbb{R}_{\geq 0} \rightarrow \mathcal{X}$:

$$\phi_B(x, \alpha) = x * G_\alpha \quad (15)$$

where $*$ denotes the convolution operator. The following Lemma shows that Gaussian blur is an *additive transform*.

Lemma 1. Let $\phi_B: \mathcal{X} \times \mathbb{R}_{\geq 0} \rightarrow \mathbb{R}_{\geq 0}$ denote the Gaussian blur transform. Then, for any $\alpha, \beta \in \mathbb{R}_{\geq 0}$

$$\phi_B(\phi_B(x, \alpha), \beta) = \phi_B(x, \alpha + \beta) \quad \forall x. \quad (16)$$

We notice that an attacker can only use positive parameters for the Gaussian blur transform. We therefore consider uniform noise on $[0, a]$ for $a > 0$, folded Gaussians and exponential distribution for smoothing.

5.2 Brightness and contrast

Brightness and contrast transformations first add a constant value $b \in \mathbb{R}$ to every pixel and then change the contrast by multiplying each pixel with a positive factor e^k , for some $k \in \mathbb{R}$. Given an image $x \in \mathcal{X}$, we define the brightness and contrast transform $\phi_{BC}: \mathcal{X} \times \mathbb{R}^2 \rightarrow \mathcal{X}$ as

$$\phi_{BC}(x, k, b) = e^k(x + b). \quad (17)$$

where $k, b \in \mathbb{R}$ are contrast and brightness parameters. We notice that ϕ_{BC} is not an additive transform. We therefore cannot simply set $\delta = \alpha + \varepsilon$ and directly apply Theorem 1. However, if $\varepsilon_1, \varepsilon_2$ are independent Gaussians, we can circumvent the issue of non-additivity using the following idea. Given ε , we derive a distribution δ such that using g_h^ε to classify $\phi_{BC}(x, \alpha)$ is the same as using $g_h^{\alpha+\delta}$ to classify the original input x . We then show a connection between the confidence of g_h^ε and g_h^δ such that we can apply Corollary 1 to δ and $\alpha + \delta$. These relations allow us to certify the brightness and contrast transformation. The following Lemmas justify this approach.

Lemma 2. Let $\varepsilon \sim \mathcal{N}(0, \text{diag}(\sigma_1^2, \sigma_2^2))$, $\alpha = (k, b)^T \in \mathbb{R}^2$ and $\delta \sim \mathcal{N}(0, \text{diag}(\sigma_1^2, e^{-2k}\sigma_2^2))$. Then

$$g_h^\varepsilon(\phi_{BC}(x, \alpha)) = g_h^{\alpha+\delta}(x) \quad \forall x. \quad (18)$$

Lemma 3. Let $x_0 \in \mathcal{X}$, $k \in \mathbb{R}$, $\varepsilon \sim \mathcal{N}(0, \Sigma)$ and $\delta \sim \mathcal{N}(0, \text{diag}(\sigma_1^2, e^{-2k}\sigma_2^2))$. Suppose that $g_h^\varepsilon(x_0)_c \geq p$ for some $p \in [0, 1]$ and $c \in \mathcal{Y}$. Then

$$g_h^\delta(x)_c \geq \begin{cases} 2\Phi(e^k\Phi^{-1}(\frac{1+p}{2})) - 1 & k \leq 0 \\ 2(1 - \Phi(e^k\Phi^{-1}(1 - \frac{p}{2}))) & k > 0 \end{cases} \quad (19)$$

Now suppose that g_h^ε makes the prediction c_A at x_0 with probability at least p_A . Then, the above Lemma tells us that g_h^δ is similarly confident in predicting the same class. If, in addition, p_A is large enough such that $g_h^\delta(x_0)_{c_A} > 0.5$, we can apply Corollary 1: as long as $\alpha = (k, b)^T$ satisfies

$$\sqrt{\left(\frac{k}{\sigma_1}\right)^2 + \left(\frac{b}{e^{-k}\sigma_2}\right)^2} < \Phi^{-1}(g_h^\delta(x)_{c_A}), \quad (20)$$

we will get the correct prediction by

$$g_h^\varepsilon(\phi_{BC}(x, \alpha))_{c_A} > \max_{c \neq c_A} g_h^\varepsilon(\phi_{BC}(x, \alpha))_c \quad (21)$$

5.3 Translation

Let $\bar{\phi}_T: \mathcal{X} \times \mathbb{Z}^2 \rightarrow \mathcal{X}$ be the transform moving an image k_1 pixels to the right and k_2 pixels to the bottom with reflection padding. In order to handle continuous noise distributions, we define the translation transform $\phi_T: \mathcal{X} \times \mathbb{R}^2 \rightarrow \mathcal{X}$ as

$$\phi_T(x, \alpha) = \bar{\phi}_T(x, [\alpha]) \quad (22)$$

where $\lceil \cdot \rceil$ denotes rounding to the nearest integer, applied element-wise. With this definition we note that ϕ_T is an *additive transform* which allows us to directly apply Corollaries 1- 5 and derive robustness bounds. We note that if we use black-padding instead of reflection-padding, the transform is not additive. However, since the number of possible translations is finite, another possibility is to use a simple brute force approach which can handle black-padding.

5.4 Rotations and Scaling

We now present our method to certify rotation and scaling transformations. The dynamics of these two transforms are more involved and require careful analysis, due to their use of bilinear interpolation. Our approach is based on the observation that when transformation parameters are close to each other, then the resulting images are also close. In order to certify an interval $[a, b]$, we sample a number of parameters $\{\alpha_i\}_{i=1}^N$ such that the maximum ℓ_2 sampling error is bounded by some constant $M \geq 0$. We then compute the ℓ_2 robustness guarantee for each sampled α_i using element-wise addition and Gaussian noise. Finally, as long as M is less than the smallest certified radius for the α_i , we know that the smoothed classifier is provably robust with respect to any parameter within the interval $[a, b]$. The following Theorem justifies this approach.

Definition 4 (Maximum ℓ_2 sampling error). Let $x \in \mathcal{X}$, $\phi: \mathcal{X} \times \mathcal{Z} \rightarrow \mathcal{X}$ be a transform, $a < b$ real numbers, $N \in \mathbb{N}$, and let $\{\alpha_i\}_{i=1}^N \subseteq [a, b]$. We define the maximum ℓ_2 sampling error as

$$M_{a,b} := \max_{a \leq \alpha \leq b} \min_{1 \leq i \leq N} \|\phi(x, \alpha) - \phi(x, \alpha_i)\|_2 \quad (23)$$

Theorem 2 (Sampling-based certification). Let $a < b$ be real numbers, $N \in \mathbb{N}$ and suppose $\{\alpha_i\}_{i=1}^N \subseteq [a, b]$. Furthermore, let $\phi: \mathcal{X} \times \mathbb{R} \rightarrow \mathcal{X}$ be a transform, $x_0 \in \mathcal{X}$, $c_A \in \mathcal{Y}$, $\varepsilon \sim \mathcal{N}(0, \sigma^2 \mathbb{1})$ isotropic Gaussian noise. Suppose that the ε -smoothed classifier $g_h^\varepsilon: \mathcal{X} \rightarrow \mathcal{S}_C$,

$$g_h^\varepsilon(x) = \mathbb{E}_\varepsilon[h(x + \varepsilon)] \quad (24)$$

is (p_A, p_B) -confident at x_0 for some $p_A, p_B \in [0, 1]$. If

$$M_{a,b} < \sigma \min_{1 \leq i \leq N} \Phi^{-1}(g_h^\varepsilon(\phi(x_0, \alpha_i))_{c_A}), \quad (25)$$

then for any $\alpha \in [a, b]$, the ε -smoothed classifier predicts class c_A on $\phi(x_0, \alpha)$, that is

$$g_h^\varepsilon(\phi(x_0, \alpha))_{c_A} > \max_{c \neq c_A} g_h^\varepsilon(\phi(x_0, \alpha))_c. \quad (26)$$

In essence, the above Theorem states that if the smoothed classifier classifies a collection of simulated transformations correctly and confidently, then it will be guaranteed to classify any similar transformation of the same input correctly. In order to use this Theorem, we first need to compute the maximum sampling error $M_{a,b}$ on a collection of sampled parameters. In the second step, we compute the robustness radius for each of those parameters and compare whether the smallest such radius is bigger than $M_{a,b}$. If this is true, then the smoothed classifier is guaranteed to make the expected prediction for all parameters in the interval $[a, b]$.

Computing the Sampling Error In order to apply Theorem 2 in practice, we need to compute the maximum ℓ_2 sampling error given in (23), which is not trivial. Our approach is based on computing an upper bound on $M_{a,b}$. For transformations, such as rotations, we compute this upper bound based on the Lipschitz constant. We refer the reader to Appendix E.3 for details.

Rotations We denote rotations as $\phi_R: \mathcal{X} \times \mathbb{R} \rightarrow \mathcal{X}$, transforming images by first rotating the input x by α degrees counter-clockwise. Subsequently, zero-padding and bilinear interpolation is applied in order to determine the color of intermediate pixels.

Scaling We denote the scaling transformation by $\phi_S: \mathcal{X} \times \mathbb{R} \rightarrow \mathcal{X}$, transforming images by first multiplying the height and width by a constant factor $\alpha \in \mathbb{R}$ and then using bilinear interpolation in order to determine the pixel values.

Detailed descriptions of both transforms are provided in Appendix D.2 and D.3.

6 Theoretic Barriers

In this section we provide a brief analysis highlighting the generalization gaps of randomized smoothing. Recall that we consider base classifiers to be deterministic functions $h: \mathcal{X} \rightarrow \mathcal{S}_C$. Denote the family of such classifiers by \mathcal{H} . Throughout this section we consider smoothed classifiers with additive isotropic Gaussian Noise

$$g_h^\varepsilon(x) = \mathbb{E}_\varepsilon [h(x + \varepsilon)], \quad \varepsilon \sim \mathcal{N}(0, \sigma^2 \mathbb{1}). \quad (27)$$

In the first step, we would like to compare classes of smoothed classifiers corresponding to different levels of noise variance. Let

$$\mathcal{G}_0 := \mathcal{H}, \quad \mathcal{G}_\sigma := \{g_h^\varepsilon \mid \varepsilon \sim \mathcal{N}(0, \sigma^2 \mathbb{1}), h \in \mathcal{H}\} \quad (28)$$

For any $\sigma > 0$, the smoothed classifiers are deterministic classifiers and hence $\mathcal{G}_\sigma \subseteq \mathcal{H}$. The next result relates families of smoothed classifier with different levels of noise.

Lemma 4. *If $\sigma_1 < \sigma_2$, then $\mathcal{G}_{\sigma_2} \subsetneq \mathcal{G}_{\sigma_1}$.*

The proof (Appendix F) relies on the fact that smoothing with σ_2^2 is equivalent to first smoothing with variance $\sigma_2^2 - \sigma_1^2$ and subsequently smoothing with σ_1^2 . The next Corollary is a direct consequence of the above Lemma.

Corollary 6. *Let $\text{Rad}(\mathcal{G})$ denote the Rademacher complexity of the function class \mathcal{G} and $\text{bestacc}(\mathcal{G}) = \sup_{h \in \mathcal{G}} \text{acc}(h)$ the best achievable classification accuracy of the function class \mathcal{G} . If $0 \leq \sigma_1 < \sigma_2$, then*

$$\text{bestacc}(\mathcal{G}_{\sigma_1}) \geq \text{bestacc}(\mathcal{G}_{\sigma_2}), \quad (29)$$

$$\text{Rad}(\mathcal{G}_{\sigma_1}) \geq \text{Rad}(\mathcal{G}_{\sigma_2}). \quad (30)$$

The above Corollary intuitively depicts the following trade-off between certified and clean accuracy: larger noise variance leads to better generalization bound and likely better certified accuracy, but comes at the cost of reduced clean accuracy.

Finite Sampling The prediction of a smoothed classifier is defined as an expectation which, in practice, needs to be estimated and often cannot be computed exactly. Evaluating a smoothed classifier and computing its generalization bound is therefore a non-trivial statistical problem and needs to be treated carefully. This problem has also been addressed in (Cohen et al., 2019), where a non-trivial gap between true and estimated robust radius is shown.

7 Experiments

We validate our approach to certifying robustness over semantic transformations experimentally on the publicly available MNIST, CIFAR-10 and ImageNet-1k datasets. We compare with state-of-the-art methods for each semantic transformation and highlight our main results.

Setup We implement all methods in Python using the PyTorch library. All experiments were run on a single NVIDIA GTX 1080Ti GPU and 24-core Intel Xeon E5-2650 CPU running at 2.2 GHz. On ImageNet we use a pretrained ResNet-50 architecture (He et al., 2016) as base classifier while on CIFAR-10 we use ResNet-110 and on MNIST we use a small CNN. We refer the reader to Appendix H.2 for experimental details.

Evaluation Procedure In adversarially robust classification we are interested in the *robust accuracy* at radius r . This metric is defined as the fraction of the test which is classified correctly with a prediction that is

Table 2: Overview of the best robust accuracy for different semantic transformations. The current state-of-the-art is **bolded**. * Within our best knowledge, we are the first to provide provable robustness against these semantic transformations.

Transformation	Dataset	Robustness Radii	Robust Acc.		
			Ours	Literature	
Gaussian Blur	MNIST	Kernel Rad. $\alpha \leq 9$	90.4%	-	
	CIFAR-10	Kernel Rad. $\alpha \leq 9$	52.0%	-	
	ImageNet	Kernel Rad. $\alpha \leq 9$	47.0%	-	
Translation (Reflection Pad.)	MNIST	$\sqrt{\Delta x^2 + \Delta y^2} \leq 5$	96.8%	-	
	CIFAR-10	$\sqrt{\Delta x^2 + \Delta y^2} \leq 5$	84.8%	-	
	ImageNet	$\sqrt{\Delta x^2 + \Delta y^2} \leq 5$	63.0%	-	
Brightness	MNIST	$b \pm 0.1^{(25.5/255)}$	98.6%	-	
	CIFAR-10	$b \pm 0.1^{(25.5/255)}$	84.2%	-	
	ImageNet	$b \pm 0.1^{(25.5/255)}$	64.0%	64.0% ^a	(Fischer et al., 2020)
Contrast	MNIST	$c \pm 30\%$	98.6%	-	
	CIFAR-10	$c \pm 30\%$	76.8%	-	
	ImageNet	$c \pm 30\%$	56.0%	45.0% ^a	(Fischer et al., 2020)
Contrast and Brightness	MNIST	$c \pm 20\%, b \pm 0.2^{(51/255)}$	98.6%	-	
	CIFAR-10	$c \pm 20\%, b \pm 0.2^{(51/255)}$	77.4%	-	
	ImageNet	$c \pm 20\%, b \pm 0.2^{(51/255)}$	57.0%	-	
Rotation	MNIST	$\pm 30^\circ$	95.6%	87.0%	(Balunovic et al., 2019)
	CIFAR-10	$\pm 10^\circ$	63.8%	62.5%	(Balunovic et al., 2019)
	ImageNet	$\pm 10^\circ$	33.0%	9.0% ^a	(Fischer et al., 2020)
Scaling	MNIST	$\pm 20\%$	96.8%	-	
	CIFAR-10	$\pm 20\%$	58.4%	-	
	ImageNet	$\pm 15\%$	31.0%	-	

^aFor brightness on ImageNet, Fischer et al. uses a slightly smaller radius than $20.37/255$; for contrast on ImageNet, Fischer et al. uses a smaller radius than $\pm 21\%$; for rotation on ImageNet, Fischer et al. uses a smaller radius than 8.13° .

certifiably robust within a ball of radius r . However, since we use randomized smoothing classifiers for inference, computing this quantity exactly is not possible. Instead we report the *approximate robust accuracy* on a subset of the test set using adapted versions of PREDICT and CERTIFY presented in (Cohen et al., 2019). The error rate is set to $\alpha = 0.001$ such that the certification holds with probability at least $1 - \alpha$.

Main Results Table 2 summarizes our results. We observe that across transformations, our approach significantly outperforms state-of-the-art, if present, in terms of robust accuracy. In particular, for Gaussian Blur, translation with reflection padding, scaling and the compositional contrast and brightness transformation, to our best knowledge, we are the first to provide their provable robustness accuracy.

Noise Distribution Tuning Our theoretical results allow us to derive robustness bounds for different types of noise distributions. Therefore we explore smoothing using exponential, uniform and Gaussian distributions for a fixed variance level. We use Gaussian blur to showcase our findings. We leave the detailed result to Appendix H.3 where we show that smoothing with exponential distribution typically performs best, confirming our theoretical analysis.

Summary of Results for Specific Transformations In the following, we summarize the experimental setup and observations for our transformation-specific results. In addition to Table 2, we provide detailed results for each specific transform in the appendix.

- For Gaussian Blur we choose the exponential distribution $\text{Exp}(1/\lambda)$ for smoothing. During training, we use the same distribution to sample blurring parameters for data augmentation. We repeat the same experiment for different values of λ . We observe a pronounced trade-off between robust and clean accuracy: *with more noise, we achieve higher certification radii, which comes at the cost of decreased clean accuracy*. This phenomenon is in line with what has been reported in previous works.
- For brightness and contrast transformations we use Gaussian noise for data augmentation during training and smoothing during inference. We report robust and clean accuracy for (1) brightness, (2) contrast, and (3) compositional brightness and contrast transformations in the Appendix.
- We certify translation transformations with black-padding and reflection padding. For black-padding we only use brute-force enumeration for certification, while for reflection padding we also use the randomized smoothing framework with Gaussian noise varying the standard deviation. We observe that in general, randomized smoothing does slightly better than the enumeration approach.
- To certify rotations we obtain base classifiers with data augmentation during training. Specifically, we rotate images with angles α_{train} sampled uniformly at random and add Gaussian noise with variance σ_{train}^2 . During inference with smoothed classifiers we use isotropic Gaussian noise for smoothing with variance σ_{test}^2 . We notice that, generally, an increase in σ_{train}^2 hurts clean accuracy, while it benefits robust accuracy.
- The procedure to certify scaling transformation is similar in nature to rotations. That is, we apply data augmentation during training and scale images with a scaling parameter s_{train} sampled uniformly at random. After scaling, we add iid Gaussian noise with variance σ_{train}^2 . We then use randomized smoothing classifiers with additive Gaussian noise to perform inference and obtain robustness bounds. Although we observe a clear trade-off between clean accuracy and noise variance, the relation between robust accuracy and variance is not obvious.

8 Conclusion

In this paper we provide a unified framework for certifying ML robustness against general adversarial transformations using function smoothing. We show that our theoretical results can be used to derive provable robustness bounds against a series of transformations based on different smoothing strategies. We then propose novel methods to certify the robust accuracy for several distinct semantic transformations. In addition, for the first time we provide the generalization gaps for function smoothing strategies, which leads to further understanding about the tradeoffs. Extensive experiments show that our transformation specific smoothing approaches significantly outperform the state-of-the-art or, if no previous methods exist, set new baselines.

Our theoretical and empirical results indicate that the utility of function smoothing goes beyond certifying additive adversarial perturbations and delivers possibilities to certify robustness against a far broader class of attacks.

References

- Abramowitz, M. and Stegun, I. A. E. *Handbook of Mathematical Functions with Formulas, Graphs, and Mathematical Tables, 9th printing*. New York: Dover, 1972.
- Athalye, A., Carlini, N., and Wagner, D. Obfuscated gradients give a false sense of security: Circumventing defenses to adversarial examples. *arXiv preprint arXiv:1802.00420*, 2018.
- Balunovic, M., Baader, M., Singh, G., Gehr, T., and Vechev, M. Certifying geometric robustness of neural networks. In *Advances in Neural Information Processing Systems*, pp. 15287–15297, 2019.

- Carmon, Y., Raghuathan, A., Schmidt, L., Liang, P., and Duchi, J. C. Unlabeled data improves adversarial robustness. *arXiv preprint arXiv:1905.13736*, 2019.
- Cohen, J. M., Rosenfeld, E., and Kolter, J. Z. Certified adversarial robustness via randomized smoothing. *arXiv preprint arXiv:1902.02918*, 2019.
- Deng, J., Dong, W., Socher, R., Li, L.-J., Li, K., and Fei-Fei, L. Imagenet: A large-scale hierarchical image database. In *2009 IEEE conference on computer vision and pattern recognition*, pp. 248–255. Ieee, 2009.
- Engstrom, L., Tsipras, D., Schmidt, L., and Madry, A. A rotation and a translation suffice: Fooling cnns with simple transformations. *arXiv preprint arXiv:1712.02779*, 1(2):3, 2017.
- Eykholt, K., Evtimov, I., Fernandes, E., Li, B., Rahmati, A., Xiao, C., Prakash, A., Kohno, T., and Song, D. Robust physical-world attacks on deep learning visual classification. In *Proceedings of the IEEE Conference on Computer Vision and Pattern Recognition*, pp. 1625–1634, 2018.
- Fischer, M., Baader, M., and Vechev, M. Statistical verification of general perturbations by gaussian smoothing. <https://openreview.net/forum?id=B1eZweHFwr>, 2020.
- Ghiasi, A., Shafahi, A., and Goldstein, T. Breaking certified defenses: semantic adversarial examples with spoofed robustness certificates. In *International Conference on Learning Representations*, 2020. URL <https://openreview.net/forum?id=HJxdTxHYvB>.
- Goodfellow, I. J., Shlens, J., and Szegedy, C. Explaining and harnessing adversarial examples. *arXiv preprint arXiv:1412.6572*, 2014.
- Gowal, S., Dvijotham, K., Stanforth, R., Bunel, R., Qin, C., Uesato, J., Mann, T., and Kohli, P. On the effectiveness of interval bound propagation for training verifiably robust models. *arXiv preprint arXiv:1810.12715*, 2018.
- He, K., Zhang, X., Ren, S., and Sun, J. Delving deep into rectifiers: Surpassing human-level performance on ImageNet classification. In *Proceedings of the IEEE International Conference on Computer Vision*, pp. 1026–1034, 2015.
- He, K., Zhang, X., Ren, S., and Sun, J. Deep residual learning for image recognition. In *Proceedings of the IEEE conference on computer vision and pattern recognition*, pp. 770–778, 2016.
- Jacobsen, J.-H., Behrmann, J., Carlini, N., Tramer, F., and Papernot, N. Exploiting excessive invariance caused by norm-bounded adversarial robustness. *arXiv preprint arXiv:1903.10484*, 2019.
- Jacod, J. and Protter, P. *Probability Essentials*. Springer, 2000.
- Kolter, J. Z. and Wong, E. Provable defenses against adversarial examples via the convex outer adversarial polytope. *arXiv preprint arXiv:1711.00851*, 2017.
- Krizhevsky, A., Hinton, G., et al. Learning multiple layers of features from tiny images. 2009.
- LeCun, Y., Bottou, L., Bengio, Y., and Haffner, P. Gradient-based learning applied to document recognition. *Proceedings of the IEEE*, 86(11):2278–2324, 1998.
- Li, L., Zhong, Z., Li, B., and Xie, T. Robustra: training provable robust neural networks over reference adversarial space. In *Proceedings of the 28th International Joint Conference on Artificial Intelligence*, pp. 4711–4717. AAAI Press, 2019.
- Ma, X., Li, B., Wang, Y., Erfani, S. M., Wijewickrema, S., Schoenebeck, G., Song, D., Houle, M. E., and Bailey, J. Characterizing adversarial subspaces using local intrinsic dimensionality. *arXiv preprint arXiv:1801.02613*, 2018.

- Moravčík, M., Schmid, M., Burch, N., Lisý, V., Morrill, D., Bard, N., Davis, T., Waugh, K., Johanson, M., and Bowling, M. DeepStack: Expert-level artificial intelligence in heads-up no-limit poker. *Science*, 356(6337): 508–513, 2017.
- Neyman, J. and Pearson, E. On the problem of the most efficient tests of statistical hypotheses. 231. *Phil. Trans. Roy. Statistical Soc. A*, 289, 1933.
- Raghunathan, A., Steinhardt, J., and Liang, P. S. Semidefinite relaxations for certifying robustness to adversarial examples. In *Advances in Neural Information Processing Systems*, pp. 10877–10887, 2018.
- Salman, H., Li, J., Razenshteyn, I., Zhang, P., Zhang, H., Bubeck, S., and Yang, G. Provably robust deep learning via adversarially trained smoothed classifiers. In *Advances in Neural Information Processing Systems*, pp. 11289–11300, 2019a.
- Salman, H., Yang, G., Zhang, H., Hsieh, C.-J., and Zhang, P. A convex relaxation barrier to tight robust verification of neural networks. *arXiv preprint arXiv:1902.08722*, 2019b.
- Silver, D., Schrittwieser, J., Simonyan, K., Antonoglou, I., Huang, A., Guez, A., Hubert, T., Baker, L., Lai, M., Bolton, A., Chen, Y., Lillicrap, T., Hui, F., Sifre, L., van den Driessche, G., Graepel, T., and Hassabis, D. Mastering the game of go without human knowledge. *Nature*, 550(7676):354–359, 10 2017.
- Singh, G., Gehr, T., Püschel, M., and Vechev, M. An abstract domain for certifying neural networks. *Proceedings of the ACM on Programming Languages*, 3(POPL):41, 2019.
- Szegedy, C., Zaremba, W., Sutskever, I., Bruna, J., Erhan, D., Goodfellow, I., and Fergus, R. Intriguing properties of neural networks. *arXiv preprint arXiv:1312.6199*, 2013.
- Tjeng, V., Xiao, K. Y., and Tedrake, R. Evaluating robustness of neural networks with mixed integer programming. 2018.
- Tong, L., Li, B., Hajaj, C., Xiao, C., Zhang, N., and Vorobeychik, Y. Improving robustness of ml classifiers against realizable evasion attacks using conserved features. In *Proceedings of the 28th USENIX Conference on Security Symposium, SEC19*, pp. 285302, USA, 2019. USENIX Association. ISBN 9781939133069.
- Tramèr, F., Kurakin, A., Papernot, N., Goodfellow, I., Boneh, D., and McDaniel, P. Ensemble adversarial training: Attacks and defenses. *arXiv preprint arXiv:1705.07204*, 2017.
- Wong, E., Schmidt, F., Metzen, J. H., and Kolter, J. Z. Scaling provable adversarial defenses. *arXiv preprint arXiv:1805.12514*, 2018.
- Xiao, C., Li, B., Zhu, J.-Y., He, W., Liu, M., and Song, D. Generating adversarial examples with adversarial networks. *arXiv preprint arXiv:1801.02610*, 2018a.
- Xiao, C., Zhu, J.-Y., Li, B., He, W., Liu, M., and Song, D. Spatially transformed adversarial examples. *arXiv preprint arXiv:1801.02612*, 2018b.
- Xu, W., Qi, Y., and Evans, D. Automatically evading classifiers. In *Proceedings of the 2016 Network and Distributed Systems Symposium*, 2016.

A Proof of Theorem 1

Here we provide the proof for Theorem 1. For the sequel, suppose that \mathcal{X} is endowed with Lebesgue measure on \mathbb{R}^d and \mathcal{Z} is a measure space with measure λ which is Lebesgue if $\mathcal{Z} \subseteq \mathbb{R}^m$ and counting measure if $\mathcal{Z} \subseteq \mathbb{Z}^m$. We consider transforms ϕ such that the maps $\phi_x: \mathcal{Z} \rightarrow \mathcal{X}$, $z \mapsto \phi_x(z) := \phi(x, z)$ are measurable for each $x \in \mathcal{X}$. Finally, let ε and δ be \mathcal{Z} -valued random variables with associated probability mass functions \mathbb{P}_ε and \mathbb{P}_δ and densities μ_ε and μ_δ respectively. The probability mass of a λ -measurable set $S \subseteq \mathcal{Z}$ is then given by $\mathbb{P}_\varepsilon[S] = \int_S \mu_\varepsilon d\lambda$ and $\mathbb{P}_\delta[S] = \int_S \mu_\delta d\lambda$ respectively. Recall the following Definitions from the main part of this paper:

Definition 2 (restated). Let $x_0 \in \mathcal{X}$, $\phi: \mathcal{X} \times \mathcal{Z} \rightarrow \mathcal{X}$ an input transform, $h: \mathcal{X} \rightarrow \mathcal{S}_C$ a base classifier, $c_A \in \mathcal{Y}$ and $p_A, p_B \in [0, 1]$. We say that the ε -smoothed classifier g_h^ε is (p_A, p_B) -confident at x_0 if it satisfies

$$g_h^\varepsilon(x_0)_{c_A} \geq p_A \geq p_B \geq \max_{c \neq c_A} g_h^\varepsilon(x_0)_c. \quad (31)$$

Definition 3 (restated). For $t \geq 0$, we define strict lower and lower level sets as

$$\underline{S}_t := \left\{ z \in \mathcal{Z} : \frac{\mu_\delta(z)}{\mu_\varepsilon(z)} < t \right\}, \quad \overline{S}_t := \left\{ z \in \mathcal{Z} : \frac{\mu_\delta(z)}{\mu_\varepsilon(z)} \leq t \right\} \quad (32)$$

We now show the following Lemma which is connected to the Neyman-Pearson Lemma (Neyman & Pearson, 1933) from statistical hypothesis testing.

Lemma 5 (Extended Neyman-Pearson). Let $f: \mathcal{Z} \rightarrow \mathbb{R}_{\geq 0}$ be a measurable function such that $0 \leq \sup_x f(x) \leq M < \infty$. Then, the following implications hold

1. For any measurable set $S \subseteq \mathcal{Z}$ such that $\underline{S}_t \subseteq S \subseteq \overline{S}_t$:

$$\mathbb{E}_\varepsilon[f(\varepsilon)] \geq M \cdot \mathbb{P}_\varepsilon[S] \quad \Rightarrow \quad \mathbb{E}_\delta[f(\delta)] \geq M \cdot \mathbb{P}_\delta[S]. \quad (33)$$

2. For any measurable set $S \subseteq \mathcal{Z}$ such that $\overline{S}_t^c \subseteq S \subseteq \underline{S}_t^c$:

$$\mathbb{E}_\varepsilon[f(\varepsilon)] \leq M \cdot \mathbb{P}_\varepsilon[S] \quad \Rightarrow \quad \mathbb{E}_\delta[f(\delta)] \leq M \cdot \mathbb{P}_\delta[S]. \quad (34)$$

Proof. We only prove (1), since the second part is analogous.

$$\mathbb{E}_\delta[f(\delta)] - M \cdot \mathbb{P}_\delta[S] = \int_{\mathcal{Z}} f(z) \mu_\delta(z) d\lambda(z) - M \cdot \int_S \mu_\delta(z) d\lambda(z) \quad (35)$$

$$= \int_{\mathcal{Z}} f(z) \mu_\delta(z) d\lambda(z) - M \cdot \left[\frac{1}{M} \int_S f(z) \mu_\delta(z) d\lambda(z) + \int_S \left(1 - \frac{f(z)}{M}\right) \mu_\delta(z) d\lambda(z) \right] \quad (36)$$

$$= \int_{S^c} f(z) \mu_\delta(z) d\lambda(z) - \int_S (M - f(z)) \mu_\delta(z) d\lambda(z) \quad (37)$$

$$\geq t \cdot \left[\int_{S^c} f(z) \mu_\varepsilon(z) d\lambda(z) - \int_S (M - f(z)) \mu_\varepsilon(z) d\lambda(z) \right] \quad (38)$$

$$= t \cdot \left[\int_{\mathcal{Z}} f(z) \mu_\varepsilon(z) d\lambda(z) - M \cdot \int_S \mu_\varepsilon(z) d\lambda(z) \right] \geq 0. \quad (39)$$

The inequality in (38) follows from the fact that whenever $z \in S^c$, then $\mu_\delta(z) \geq t \cdot \mu_\varepsilon(z)$ and if $z \in S$, then $\mu_\delta(z) \leq t \cdot \mu_\varepsilon(z)$ since S is assumed to be a lower level set. Finally, (39) follows from the assumption. \square

Theorem 1 (restated). Let $\varepsilon \sim \mathbb{P}_\varepsilon$, $\delta \sim \mathbb{P}_\delta$ be two random variables with densities μ_ε and μ_δ . Let $\phi: \mathcal{X} \times \mathcal{Z} \rightarrow \mathcal{X}$ be a transform, h a base classifier, $x_0 \in \mathcal{X}$, and suppose that the ε -smoothed classifier g_h^ε is (p_A, p_B) -confident at x_0 for some $c_A \in \mathcal{Y}$. Let

$$\begin{aligned} \zeta: \mathbb{R}_{\geq 0} &\rightarrow [0, 1] \\ t &\mapsto \zeta(t) := \mathbb{P}_\varepsilon[\overline{S}_t] \end{aligned} \quad (40)$$

be the probability mass function of the lower level sets \bar{S}_t . Denote by $\zeta^{-1}(p) := \inf\{t: \zeta(t) \geq p\}$ its generalized inverse. For $t \geq 0$ and $p \in [0, 1]$ let

$$\mathcal{S}_{t,p} := \{S \subseteq \mathcal{Z} \mid \underline{S}_t \subseteq S \subseteq \bar{S}_t \wedge \mathbb{P}_\varepsilon[S] \leq p\} \quad (41)$$

and define the function $\xi: \mathbb{R}_{\geq 0} \times [0, 1] \rightarrow [0, 1]$

$$\xi(t, p) := \sup\{\mathbb{P}_\delta[S] \mid S \in \mathcal{S}_{t,p}\}. \quad (42)$$

If δ satisfies

$$1 - \xi(\zeta^{-1}(1 - p_B), 1 - p_B) < \xi(\zeta^{-1}(p_A), p_A), \quad (43)$$

then

$$g_h^\delta(x_0)_{c_A} > \max_{c \neq c_A} g_h^\delta(x_0)_c. \quad (44)$$

Lemma 6. The function $\zeta: \mathbb{R}_{\geq 0} \rightarrow [0, 1]$ $t \mapsto \zeta(t) := \mathbb{P}_\varepsilon[\bar{S}_t]$ is right-continuous.

Proof of Lemma 6. Let $t \geq 0$ and suppose that $\{t_n\}_{n \in \mathbb{N}}$ is a sequence such that $t_n \downarrow t$. In order to show right-continuity, we need to show that

$$\lim_{n \rightarrow \infty} \zeta(t_n) = \zeta(t). \quad (45)$$

It is a well known fact from Probability Theory that if a sequence of events $\{A_n\}_{n \in \mathbb{N}}$ is decreasing, in the sense that for every n , $A_{n+1} \subseteq A_n$, then for $A = \bigcap_{n=1}^{\infty} A_n$, $\mathbb{P}[A_n] \downarrow \mathbb{P}[A]$ as $n \rightarrow \infty$ (e.g. (Jacod & Protter, 2000), p. 9, Theorem 2.3). For that purpose, consider the set of events

$$A_n := \left\{ z \in \mathcal{Z} \mid \frac{\mu_\delta(z)}{\mu_\varepsilon(z)} \leq t_n \right\}. \quad (46)$$

Note that $A_n = \bar{S}_{t_n}$ and hence $\mathbb{P}_\varepsilon[A_n] = \zeta(t_n)$. Furthermore, $A_{n+1} \subseteq A_n$ since for any $z \in A_{n+1}$, we have

$$\frac{\mu_\delta(z)}{\mu_\varepsilon(z)} \leq t_{n+1} \leq t_n \quad (47)$$

and thus $z \in A_n$. Let $A := \left\{ z \in \mathcal{Z} \mid \frac{\mu_\delta(z)}{\mu_\varepsilon(z)} \leq t \right\}$. We now show that $\bigcap_{n=1}^{\infty} A_n = A$. Suppose that $z \in \bigcap_{n=1}^{\infty} A_n$. Then $\forall n$, we have $\frac{\mu_\delta(z)}{\mu_\varepsilon(z)} \leq t_n$. Taking the limit as $n \rightarrow \infty$ on both sides yields $\frac{\mu_\delta(z)}{\mu_\varepsilon(z)} \leq t$ and hence $z \in A$. If, on the other hand, $z \in A$, then $\frac{\mu_\delta(z)}{\mu_\varepsilon(z)} \leq t \leq t_n$ for any n and hence $z \in A_n \forall n$. Thus $\bigcap_{n=1}^{\infty} A_n = A$. Finally, this yields

$$\zeta(t_n) = \mathbb{P}_\varepsilon[\bar{S}_{t_n}] = \mathbb{P}_\varepsilon[A_n] \downarrow \mathbb{P}_\varepsilon[A] = \mathbb{P}_\varepsilon[\bar{S}_t] = \zeta(t) \quad (48)$$

completing the proof. \square

Lemma 7. Suppose $\zeta: \mathbb{R}_{\geq 0} \rightarrow [0, 1]$ is defined as in Theorem 1, that is $\zeta(t) := \mathbb{P}_\varepsilon\left[\frac{\mu_\delta(\varepsilon)}{\mu_\varepsilon(\varepsilon)} \leq t\right]$ and its inverse as $\zeta^{-1}(p) := \inf\{t \mid \zeta(t) \geq p\}$. Then, for any $p \in [0, 1]$

$$\mathbb{P}_\varepsilon\left[\underline{S}_{\zeta^{-1}(p)}\right] \leq p. \quad (49)$$

Proof of Lemma 7. For $p \in [0, 1]$ let $t_p := \zeta^{-1}(p)$. For $n \in \mathbb{N}$ define the sets $A_n := \left\{ z \in \mathcal{Z} \mid \frac{\mu_\delta(z)}{\mu_\varepsilon(z)} \leq t_p - \frac{1}{n} \right\}$. Note that $A_n \subseteq A_{n+1}$ since for any $z \in A_n$ we have

$$\frac{\mu_\delta(z)}{\mu_\varepsilon(z)} \leq t_p - \frac{1}{n} = t_p - \frac{1}{n+1} \frac{n+1}{n} \leq t_p - \frac{1}{n+1}. \quad (50)$$

Let $A := \cup_{n=1}^{\infty} A_n$ and note that $A = \underline{S}_{t_p}$. Indeed, if $z \in A$, $\exists n$ such that $\frac{\mu_{\delta}(z)}{\mu_{\varepsilon}(z)} \leq t_p - \frac{1}{n} < t_p$ and hence $z \in \underline{S}_{t_p}$. If, on the other hand, $z \in \underline{S}_{t_p}$, then $\exists n$ such that $\frac{\mu_{\delta}(z)}{\mu_{\varepsilon}(z)} \leq t_p - \frac{1}{n}$ and hence $z \in A_n$. Note that for any n , $t_p - \frac{1}{n} < t_p = \inf\{t \mid \zeta(t) \geq p\}$ and hence

$$\mathbb{P}_{\varepsilon}[A_n] = \zeta\left(t_p - \frac{1}{n}\right) \leq p. \quad (51)$$

Finally,

$$\mathbb{P}_{\varepsilon}\left[\underline{S}_{\zeta^{-1}(p)}\right] = \mathbb{P}_{\varepsilon}\left[\bigcup_{n=1}^{\infty} A_n\right] = \lim_{n \rightarrow \infty} \mathbb{P}_{\varepsilon}[A_n] \leq p \quad (52)$$

concluding the proof. \square

Proof of Theorem 1. Let $t_A := \zeta^{-1}(p_A)$, $t_B := \zeta^{-1}(1 - p_B)$. For ease of notation let $\underline{S}_A := \underline{S}_{t_A}$, $\underline{S}_B := \underline{S}_{t_B}$, $\overline{S}_A := \overline{S}_{t_A}$ and $\overline{S}_B := \overline{S}_{t_B}$. Note that by Lemma 6, ζ is right-continuous and hence for any $p \in [0, 1]$ we have $\zeta(\zeta^{-1}(p)) \geq p$. In particular, $\mathbb{P}_{\varepsilon}[\overline{S}_A] = \zeta(\zeta^{-1}(p_A)) \geq p_A$ and $\mathbb{P}_{\varepsilon}[\overline{S}_B] = \zeta(\zeta^{-1}(1 - p_B)) \geq 1 - p_B$. Let

$$\mathcal{S}_A := \{S \subseteq \mathcal{Z} \mid \underline{S}_A \subseteq S \subseteq \overline{S}_A \wedge \mathbb{P}_{\varepsilon}[S] \leq p_A\} = \mathcal{S}_{t_A, p_A}, \quad (53)$$

$$\mathcal{S}_B := \{S \subseteq \mathcal{Z} \mid \underline{S}_B \subseteq S \subseteq \overline{S}_B \wedge \mathbb{P}_{\varepsilon}[S] \leq 1 - p_B\} = \mathcal{S}_{t_B, 1 - p_B}. \quad (54)$$

Note that by Lemma 7, $\mathbb{P}_{\varepsilon}[\underline{S}_A] \leq p_A$ and $\mathbb{P}_{\varepsilon}[\underline{S}_B] \leq 1 - p_B$. Hence $\mathcal{S}_A \neq \emptyset$ and $\mathcal{S}_B \neq \emptyset$. Let $S_A \in \mathcal{S}_A$ and $S_B \in \mathcal{S}_B$ arbitrary. Then, since by assumption g_h^{ε} is (p_A, p_B) -confident, for any $c \neq c_A$

$$\mathbb{E}_{\varepsilon}[h(\phi(x_0, \varepsilon))_{c_A}] = g_h^{\varepsilon}(x_0)_{c_A} \geq p_A \geq \mathbb{P}_{\varepsilon}[S_A], \quad (55)$$

$$\mathbb{E}_{\varepsilon}[h(\phi(x_0, \varepsilon))_c] = g_h^{\varepsilon}(x_0)_c \leq p_B \leq 1 - \mathbb{P}_{\varepsilon}[S_B] = \mathbb{P}_{\varepsilon}[S_B^c] \quad (56)$$

Note that $\underline{S}_A \subseteq S_A \subseteq \overline{S}_A$. We can thus apply part 1 of Lemma 5 to $f = h(\phi(x_0, \cdot))_{c_A}$ and $M = 1$ and obtain

$$g_h^{\delta}(x_0)_{c_A} = \mathbb{E}_{\delta}[h(\phi(x_0, \delta))_{c_A}] \geq \mathbb{P}_{\delta}[S_A]. \quad (57)$$

Similarly, $\overline{S}_B^c \subseteq S_B^c \subseteq \underline{S}_B^c$ and applying part 2 of Lemma 5 to $f = h(\phi(x_0, \cdot))_c$ and $M = 1$ yields

$$g_h^{\delta}(x_0)_c = \mathbb{E}_{\delta}[h(\phi(x_0, \delta))_c] \leq \mathbb{P}_{\delta}[S_B^c] = 1 - \mathbb{P}_{\delta}[S_B]. \quad (58)$$

Since the choice of S_A and S_B was arbitrary, we get

$$g_h^{\delta}(x_0)_{c_A} \geq \sup_{S \in \mathcal{S}_A} \mathbb{P}_{\delta}[S] = \xi(t_A, p_A), \quad (59)$$

$$g_h^{\delta}(x_0)_c \leq \inf_{S \in \mathcal{S}_B} \mathbb{P}_{\delta}[S^c] = 1 - \sup_{S \in \mathcal{S}_B} \mathbb{P}_{\delta}[S] = 1 - \xi(t_B, 1 - p_B). \quad (60)$$

Since the above inequalities hold for all $c \neq c_A$, we find $g_h^{\delta}(x_0)_{c_A} > \max_{c \neq c_A} g_h^{\delta}(x_0)_c$ if

$$1 - \xi(t_B, 1 - p_B) < \xi(t_A, p_A) \quad (61)$$

which proves the Theorem. \square

A.1 Resolvable Transforms

The following connects the robustness over δ with robustness over parameters α for transformations that are *resolvable* (which applies to all transformations we consider in this paper.)

Definition 5 (Resolvable Transforms). Suppose $\mathcal{Z} \subseteq \mathbb{R}^m$. We call a transform $\phi: \mathcal{X} \times \mathcal{Z} \rightarrow \mathcal{X}$ resolvable, if for any $\alpha \in \mathcal{Z}$, there exists a function $\psi_\alpha: \mathcal{Z} \rightarrow \mathcal{Z}$ which is *injective, continuously differentiable, has non-vanishing Jacobian*, and

$$\phi(\phi(x, \alpha), \beta) = \phi(x, \psi_\alpha(\beta)) \quad \forall x, \beta \quad (62)$$

We notice that if a transformation is resolvable, then

$$\mathbb{E}_\varepsilon[h(\phi(\phi(x, \alpha), \varepsilon))] = \mathbb{E}_\varepsilon[h(\phi(x, \psi_\alpha(\varepsilon)))] \quad (63)$$

We can directly apply Theorem 1 to distributions δ of the form $\psi_\alpha(\varepsilon)$ and reason about the attacker parameter α . The next Lemma justifies this approach.

Lemma 8. Suppose that $\mathcal{Z} \subseteq \mathbb{R}^m$ and let $\phi: \mathcal{X} \times \mathcal{Z} \rightarrow \mathcal{X}$ be a resolvable transform. Denote by Δ the family of probability distributions such that (43) holds with respect to ϕ . Then, the random variable $\delta := \psi_\alpha(\varepsilon)$ admits a density with respect to Lebesgue measure and there exists a subset $A \subseteq \mathcal{Z}$ such that

$$\forall \alpha \in A: \psi_\alpha(\varepsilon) \in \Delta. \quad (64)$$

The above Lemma draws a connection between the abstract notion of probability distributions satisfying (43) and robustness over parameters. In other words, it states that if a transformation is resolvable, we can find a subset $A \subseteq \mathcal{Z}$ such that the random variable $\delta := \psi_\alpha(\varepsilon)$ satisfies (43) for any $\alpha \in A$. In this case, since δ is parameterized by α , Theorem 1 gives us a condition on $\alpha \in \mathcal{Z}$ such that

$$g_h^\varepsilon(\phi(x_0, \alpha)) \quad (65)$$

makes the same prediction as $g_h^\varepsilon(x_0)$. We notice that this does not yet provide us with an explicit condition on parameters α . However, for the transforms considered in this paper, ψ_α has a convenient form which lets us solve (43) directly for α .

Proof of Lemma 8. Since ϕ is a resolvable transform, we know that $\forall \alpha \in \mathcal{Z}, \exists \psi_\alpha: \mathcal{Z} \rightarrow \mathcal{Z}$ such that for any $x \in \mathcal{X}, \beta \in \mathcal{Z}$

$$\phi(\phi(x, \alpha), \beta) = \phi(x, \psi_\alpha(\beta)). \quad (66)$$

Consider the random variable $\delta := \psi_\alpha(\varepsilon)$ and recall that ψ_α is injective, continuously differentiable and has non-vanishing Jacobian for each α . We can thus apply Jacobi's Transformation Formula (Jacod & Protter, 2000) to obtain a density for δ with respect to Lebesgue measure:

$$\mu_\delta(z) = \begin{cases} \mu_\varepsilon(\psi_\alpha^{-1}(z)) \cdot |\det(J_{\psi_\alpha^{-1}(z)})| & z \in \text{Im}(\psi_\alpha) \\ 0 & \text{otherwise.} \end{cases} \quad (67)$$

Consider the set $A := \{\alpha \in \mathcal{Z} \mid \psi_\alpha(\varepsilon) \in \Delta\}$ which is well-defined since $\psi_\alpha(\varepsilon)$ admits a density. This concludes the proof. \square

Remark 1. Note that if the transform $\phi: \mathcal{X} \times \mathcal{Z} \rightarrow \mathcal{X}$ satisfies $\phi(x, 0) = x$ and $p_B < p_A$, then $\{\varepsilon\} \subseteq A$ in which case A is non-empty.

B Derivations of robustness bounds

In this section we explicitly derive robustness bounds for a collection of specific noise distributions. Throughout this section suppose that $\phi: \mathcal{X} \times \mathcal{Z} \rightarrow \mathcal{X}$ is a resolvable transform, $h: \mathcal{X} \rightarrow \mathcal{S}_C$ is a base classifier, $x_0 \in \mathcal{X}$ and $c_A \in \mathcal{Y}$ such that g_h^ε is (p_A, p_B) -confident at x_0 . We first prove a corollary that simplifies our main result for noise distributions ε and δ such that the differences $\partial_t := \overline{S}_t \setminus \underline{S}_t$ of the associated level sets have zero probability mass under both \mathbb{P}_ε and \mathbb{P}_δ . One example for noise distributions that satisfy this property are Gaussian random variables.

Corollary 7. *Suppose that the sets $\partial_t := \overline{S}_t \setminus \underline{S}_t$ satisfy $\mathbb{P}_\varepsilon[\partial_t] = \mathbb{P}_\delta[\partial_t] = 0$ for $t \geq 0$. Then for $p \in [0, 1]$*

$$\xi(\zeta^{-1}(p), p) = \mathbb{P}_\delta \left[\underline{S}_{\zeta^{-1}(p)} \right] = \mathbb{P}_\delta \left[\overline{S}_{\zeta^{-1}(p)} \right]. \quad (68)$$

In particular, condition (43) reduces to

$$1 - \mathbb{P}_\delta \left[\overline{S}_{\zeta^{-1}(1-p_B)} \right] < \mathbb{P}_\delta \left[\overline{S}_{\zeta^{-1}(p_A)} \right]. \quad (69)$$

Proof. Let $p \in [0, 1]$ and set $t := \zeta^{-1}(p)$. Note that for any S such that $\underline{S}_t \subseteq S \subseteq \overline{S}_t$ and $\eta \in \{\varepsilon, \delta\}$, we have

$$\mathbb{P}_\eta[\underline{S}_t] \leq \mathbb{P}_\eta[S] \leq \mathbb{P}_\eta[\overline{S}_t]. \quad (70)$$

Furthermore, $0 = \mathbb{P}_\eta[\partial_t] = \mathbb{P}_\eta[\overline{S}_t] - \mathbb{P}_\eta[\underline{S}_t]$ and Lemma 7 imply that

$$\mathbb{P}_\eta[\underline{S}_t] = \mathbb{P}_\eta[S] = \mathbb{P}_\eta[\overline{S}_t] \text{ and } \mathbb{P}_\varepsilon[\underline{S}_t] = p \quad (71)$$

Hence

$$S_{t,p} = \{S \subseteq \mathcal{Z} \mid \underline{S}_t \subseteq S \subseteq \overline{S}_t \wedge \mathbb{P}_\varepsilon[\varepsilon \in S] \leq p\} = \{S \subseteq \mathcal{Z} \mid \underline{S}_t \subseteq S \subseteq \overline{S}_t\} \quad (72)$$

and together with (71)

$$\xi(\zeta^{-1}(p), p) = \sup\{\mathbb{P}_\delta[S] \mid \underline{S}_{\zeta^{-1}(p)} \subseteq S \subseteq \overline{S}_{\zeta^{-1}(p)}\} = \mathbb{P}_\delta[\underline{S}_{\zeta^{-1}(p)}] = \mathbb{P}_\delta[\overline{S}_{\zeta^{-1}(p)}] \quad (73)$$

completing the proof. \square

Corollary 1 (restated). *Suppose $\mathcal{Z} = \mathbb{R}^m$, $\Sigma := \text{diag}(\sigma_1^2, \dots, \sigma_m^2)$ and $\varepsilon \sim \mathcal{N}(0, \Sigma)$ and $\delta := \alpha + \varepsilon$ for some $\alpha \in \mathbb{R}^m$. Then, we have $g_h^\delta(x_0)_{c_A} > \max_{c \neq c_A} g_h^\delta(x_0)_c$ if α satisfies*

$$\sqrt{\sum_{i=1}^m \left(\frac{\alpha_i}{\sigma_i} \right)^2} < \frac{1}{2} (\Phi^{-1}(p_A) - \Phi^{-1}(p_B)). \quad (74)$$

Proof. By Theorem 1 we know that $g_h^\delta(x_0)_{c_A} > \max_{c \neq c_A} g_h^\delta(x_0)_c$ if δ satisfies

$$1 - \xi(\zeta^{-1}(1-p_B), 1-p_B) < \xi(\zeta^{-1}(p_A), p_A). \quad (75)$$

The proof is thus complete if we show that (75) reduces to (74). For that purpose let $A := \Sigma^{-1}$ and note that the bilinear form $(z_1, z_2) \mapsto z_1^T A z_2 =: \langle z_1, z_2 \rangle_A$ defines an inner product on \mathbb{R}^m . Let $z \in \mathbb{R}^m$ and consider

$$\frac{\mu_\delta(z)}{\mu_\varepsilon(z)} = \frac{\exp\left(-\frac{1}{2}\langle z - \alpha, z - \alpha \rangle_A\right)}{\exp\left(-\frac{1}{2}\langle z, z \rangle_A\right)} = \exp\left(\langle z, \alpha \rangle_A - \frac{1}{2}\langle \alpha, \alpha \rangle_A\right). \quad (76)$$

and thus

$$\frac{\mu_\delta(z)}{\mu_\varepsilon(z)} \leq t \iff \langle z, \alpha \rangle_A \leq \log(t) + \frac{1}{2}\langle \alpha, \alpha \rangle_A. \quad (77)$$

Let $Z \sim \mathcal{N}(0, 1)$ and notice that $\frac{\langle \varepsilon, \alpha \rangle_A}{\sqrt{\langle \alpha, \alpha \rangle_A}} \stackrel{d}{=} Z \stackrel{d}{=} \frac{\langle \delta, \alpha \rangle_A - \langle \alpha, \alpha \rangle_A}{\sqrt{\langle \alpha, \alpha \rangle_A}}$. We can write $\partial_t := \bar{S}_t \setminus \underline{S}_t = \{z \in \mathbb{R}^m \mid \frac{\mu_\delta(z)}{\mu_\varepsilon(z)} = t\}$ and hence

$$\mathbb{P}_\varepsilon[\partial_t] = \mathbb{P}_Z \left[Z = \frac{\log(t) + \frac{1}{2} \langle \alpha, \alpha \rangle_A}{\sqrt{\langle \alpha, \alpha \rangle_A}} \right] = 0 = \mathbb{P}_Z \left[Z = \frac{\log(t) - \frac{1}{2} \langle \alpha, \alpha \rangle_A}{\sqrt{\langle \alpha, \alpha \rangle_A}} \right] = \mathbb{P}_\delta[\partial_t]. \quad (78)$$

We can thus apply Corollary 7 and solve

$$1 - \mathbb{P}_\delta[\bar{S}_{\zeta^{-1}(1-p_B)}] < \mathbb{P}_\delta[\bar{S}_{\zeta^{-1}(p_A)}]. \quad (79)$$

for α . We compute ζ as

$$\zeta(t) = \mathbb{P}_\varepsilon \left[\frac{\mu_\delta(\varepsilon)}{\mu_\varepsilon(\varepsilon)} \leq t \right] = \mathbb{P}_\varepsilon \left[\langle \varepsilon, \alpha \rangle_A \leq \log(t) + \frac{1}{2} \langle \alpha, \alpha \rangle_A \right] = \Phi \left(\frac{\log(t) + \frac{1}{2} \langle \alpha, \alpha \rangle_A}{\sqrt{\langle \alpha, \alpha \rangle_A}} \right) \quad (80)$$

and for $p \in [0, 1]$ its inverse

$$p = \zeta(t) \iff \Phi^{-1}(p) \sqrt{\langle \alpha, \alpha \rangle_A} = \log(t) + \frac{1}{2} \langle \alpha, \alpha \rangle_A \iff \zeta^{-1}(t) = \exp \left(\Phi^{-1}(p) \sqrt{\langle \alpha, \alpha \rangle_A} - \frac{1}{2} \langle \alpha, \alpha \rangle_A \right). \quad (81)$$

Thus

$$\begin{aligned} \mathbb{P}_\delta \left[\frac{\mu_\delta(\delta)}{\mu_\varepsilon(\delta)} \leq \zeta^{-1}(p) \right] &= \mathbb{P}_\delta \left[\frac{\langle \delta, \alpha \rangle_A - \langle \alpha, \alpha \rangle_A}{\sqrt{\langle \alpha, \alpha \rangle_A}} \leq \frac{\log(\zeta^{-1}(p)) - \frac{1}{2} \langle \alpha, \alpha \rangle_A}{\sqrt{\langle \alpha, \alpha \rangle_A}} \right] \quad (82) \\ &= \Phi \left(\frac{\left(\Phi^{-1}(p) \sqrt{\langle \alpha, \alpha \rangle_A} - \frac{1}{2} \langle \alpha, \alpha \rangle_A \right) - \frac{1}{2} \langle \alpha, \alpha \rangle_A}{\sqrt{\langle \alpha, \alpha \rangle_A}} \right) = \Phi \left(\Phi^{-1}(p) - \sqrt{\langle \alpha, \alpha \rangle_A} \right). \quad (83) \end{aligned}$$

Finally, (75) reduces to

$$1 - \Phi \left(\Phi^{-1}(1-p_B) - \sqrt{\langle \alpha, \alpha \rangle_A} \right) < \Phi \left(\Phi^{-1}(p_A) - \sqrt{\langle \alpha, \alpha \rangle_A} \right) \quad (84)$$

$$\iff \Phi \left(\sqrt{\langle \alpha, \alpha \rangle_A} + \Phi^{-1}(p_B) \right) < \Phi \left(\Phi^{-1}(p_A) - \sqrt{\langle \alpha, \alpha \rangle_A} \right) \quad (85)$$

$$\iff \sqrt{\langle \alpha, \alpha \rangle_A} + \Phi^{-1}(p_B) < \Phi^{-1}(p_A) - \sqrt{\langle \alpha, \alpha \rangle_A} \quad (86)$$

$$\iff \sqrt{\sum_{i=1}^m \left(\frac{\alpha_i}{\sigma_i} \right)^2} < \frac{1}{2} (\Phi^{-1}(p_A) - \Phi^{-1}(p_B)) \quad (87)$$

concluding the proof. \square

Corollary 2 (restated). *Suppose $\mathcal{Z} = \mathbb{R}_{\geq 0}^m$, fix some $\lambda > 0$ and let $\varepsilon_i \sim \text{Exp}(1/\lambda)$ be independent and identically distributed. Let $\varepsilon := (\varepsilon_1, \dots, \varepsilon_m)^T$ and $\delta := \alpha + \varepsilon$ for some $\alpha \in \mathbb{R}_{\geq 0}^m$. Then, we have $g_h^\delta(x_0)_{c_A} > \max_{c \neq c_A} g_h^\delta(x_0)_c$ whenever α satisfies*

$$\|\alpha\|_1 < -\frac{\log(1-p_A+p_B)}{\lambda}. \quad (88)$$

Proof. By Theorem 1 we know that $g_h^\delta(x_0)_{c_A} > \max_{c \neq c_A} g_h^\delta(x_0)_c$ if δ satisfies

$$1 - \xi(\zeta^{-1}(1-p_B), 1-p_B) < \xi(\zeta^{-1}(p_A), p_A). \quad (89)$$

The proof is thus complete if we show that (89) reduces to (88). For that purpose, consider

$$\mu_\varepsilon(z) = \begin{cases} \lambda \cdot \exp(-\lambda \|z\|_1), & \min_i(z_i) \geq 0, \\ 0, & \text{otherwise.} \end{cases} \quad \mu_\delta(z) = \begin{cases} \lambda \cdot \exp(-\lambda \|z - \alpha\|_1), & \min_i(z_i - \alpha_i) \geq 0, \\ 0, & \text{otherwise.} \end{cases} \quad (90)$$

Note that $\forall i, z_i - \alpha_i \leq z_i$ and hence $\mu_\varepsilon(z) = 0 \Rightarrow \mu_\delta(z) = 0$. Thus

$$\frac{\mu_\delta(z)}{\mu_\varepsilon(z)} = \begin{cases} \exp(\lambda \cdot \|\alpha\|_1) & \min_i(z_i - \alpha_i) \geq 0, \\ 0, & \text{otherwise.} \end{cases} \quad (91)$$

Let $S_0 := \{z \in \mathbb{R}_{\geq 0}^m \mid \min_i(z_i - \alpha_i) < 0\}$ and note that

$$\mathbb{P}_\varepsilon[S_0] = \mathbb{P}_\varepsilon\left[\bigcup_{i=1}^m \{\varepsilon_i < \alpha_i\}\right] = 1 - \mathbb{P}_\varepsilon\left[\bigcap_{i=1}^m \{\varepsilon_i \geq \alpha_i\}\right] = 1 - \prod_{i=1}^m \mathbb{P}_{\varepsilon_i}[\varepsilon_i \geq \alpha_i] \quad (92)$$

$$= 1 - \prod_{i=1}^m (1 - (1 - \exp(-\lambda \alpha_i))) = 1 - \exp(-\lambda \|\alpha\|_1). \quad (93)$$

Let $t_\alpha := \exp(\lambda \|\alpha\|_1)$ and compute ζ as

$$\zeta(t) = \mathbb{P}_\varepsilon\left[\frac{\mu_\delta(\varepsilon)}{\mu_\varepsilon(\varepsilon)} \leq t\right] = \mathbb{P}_\varepsilon\left[\mathbb{1}\{\min_i(\varepsilon_i - \alpha_i) \geq 0\} \leq t \cdot \exp(-\lambda \|\alpha\|_1)\right] = \begin{cases} 1 - \exp(-\lambda \|\alpha\|_1) & t < t_\alpha, \\ 1 & t \geq t_\alpha. \end{cases} \quad (94)$$

Recall that $\zeta^{-1}(p) := \inf\{t \mid \zeta(t) \geq p\}$ for $p \in [0, 1]$ and hence

$$\zeta^{-1}(p) = \begin{cases} 0 & p \leq 1 - \exp(-\lambda \|\alpha\|_1), \\ \exp(\lambda \|\alpha\|_1) & p > 1 - \exp(-\lambda \|\alpha\|_1). \end{cases} \quad (95)$$

In order to evaluate ξ we compute the lower and strict lower level sets at $t = \zeta^{-1}(p)$. Recall that $\underline{S}_t = \{z \in \mathbb{R}_{\geq 0}^m \mid \frac{\mu_\delta(z)}{\mu_\varepsilon(z)} < t\}$ and $\overline{S}_t = \{z \in \mathbb{R}_{\geq 0}^m \mid \frac{\mu_\delta(z)}{\mu_\varepsilon(z)} \leq t\}$ and consider

$$\underline{S}_{\zeta^{-1}(p)} = (S_0^c \cap \{z \in \mathbb{R}_{\geq 0}^m \mid \exp(\lambda \|\alpha\|_1) < \zeta^{-1}(p)\}) \cup (S_0 \cap \{z \in \mathbb{R}_{\geq 0}^m \mid 0 < \zeta^{-1}(p)\}) \quad (96)$$

$$= \begin{cases} \emptyset & p \leq 1 - \exp(-\lambda \|\alpha\|_1), \\ S_0 & p > 1 - \exp(-\lambda \|\alpha\|_1) \end{cases} \quad (97)$$

and

$$\overline{S}_{\zeta^{-1}(p)} = (S_0^c \cap \{z \in \mathbb{R}_{\geq 0}^m \mid \exp(\lambda \|\alpha\|_1) \leq \zeta^{-1}(p)\}) \cup (S_0 \cap \{z \in \mathbb{R}_{\geq 0}^m \mid 0 \leq \zeta^{-1}(p)\}) \quad (98)$$

$$= \begin{cases} S_0 & p \leq 1 - \exp(-\lambda \|\alpha\|_1), \\ \mathbb{R}_{\geq 0}^m & p > 1 - \exp(-\lambda \|\alpha\|_1). \end{cases} \quad (99)$$

Suppose $p \leq 1 - \exp(-\lambda \|\alpha\|_1)$. Then $\underline{S}_{\zeta^{-1}(p)} = \emptyset$ and $\overline{S}_{\zeta^{-1}(p)} = S_0$ and hence

$$p \leq 1 - \exp(-\lambda \|\alpha\|_1) \Rightarrow \xi(\zeta^{-1}(p), p) = \sup\{\mathbb{P}_\delta[S] \mid S \subseteq S_0 \wedge \mathbb{P}_\varepsilon[S] \leq p\} = 0. \quad (100)$$

Condition (89) can thus only be satisfied, if $p_A > 1 - \exp(-\lambda \|\alpha\|_1)$ and $1 - p_B > 1 - \exp(-\lambda \|\alpha\|_1)$. In this case $\underline{S}_{\zeta^{-1}(p)} = S_0$ and $\overline{S}_{\zeta^{-1}(p)} = \mathbb{R}_{\geq 0}^m$. For $p \in [0, 1]$ let $\mathcal{S}_p = \{S \subseteq \mathbb{R}_{\geq 0}^m \mid S_0 \subseteq S \subseteq \mathbb{R}_{\geq 0}^m \wedge \mathbb{P}_\varepsilon[S] \leq p\}$. Then

$$p > 1 - \exp(-\lambda \|\alpha\|_1) \Rightarrow \xi(\zeta^{-1}(p), p) = \sup_{S \in \mathcal{S}_p} \mathbb{P}_\delta[S]. \quad (101)$$

We can write any $S \in \mathcal{S}_p$ as the disjoint union $S = S_0 \dot{\cup} S_1$ for some $S_1 \subseteq \mathbb{R}_{\geq 0}^m$ such that $\mathbb{P}_\varepsilon[S_0 \dot{\cup} S_1] \leq p$. Note that $\mathbb{P}_\delta[S_0] = 0$ and since $S_0 \cap S_1 = \emptyset$ any $z \in S_1$ satisfies $0 \leq \min_i (z_i - \alpha_i) \leq \min_i z_i$ and hence $\frac{\mu_\delta(z)}{\mu_\varepsilon(z)} = \exp(\lambda \|\alpha\|_1)$. Thus

$$\mathbb{P}_\delta[S] = \mathbb{P}_\delta[S_1] = \int_{S_1} \mu_\delta(z) dz = \int_{S_1} \exp(\lambda \|\alpha\|_1) \mu_\varepsilon(z) dz = \exp(\lambda \|\alpha\|_1) \cdot \mathbb{P}_\varepsilon[S_1]. \quad (102)$$

Thus, The supremum of the left hand side over all $S \in \mathcal{S}_p$ equals the supremum of the right hand side over all $S_1 \in \{S' \subseteq S_0^c \mid \mathbb{P}_\varepsilon[S'] \leq 1 - \mathbb{P}_\varepsilon[S_0]\}$

$$\sup_{S \in \mathcal{S}_p} \mathbb{P}_\delta[S] = \exp(\lambda \|\alpha\|_1) \cdot \sup \{\mathbb{P}_\delta[S'] \mid S' \subseteq S_0^c \wedge \mathbb{P}_\varepsilon[S'] \leq 1 - \mathbb{P}_\varepsilon[S_0]\} \quad (103)$$

$$= \exp(\lambda \|\alpha\|_1) \cdot (p - \mathbb{P}_\varepsilon[S_0]). \quad (104)$$

Computing ξ at $(\zeta^{-1}(p_A), p_A)$ yields

$$\xi(\zeta^{-1}(p_A), p_A) = \sup_{S \in \mathcal{S}_{p_A}} \mathbb{P}_\delta[S] = \exp(\lambda \|\alpha\|_1) \cdot (p_A - \mathbb{P}_\varepsilon[S_0]) \quad (105)$$

$$\stackrel{(93)}{=} \exp(\lambda \|\alpha\|_1) \cdot (p_A - (1 - \exp(-\lambda \|\alpha\|_1))) = \exp(\lambda \|\alpha\|_1) \cdot (p_A + \exp(-\lambda \|\alpha\|_1) - 1) \quad (106)$$

and at $(\zeta^{-1}(1 - p_B), 1 - p_B)$ as

$$\xi(\zeta^{-1}(1 - p_B), 1 - p_B) = \sup_{S \in \mathcal{S}_{1-p_B}} \mathbb{P}_\delta[S] = \exp(\lambda \|\alpha\|_1) \cdot (1 - p_B - \mathbb{P}_\varepsilon[S_0]) \quad (107)$$

$$\stackrel{(93)}{=} \exp(\lambda \|\alpha\|_1) \cdot (1 - p_B - (1 - \exp(-\lambda \|\alpha\|_1))) = \exp(\lambda \|\alpha\|_1) \cdot (-p_B + \exp(-\lambda \|\alpha\|_1)). \quad (108)$$

Finally, condition (89) is satisfied whenever α satisfies

$$1 - \exp(\lambda \|\alpha\|_1) \cdot (-p_B + \exp(-\lambda \|\alpha\|_1)) < \exp(\lambda \|\alpha\|_1) \cdot (p_A + \exp(-\lambda \|\alpha\|_1) - 1) \quad (109)$$

$$\iff \exp(-\lambda \|\alpha\|_1) + p_B - \exp(-\lambda \|\alpha\|_1) < p_A + \exp(-\lambda \|\alpha\|_1) - 1 \quad (110)$$

$$\iff 1 - p_A + p_B < \exp(-\lambda \|\alpha\|_1) \quad (111)$$

$$\iff \|\alpha\|_1 < -\frac{\log(1 - p_A + p_B)}{\lambda} \quad (112)$$

completing the proof. \square

Corollary 3 (restated). *Suppose $\mathcal{Z} = \mathbb{R}^m$, and $\varepsilon \sim \mathcal{U}([a, b]^m)$ for some $a < b$. Set $\delta := \alpha + \varepsilon$ for $\alpha \in \mathbb{R}^m$. Then $g_h^\delta(x_0)_{c_A} > \max_{c \neq c_A} g_h^\delta(x_0)_c$ if α satisfies*

$$1 - \left(\frac{p_A - p_B}{2}\right) < \prod_{i=1}^m \left(1 - \frac{|\alpha_i|}{b - a}\right)_+ \quad (113)$$

where $(x)_+ := \max\{x, 0\}$.

Proof. By Theorem 1 we know that $g_h^\delta(x_0)_{c_A} > \max_{c \neq c_A} g_h^\delta(x_0)_c$ if δ satisfies

$$1 - \xi(\zeta^{-1}(1 - p_B), 1 - p_B) < \xi(\zeta^{-1}(p_A), p_A). \quad (114)$$

The proof is thus complete if we show that (114) reduces to (113). For that purpose, let $I_\varepsilon = [a, b]^m$ and $I_\delta := \prod_{i=1}^m [a + \alpha_i, b + \alpha_i]$ and consider

$$\mu_\varepsilon(z) = \begin{cases} (b - a)^{-m} & z \in I_\varepsilon, \\ 0 & \text{otherwise} \end{cases} \quad \mu_\delta(z) = \begin{cases} (b - a)^{-m} & z \in I_\delta, \\ 0 & \text{otherwise.} \end{cases} \quad (115)$$

Let $S_0 := I_\varepsilon \setminus I_\delta$. Then, for any $z \in I_\varepsilon \cup I_\delta$

$$\frac{\mu_\delta(z)}{\mu_\varepsilon(z)} = \begin{cases} 0 & z \in S_0, \\ 1 & z \in I_\varepsilon \cap I_\delta, \\ \infty & z \in I_\delta \setminus I_\varepsilon. \end{cases} \quad (116)$$

Note that

$$\mathbb{P}_\varepsilon[S_0] = 1 - \mathbb{P}_\varepsilon[I_\delta] = 1 - \prod_{i=1}^m \mathbb{P}_{\varepsilon_i}[a + \alpha_i \leq \varepsilon_i \leq b + \alpha_i] = 1 - \prod_{i=1}^m \left(1 - \frac{|\alpha_i|}{b-a}\right)_+ \quad (117)$$

where $(x)_+ = \max\{x, 0\}$. We then compute ζ for $t \geq 0$

$$\zeta(t) = \mathbb{P}_\varepsilon \left[\frac{\mu_\delta(\varepsilon)}{\mu_\varepsilon(\varepsilon)} \leq t \right] = \begin{cases} \mathbb{P}_\varepsilon[S_0] & t < 1, \\ \mathbb{P}_\varepsilon[I_\varepsilon] & t \geq 1. \end{cases} = \begin{cases} 1 - \prod_{i=1}^m \left(1 - \frac{|\alpha_i|}{b-a}\right)_+ & t < 1, \\ 1 & t \geq 1. \end{cases} \quad (118)$$

Recall that $\zeta^{-1}(p) := \inf\{t \mid \zeta(t) \geq p\}$ for $p \in [0, 1]$ and hence

$$\zeta^{-1}(p) = \begin{cases} 0 & p \leq 1 - \prod_{i=1}^m \left(1 - \frac{|\alpha_i|}{b-a}\right)_+, \\ 1 & p > 1 - \prod_{i=1}^m \left(1 - \frac{|\alpha_i|}{b-a}\right)_+. \end{cases} \quad (119)$$

In order to evaluate ξ we compute the lower and strict lower level sets at $t = \zeta^{-1}(p)$. Recall that $\underline{S}_t = \{z \in \mathbb{R}_{\geq 0}^m \mid \frac{\mu_\delta(z)}{\mu_\varepsilon(z)} < t\}$ and $\bar{S}_t = \{z \in \mathbb{R}_{\geq 0}^m \mid \frac{\mu_\delta(z)}{\mu_\varepsilon(z)} \leq t\}$ and consider

$$\underline{S}_{\zeta^{-1}(p)} = \begin{cases} \emptyset & p \leq 1 - \prod_{i=1}^m \left(1 - \frac{|\alpha_i|}{b-a}\right)_+, \\ S_0 & p > 1 - \prod_{i=1}^m \left(1 - \frac{|\alpha_i|}{b-a}\right)_+ \end{cases} \quad (120)$$

and

$$\bar{S}_{\zeta^{-1}(p)} = \begin{cases} S_0 & p \leq 1 - \prod_{i=1}^m \left(1 - \frac{|\alpha_i|}{b-a}\right)_+, \\ I_\varepsilon & p > 1 - \prod_{i=1}^m \left(1 - \frac{|\alpha_i|}{b-a}\right)_+ \end{cases} \quad (121)$$

Suppose $p \leq 1 - \prod_{i=1}^m \left(1 - \frac{|\alpha_i|}{b-a}\right)_+$. Then $\underline{S}_{\zeta^{-1}(p)} = \emptyset$ and $\bar{S}_{\zeta^{-1}(p)} = S_0$ and hence

$$p \leq 1 - \prod_{i=1}^m \left(1 - \frac{|\alpha_i|}{b-a}\right)_+ \Rightarrow \xi(\zeta^{-1}(p), p) = \sup\{\mathbb{P}_\delta[S] \mid S \subseteq S_0 \wedge \mathbb{P}_\varepsilon[S] \leq p\} = 0. \quad (122)$$

Condition (114) can thus only be satisfied, if $p_A > 1 - \prod_{i=1}^m \left(1 - \frac{|\alpha_i|}{b-a}\right)_+$ and $1 - p_B > 1 - \prod_{i=1}^m \left(1 - \frac{|\alpha_i|}{b-a}\right)_+$. In this case $\underline{S}_{\zeta^{-1}(p)} = S_0$ and $\bar{S}_{\zeta^{-1}(p)} = I_\varepsilon$. For $p \in [0, 1]$ let $\mathcal{S}_p = \{S \subseteq \mathbb{R}_{\geq 0}^m \mid S_0 \subseteq S \subseteq I_\varepsilon \wedge \mathbb{P}_\varepsilon[S] \leq p\}$. Then

$$p > 1 - \prod_{i=1}^m \left(1 - \frac{|\alpha_i|}{b-a}\right)_+ \Rightarrow \xi(\zeta^{-1}(p), p) = \sup_{S \in \mathcal{S}_p} \mathbb{P}_\delta[S]. \quad (123)$$

We can write any $S \in \mathcal{S}_p$ as the disjoint union $S = S_0 \dot{\cup} S_1$ for some $S_1 \subseteq I_\varepsilon \cap I_\delta$ such that $\mathbb{P}_\varepsilon[S_0 \dot{\cup} S_1] \leq p$. Note that $\mathbb{P}_\delta[S_0] = 0$ and for any $z \in S_1$, we have $\mu_\varepsilon(z) = \mu_\delta(z)$. Hence

$$\mathbb{P}_\delta[S] = \mathbb{P}_\delta[S_1] = \mathbb{P}_\varepsilon[S_1] \leq p - \mathbb{P}_\varepsilon[S_0] = p - \left(1 - \prod_{i=1}^m \left(1 - \frac{|\alpha_i|}{b-a}\right)_+\right) \quad (124)$$

Thus, The supremum of the left hand side over all $S \in \mathcal{S}_p$ equals the supremum of the right hand side over all $S_1 \in \{S' \subseteq I_\varepsilon \cap I_\delta \mid \mathbb{P}_\varepsilon[S'] \leq 1 - \mathbb{P}_\varepsilon[S_0]\}$

$$\sup_{S \in \mathcal{S}_p} \mathbb{P}_\delta[S] = \sup \{\mathbb{P}_\delta[S'] \mid S' \subseteq I_\varepsilon \cap I_\delta \wedge \mathbb{P}_\varepsilon[S'] \leq p - \mathbb{P}_\varepsilon[S_0]\} \quad (125)$$

$$= p - \left(1 - \prod_{i=1}^m \left(1 - \frac{|\alpha_i|}{b-a}\right)_+\right). \quad (126)$$

Hence, computing ξ at $(\zeta^{-1}(p_A), p_A)$ and $(\zeta^{-1}(1-p_B), 1-p_B)$ yields

$$\xi(\zeta^{-1}(p_A), p_A) = p_A - \left(1 - \prod_{i=1}^m \left(1 - \frac{|\alpha_i|}{b-a}\right)_+\right), \quad (127)$$

$$\xi(\zeta^{-1}(1-p_B), 1-p_B) = 1 - p_B - \left(1 - \prod_{i=1}^m \left(1 - \frac{|\alpha_i|}{b-a}\right)_+\right). \quad (128)$$

Finally, condition (114) is satisfied whenever α satisfies

$$1 - \left(1 - p_B - \left(1 - \prod_{i=1}^m \left(1 - \frac{|\alpha_i|}{b-a}\right)_+\right)\right) < p_A - \left(1 - \prod_{i=1}^m \left(1 - \frac{|\alpha_i|}{b-a}\right)_+\right) \quad (129)$$

$$\iff p_B + 1 - \prod_{i=1}^m \left(1 - \frac{|\alpha_i|}{b-a}\right)_+ < p_A - 1 + \prod_{i=1}^m \left(1 - \frac{|\alpha_i|}{b-a}\right)_+ \quad (130)$$

$$\iff 2 - p_A + p_B < 2 \cdot \prod_{i=1}^m \left(1 - \frac{|\alpha_i|}{b-a}\right)_+ \quad (131)$$

$$\iff 1 - \left(\frac{p_A - p_B}{2}\right) < \prod_{i=1}^m \left(1 - \frac{|\alpha_i|}{b-a}\right)_+ \quad (132)$$

concluding the proof. \square

Corollary 4 (restated). *Suppose $\mathcal{Z} = \mathbb{R}$ and $\varepsilon \sim \mathcal{L}(0, b)$ follows a Laplace distribution with mean 0 and scale parameter $b > 0$. Let $\delta := \alpha + \varepsilon$ for $\alpha \in \mathbb{R}$. Then $g_h^\delta(x_0)_{c_A} > \max_{c \neq c_A} g_h^\delta(x_0)_c$ if α satisfies*

$$|\alpha| < \begin{cases} -b \cdot \log(4p_B(1-p_A)) & (p_A = \frac{1}{2} \wedge p_B < \frac{1}{2}) \vee (p_A > \frac{1}{2} \wedge p_B = \frac{1}{2}) \\ -b \cdot \log(1-p_A+p_B) & p_A > \frac{1}{2} \wedge p_B < \frac{1}{2}. \end{cases} \quad (133)$$

Proof. By Theorem 1 we know that $g_h^\delta(x_0)_{c_A} > \max_{c \neq c_A} g_h^\delta(x_0)_c$ if δ satisfies

$$1 - \xi(\zeta^{-1}(1-p_B), 1-p_B) < \xi(\zeta^{-1}(p_A), p_A). \quad (134)$$

The proof is thus complete if we show that (134) reduces to (133). For that purpose, consider

$$\mu_\varepsilon(z) = \frac{1}{2b} \exp\left(-\frac{|z|}{b}\right), \quad \mu_\delta(z) = \frac{1}{2b} \exp\left(-\frac{|z-\alpha|}{b}\right). \quad (135)$$

Due to symmetry, assume without loss of generality that $\alpha \geq 0$. Then for $z \in \mathbb{R}$

$$\frac{\mu_\delta(z)}{\mu_\varepsilon(z)} = \exp\left(-\frac{|z-\alpha|-|z|}{b}\right) = \begin{cases} \exp\left(-\frac{\alpha}{b}\right) & z < 0, \\ \exp\left(\frac{2z-\alpha}{b}\right) & 0 \leq z < \alpha, \\ \exp\left(\frac{\alpha}{b}\right) & z \geq \alpha. \end{cases} \quad (136)$$

Note that the CDFs for ε and δ are given by

$$F_\varepsilon(z) = \begin{cases} \frac{1}{2} \exp\left(\frac{z}{b}\right) & z \leq 0, \\ 1 - \frac{1}{2} \exp\left(-\frac{z}{b}\right) & z > 0, \end{cases} \quad F_\delta(z) = \begin{cases} \frac{1}{2} \exp\left(\frac{z-\alpha}{b}\right) & z \leq \alpha, \\ 1 - \frac{1}{2} \exp\left(-\frac{z-\alpha}{b}\right) & z > \alpha. \end{cases} \quad (137)$$

Note that for $\exp\left(-\frac{\alpha}{b}\right) \leq t < \exp\left(\frac{\alpha}{b}\right)$ we have

$$\mathbb{P}_\varepsilon \left[\exp\left(\frac{2\varepsilon - \alpha}{b}\right) \leq t \wedge 0 \leq \varepsilon < \alpha \right] = \mathbb{P}_\varepsilon \left[\exp\left(-\frac{\alpha}{b}\right) \leq \exp\left(\frac{2\varepsilon - \alpha}{b}\right) \leq t \right] \quad (138)$$

$$= \mathbb{P}_\varepsilon \left[0 \leq \varepsilon \leq \frac{b \log(t) + \alpha}{2} \right] = F_\varepsilon\left(\frac{b \log(t) + \alpha}{2}\right) - F_\varepsilon(0) \quad (139)$$

$$= \frac{1}{2} - \frac{1}{2} \exp\left(-\frac{1}{b} \left(\frac{b \log(t) + \alpha}{2}\right)\right) = \frac{1}{2} - \frac{1}{2\sqrt{t}} \exp\left(-\frac{\alpha}{2b}\right). \quad (140)$$

Computing ζ yields

$$\zeta(t) = \mathbb{P}_\varepsilon \left[\frac{\mu_\delta(\varepsilon)}{\mu_\varepsilon(\varepsilon)} \leq t \right] \quad (141)$$

$$= \mathbb{P}_\varepsilon \left[\exp\left(-\frac{\alpha}{b}\right) \leq t \wedge \varepsilon < 0 \right] + \mathbb{P}_\varepsilon \left[\exp\left(\frac{\alpha}{b}\right) \leq t \wedge \varepsilon \geq \alpha \right] + \mathbb{P}_\varepsilon \left[\exp\left(\frac{2\varepsilon - \alpha}{b}\right) \leq t \wedge 0 \leq \varepsilon < \alpha \right] \quad (142)$$

$$= \begin{cases} 0 & t < \exp\left(-\frac{\alpha}{b}\right), \\ 1 - \frac{1}{2\sqrt{t}} \exp\left(-\frac{\alpha}{2b}\right) & \exp\left(-\frac{\alpha}{b}\right) \leq t < \exp\left(\frac{\alpha}{b}\right), \\ 1 & t \geq \exp\left(\frac{\alpha}{b}\right). \end{cases} \quad (143)$$

The inverse is then given by

$$\zeta^{-1}(p) = \begin{cases} 0 & p < \frac{1}{2}, \\ \frac{1}{4(1-p)^2} \exp\left(-\frac{\alpha}{b}\right) & \frac{1}{2} \leq p < 1 - \frac{1}{2} \exp\left(-\frac{\alpha}{b}\right), \\ \exp\left(\frac{\alpha}{b}\right) & p \geq 1 - \frac{1}{2} \exp\left(-\frac{\alpha}{b}\right). \end{cases} \quad (144)$$

In order to evaluate ξ we compute the lower and strict lower level sets at $t = \zeta^{-1}(p)$. Recall that $\underline{S}_t = \{z \in \mathbb{R} \mid \frac{\mu_\delta(z)}{\mu_\varepsilon(z)} < t\}$ and $\overline{S}_t = \{z \in \mathbb{R} \mid \frac{\mu_\delta(z)}{\mu_\varepsilon(z)} \leq t\}$ and consider

$$\underline{S}_{\zeta^{-1}(p)} = \begin{cases} \emptyset & p \leq \frac{1}{2}, \\ \left(-\infty, b \cdot \log\left(\frac{1}{2(1-p)}\right)\right) & \frac{1}{2} < p < 1 - \frac{1}{2} \exp\left(-\frac{\alpha}{b}\right), \\ \left(-\infty, \alpha\right], & p \geq 1 - \frac{1}{2} \exp\left(-\frac{\alpha}{b}\right) \end{cases} \quad (145)$$

and

$$\overline{S}_{\zeta^{-1}(p)} = \begin{cases} \emptyset & p < \frac{1}{2}, \\ \left(-\infty, b \cdot \log\left(\frac{1}{2(1-p)}\right)\right] & \frac{1}{2} \leq p < 1 - \frac{1}{2} \exp\left(-\frac{\alpha}{b}\right), \\ \mathbb{R} & p \geq 1 - \frac{1}{2} \exp\left(-\frac{\alpha}{b}\right). \end{cases} \quad (146)$$

Suppose $p < \frac{1}{2}$. Then $\underline{S}_{\zeta^{-1}(p)} = \overline{S}_{\zeta^{-1}(p)} = \emptyset$ and hence $\xi(\zeta^{-1}(p), p) = 0$ and condition (134) cannot be satisfied. If $p = \frac{1}{2}$, then $\underline{S}_{\zeta^{-1}(p)} = \emptyset$ and $\overline{S}_{\zeta^{-1}(p)} = (-\infty, 0]$. Note that for $z \leq 0$ we have $\mu_\delta(z) =$

$\mu_\varepsilon(z) \exp(-\frac{\alpha}{b})$ and hence for any $S \subseteq \bar{S}_{\zeta^{-1}(\frac{1}{2})}$ we have $\mathbb{P}_\delta[S] = \exp(-\frac{\alpha}{b}) \cdot \mathbb{P}_\varepsilon[S]$. We can thus compute ξ at $(\zeta^{-1}(\frac{1}{2}), \frac{1}{2})$ as

$$p = \frac{1}{2} \Rightarrow \xi\left(\zeta^{-1}\left(\frac{1}{2}\right), \frac{1}{2}\right) = \sup\left\{\mathbb{P}_\delta[S] \mid S \subseteq (-\infty, 0] \wedge \mathbb{P}_\varepsilon[S] \leq \frac{1}{2}\right\} = \frac{1}{2}. \quad (147)$$

Now suppose $\frac{1}{2} < p < 1 - \frac{1}{2} \exp(-\frac{\alpha}{b})$. In this case, $\underline{S}_{\zeta^{-1}(p)} = (-\infty, b \cdot \log(\frac{1}{2(1-p)}))$ and $\bar{S}_{\zeta^{-1}(p)} = (-\infty, b \cdot \log(\frac{1}{2(1-p)})]$. Since the singleton $\{b \cdot \log(\frac{1}{2(1-p)})\}$ has no probability mass under both \mathbb{P}_ε and \mathbb{P}_δ , the function ξ is straight forward to compute

$$\frac{1}{2} < p < 1 - \frac{1}{2} \exp(-\frac{\alpha}{b}) \Rightarrow \xi(\zeta^{-1}(p), p) = \mathbb{P}_\delta\left[\delta \leq \overbrace{b \cdot \log\left(\frac{1}{2(1-p)}\right)}^{< \alpha}\right] = \frac{1}{2} \exp\left(\frac{b \cdot \log\left(\frac{1}{2(1-p)}\right) - \alpha}{b}\right) \quad (148)$$

$$= \frac{1}{4(1-p)} \exp\left(-\frac{\alpha}{b}\right). \quad (149)$$

Finally, consider the case where $p \geq 1 - \frac{1}{2} \exp(-\frac{\alpha}{b})$. Then $\underline{S}_{\zeta^{-1}(p)} = (-\infty, \alpha]$ and $\bar{S}_{\zeta^{-1}(p)} = \mathbb{R}$. Any $(-\infty, \alpha] \subseteq S \subseteq \mathbb{R}$ can then be written as $S = (-\infty, \alpha] \dot{\cup} S_1$ for some $S_1 \subseteq (\alpha, \infty)$. Thus

$$\mathbb{P}_\delta[S] = \mathbb{P}_\delta[\delta \leq \alpha] + \mathbb{P}_\delta[S_1] = \frac{1}{2} + \exp\left(\frac{\alpha}{b}\right) \mathbb{P}_\varepsilon[S_1], \quad (150)$$

$$\mathbb{P}_\varepsilon[S] = \mathbb{P}_\varepsilon[\varepsilon \leq \alpha] + \mathbb{P}_\varepsilon[S_1] = 1 - \frac{1}{2} \exp(-\frac{\alpha}{b}) + \mathbb{P}_\varepsilon[S_1]. \quad (151)$$

Computing ξ thus yields

$$p \geq 1 - \frac{1}{2} \exp(-\frac{\alpha}{b}) \Rightarrow \xi(\zeta^{-1}(p), p) = \sup\{\mathbb{P}_\delta[S] \mid (-\infty, \alpha] \subseteq S \subseteq \mathbb{R} \wedge \mathbb{P}_\varepsilon[S] \leq p\} \quad (152)$$

$$= \frac{1}{2} + \sup\left\{\mathbb{P}_\delta[S_1] \mid S_1 \subseteq (\alpha, \infty) \wedge \mathbb{P}_\varepsilon[S_1] \leq p - 1 + \frac{1}{2} \exp(-\frac{\alpha}{b})\right\} \quad (153)$$

$$= \frac{1}{2} + \exp\left(\frac{\alpha}{b}\right) \left(p - 1 + \frac{1}{2} \exp(-\frac{\alpha}{b})\right) = 1 - \exp\left(\frac{\alpha}{b}\right) (1-p) \quad (154)$$

In order to evaluate condition (134), consider

$$1 - \xi(\zeta^{-1}(1-p_B), 1-p_B) = \begin{cases} 1 & p_B > \frac{1}{2} \\ \frac{1}{2} & p_B = \frac{1}{2} \\ 1 - \frac{1}{4p_B} \exp(-\frac{\alpha}{b}) & \frac{1}{2} > p_B > \exp(-\frac{\alpha}{b}) \\ \exp(\frac{\alpha}{b}) p_B & \exp(-\frac{\alpha}{b}) \geq p_B, \end{cases} \quad (155)$$

$$\xi(\zeta^{-1}(p_A), p_A) = \begin{cases} 0 & p_A < \frac{1}{2} \\ \frac{1}{2} & p_A = \frac{1}{2} \\ \frac{1}{4(1-p_A)} \exp(-\frac{\alpha}{b}) & \frac{1}{2} < p_A < 1 - \frac{1}{2} \exp(-\frac{\alpha}{b}) \\ 1 - \exp(\frac{\alpha}{b}) (1-p_A) & p_A \geq 1 - \frac{1}{2} \exp(-\frac{\alpha}{b}). \end{cases} \quad (156)$$

$$(157)$$

Note that the case $p_B > \frac{1}{2}$ can be ruled out, since by assumption $p_A \geq p_B$. Furthermore, if $p_B > \frac{1}{2}$, then condition (134) cannot be satisfied. Similarly, if $p_A = \frac{1}{2}$, then we need $p_B < \frac{1}{2}$. Thus, if $p_A = \frac{1}{2}$, then

condition (134) is satisfied if $p_B < \frac{1}{2}$ and

$$\max \left\{ 1 - \frac{1}{4p_B} \exp\left(-\frac{\alpha}{b}\right), \exp\left(\frac{\alpha}{b}\right) \cdot p_B \right\} < \frac{1}{2} \quad (158)$$

$$\iff p_B \cdot \exp\left(\frac{\alpha}{b}\right) < \frac{1}{2} \quad (159)$$

$$\iff \alpha < -b \cdot \log(2p_B). \quad (160)$$

Now consider the case where $p_A > \frac{1}{2}$. If $p_B = \frac{1}{2}$, then condition (134) is satisfied if

$$\frac{1}{2} < \min \left\{ \frac{1}{4(1-p_A)} \exp\left(-\frac{\alpha}{b}\right), 1 - \exp\left(\frac{\alpha}{b}\right) (1-p_A) \right\} \quad (161)$$

$$\iff \frac{1}{2} < 1 - \exp\left(\frac{\alpha}{b}\right) (1-p_A) \quad (162)$$

$$\iff \alpha < -b \cdot \log(2(1-p_A)). \quad (163)$$

If on the other hand, $p_A > \frac{1}{2}$ and $p_B < \frac{1}{2}$, condition (134) is satisfied if

$$\max \left\{ 1 - \frac{1}{4p_B} \exp\left(-\frac{\alpha}{b}\right), \exp\left(\frac{\alpha}{b}\right) \cdot p_B \right\} < \min \left\{ \frac{1}{4(1-p_A)} \exp\left(-\frac{\alpha}{b}\right), 1 - \exp\left(\frac{\alpha}{b}\right) (1-p_A) \right\} \quad (164)$$

$$p_B \cdot \exp\left(\frac{\alpha}{b}\right) < 1 - \exp\left(\frac{\alpha}{b}\right) (1-p_A) \quad (165)$$

$$\alpha < -b \cdot \log(1-p_A+p_B). \quad (166)$$

Finally, we get that condition (134) is satisfied, if

$$|\alpha| < \begin{cases} -b \cdot \log(4p_B(1-p_A)) & (p_A = \frac{1}{2} \wedge p_B < \frac{1}{2}) \vee (p_A > \frac{1}{2} \wedge p_B = \frac{1}{2}) \\ -b \cdot \log(1-p_A+p_B) & p_A > \frac{1}{2} \wedge p_B < \frac{1}{2}. \end{cases} \quad (167)$$

□

Corollary 5 (restated). *Suppose $\mathcal{Z} = \mathbb{R}_{\geq 0}$, $\varepsilon \sim |\mathcal{N}(0, \sigma)|$ and $\delta := \alpha + \varepsilon$ for some $\alpha > 0$. Then $g_h^\delta(x_0)_{c_A} > \max_{c \neq c_A} g_h^\delta(x_0)_c$ if $p_B < p_A$ and α satisfies*

$$\alpha < \sigma \cdot \left(\Phi^{-1} \left(\frac{1 + \min\{p_A, 1-p_B\}}{2} \right) - \Phi^{-1} \left(\frac{3}{4} \right) \right), \quad (168)$$

Proof. By Theorem 1 we know that $g_h^\delta(x_0)_{c_A} > \max_{c \neq c_A} g_h^\delta(x_0)_c$ if δ satisfies

$$1 - \xi(\zeta^{-1}(1-p_B), 1-p_B) < \xi(\zeta^{-1}(p_A), p_A). \quad (169)$$

The proof is thus complete if we show that (169) reduces to (168). For that purpose, consider

$$\mu_\varepsilon(z) = \begin{cases} \frac{2}{\sqrt{2\pi}\sigma} \exp\left(-\frac{z^2}{2\sigma^2}\right) & z \geq 0 \\ 0 & z < 0 \end{cases} \quad \mu_\delta(z) = \begin{cases} \frac{2}{\sqrt{2\pi}\sigma} \exp\left(-\frac{(z-\alpha)^2}{2\sigma^2}\right) & z \geq \alpha \\ 0 & z < \alpha. \end{cases} \quad (170)$$

Then, for $z \geq 0$,

$$\frac{\mu_\delta(z)}{\mu_\varepsilon(z)} = \begin{cases} 0 & z < \alpha, \\ \exp\left(\frac{z\alpha}{\sigma^2} - \frac{\alpha^2}{2\sigma^2}\right) & z \geq \alpha. \end{cases} \quad (171)$$

Let $t_\alpha := \exp\left(\frac{\alpha^2}{2\sigma^2}\right)$ and suppose $t < t_\alpha$. Then

$$\zeta(t) = \mathbb{P}_\varepsilon \left[\frac{\mu_\delta(\varepsilon)}{\mu_\varepsilon(\varepsilon)} \leq t \right] = \mathbb{P}_\varepsilon [\varepsilon < \alpha] = \int_0^\alpha \frac{2}{\sqrt{2\pi}\sigma} \exp\left(-\frac{z^2}{2\sigma^2}\right) dz = 2 \cdot \int_0^{\alpha/\sigma} \frac{1}{\sqrt{2\pi}} \exp\left(-\frac{s^2}{2}\right) ds \quad (172)$$

$$= 2 \cdot \Phi\left(\frac{\alpha}{\sigma}\right) - 1. \quad (173)$$

If $t \geq t_\alpha$, then

$$\zeta(t) = \mathbb{P}_\varepsilon \left[\frac{\mu_\delta(\varepsilon)}{\mu_\varepsilon(\varepsilon)} \leq t \right] = \mathbb{P}_\varepsilon \left[\frac{\varepsilon \alpha}{\sigma^2} - \frac{\alpha^2}{2\sigma^2} \leq \log(t) \wedge \varepsilon \geq \alpha \right] + \mathbb{P}_\varepsilon [\varepsilon < \alpha] = \mathbb{P}_\varepsilon \left[\varepsilon \leq \frac{\sigma^2}{\alpha} \log(t) + \frac{1}{2}\alpha \right] \quad (174)$$

$$= 2 \cdot \Phi\left(\frac{\sigma}{\alpha} \log(t) + \frac{\alpha}{2\sigma}\right) - 1. \quad (175)$$

and hence

$$\zeta(t) = \begin{cases} 2 \cdot \Phi\left(\frac{\alpha}{\sigma}\right) - 1 & t < t_\alpha \\ 2 \cdot \Phi\left(\frac{\sigma}{\alpha} \log(t) + \frac{\alpha}{2\sigma}\right) - 1 & t \geq t_\alpha. \end{cases} \quad (176)$$

Note that $\zeta(t_\alpha) = 2 \cdot \Phi\left(\frac{\alpha}{\sigma}\right) - 1$ and let $p_\alpha := \zeta(t_\alpha)$. Recall that $\zeta^{-1}(p) := \inf\{t \mid \zeta(t) \geq p\}$ which yields

$$\zeta^{-1}(p) = \begin{cases} 0 & p \leq p_\alpha \\ \exp\left(\frac{\alpha}{\sigma} \Phi^{-1}\left(\frac{1+p}{2}\right) - \frac{\alpha^2}{2\sigma^2}\right) & p > p_\alpha. \end{cases} \quad (177)$$

In order to evaluate ξ we compute the lower and strict lower level sets at $t = \zeta^{-1}(p)$. Recall that $\underline{S}_t = \{z \in \mathbb{R}_{\geq 0} \mid \frac{\mu_\delta(z)}{\mu_\varepsilon(z)} < t\}$ and $\bar{S}_t = \{z \in \mathbb{R}_{\geq 0} \mid \frac{\mu_\delta(z)}{\mu_\varepsilon(z)} \leq t\}$. Let $S_0 := [0, \alpha]$ and note that if $p \leq p_\alpha$, we have $\zeta^{-1}(p) = 0$ and hence $\underline{S}_{\zeta^{-1}(p)} = \emptyset$ and $\bar{S}_{\zeta^{-1}(p)} = S_0$. If, on the other hand $p > p_\alpha$, then

$$\underline{S}_{\zeta^{-1}(p)} = \left\{ z \geq 0 : \frac{\mu_\delta(z)}{\mu_\varepsilon(z)} < \zeta^{-1}(p) \right\} = S_0 \cup \left\{ z \geq \alpha : \frac{z\alpha}{\sigma^2} - \frac{\alpha^2}{2\sigma^2} < \frac{\alpha}{\sigma} \Phi^{-1}\left(\frac{1+p}{2}\right) - \frac{\alpha^2}{2\sigma^2} \right\} \quad (178)$$

$$= S_0 \cup \left\{ z \geq \alpha : z < \sigma \cdot \Phi^{-1}\left(\frac{1+p}{2}\right) \right\} = S_0 \cup \left[\alpha, \sigma \cdot \Phi^{-1}\left(\frac{1+p}{2}\right) \right) \quad (179)$$

and

$$\bar{S}_{\zeta^{-1}(p)} = \left\{ z \geq 0 : \frac{\mu_\delta(z)}{\mu_\varepsilon(z)} \leq \zeta^{-1}(p) \right\} = S_0 \cup \left\{ z \geq \alpha : \frac{z\alpha}{\sigma^2} - \frac{\alpha^2}{2\sigma^2} \leq \frac{\alpha}{\sigma} \Phi^{-1}\left(\frac{1+p}{2}\right) - \frac{\alpha^2}{2\sigma^2} \right\} \quad (180)$$

$$= S_0 \cup \left\{ z \geq \alpha : z \leq \sigma \cdot \Phi^{-1}\left(\frac{1+p}{2}\right) \right\} = S_0 \cup \left[\alpha, \sigma \cdot \Phi^{-1}\left(\frac{1+p}{2}\right) \right] \quad (181)$$

$$= \underline{S}_{\zeta^{-1}(p)} \cup \left\{ \sigma \cdot \Phi^{-1}\left(\frac{1+p}{2}\right) \right\}. \quad (182)$$

In other words

$$\underline{S}_{\zeta^{-1}(p)} = \begin{cases} \emptyset & p \leq p_\alpha, \\ S_0 \cup \left[\alpha, \sigma \cdot \Phi^{-1}\left(\frac{1+p}{2}\right) \right) & p > p_\alpha, \end{cases} \quad (183)$$

$$\bar{S}_{\zeta^{-1}(p)} = \begin{cases} S_0 & p \leq p_\alpha, \\ S_0 \cup \left[\alpha, \sigma \cdot \Phi^{-1}\left(\frac{1+p}{2}\right) \right] & p > p_\alpha. \end{cases} \quad (184)$$

$$(185)$$

Let $\mathcal{S}_{t,p} := \{S \subseteq \mathbb{R}_{\geq 0} \mid \underline{S}_t \subseteq S \subseteq \bar{S}_t \wedge \mathbb{P}_\varepsilon[S] \leq p\}$ and recall that $\xi(t, p) = \sup_{S \in \mathcal{S}_{t,p}} \mathbb{P}_\delta[S]$. Note that for $p \leq p_\alpha$, we have $\mathcal{S}_{\zeta^{-1}(p), p} = \{S \subseteq \mathbb{R}_{\geq 0} \mid S \subseteq S_0 \wedge \mathbb{P}_\varepsilon[S] \leq p\}$ and for $S \subseteq S_0$, it holds that $\mathbb{P}_\delta[S] = 0$. Hence

$$p \leq p_\alpha \Rightarrow \xi(\zeta^{-1}(p), p) = \sup_{S \in \mathcal{S}_{\zeta^{-1}(p), p}} \mathbb{P}_\delta[S] = 0. \quad (186)$$

If $p > p_\alpha$, then

$$\mathcal{S}_{\zeta^{-1}(p), p} = \{S \subseteq \mathbb{R}_{\geq 0} \mid S_0 \cup \left[\alpha, \sigma \cdot \Phi^{-1} \left(\frac{1+p}{2} \right) \right] \subseteq S \subseteq S_0 \cup \left[\alpha, \sigma \cdot \Phi^{-1} \left(\frac{1+p}{2} \right) \right] \wedge \mathbb{P}_\varepsilon[S] \leq p\}. \quad (187)$$

Since the singleton $\{\sigma \cdot \Phi^{-1}(\frac{1+p}{2})\}$ has no mass under \mathbb{P}_ε and \mathbb{P}_δ , we compute

$$p > p_\alpha \Rightarrow \xi(\zeta^{-1}(p), p) = \mathbb{P}_\delta \left[0 \leq \delta \leq \sigma \cdot \Phi^{-1} \left(\frac{1+p}{2} \right) \right] = \mathbb{P}_\varepsilon \left[0 \leq \varepsilon \leq \sigma \cdot \Phi^{-1} \left(\frac{1+p}{2} \right) - \alpha \right] \quad (188)$$

$$= 2 \cdot \Phi \left(\Phi^{-1} \left(\frac{1+p}{2} \right) - \frac{\alpha}{\sigma} \right) - 1. \quad (189)$$

Condition 169 can thus only be satisfied if $p_B < p_A$ and

$$2 \cdot \Phi \left(\frac{\alpha}{\sigma} \right) - 1 < \min\{p_A, 1 - p_B\} \wedge 1 - \xi(\zeta^{-1}(1 - p_B), 1 - p_B) < \xi(\zeta^{-1}(p_A), p_A) \quad (190)$$

$$\Leftrightarrow \alpha < \sigma \cdot \Phi^{-1} \left(\frac{1 + \min\{p_A, 1 - p_B\}}{2} \right) \wedge \Phi \left(\Phi^{-1} \left(\frac{1 + (1 - p_B)}{2} \right) - \frac{\alpha}{\sigma} \right) + \quad (191)$$

$$+ \Phi \left(\Phi^{-1} \left(\frac{1 + p_A}{2} \right) - \frac{\alpha}{\sigma} \right) > \frac{3}{2}. \quad (192)$$

Thus, the following is a sufficient condition for the two inequalities in (192) and hence (169) to hold

$$\alpha < \sigma \cdot \left(\Phi^{-1} \left(\frac{1 + \min\{p_A, 1 - p_B\}}{2} \right) - \Phi^{-1} \left(\frac{3}{4} \right) \right), \quad (193)$$

completing the proof. □

C Comparison of smoothing noise distributions: Detailed Figures and Tables

In this section we provide more detailed graphical illustrations and tables accompanying our findings from section 4.1.

Table 3: Comparison of certification radii. The variance is normalized to 1 and dimensionality of the noise space is $m = 1$. Note that for Exponential and Folded Gaussian distributions the perturbations are restricted to $\mathbb{R}_{\geq 0}$.

Distribution	Robust Radius
$\mathcal{N}(0, 1)$	$\Phi^{-1}(p_A)$
$\mathcal{L}(0, \frac{1}{\sqrt{2}})$	$-\frac{1}{\sqrt{2}} \cdot \log(2 - 2p_A)$
$\mathcal{U}([-\sqrt{3}, -\sqrt{3}])$	$2\sqrt{3} \cdot (p_A - \frac{1}{2})$
Exp(1)	$-\log(2 - 2p_A)$
$ \mathcal{N}(0, \sqrt{\frac{\pi}{\pi-2}}) $	$\sqrt{\frac{\pi}{\pi-2}} \cdot (\Phi^{-1}(\frac{1+p_A}{2}) - \Phi^{-1}(\frac{3}{4}))$

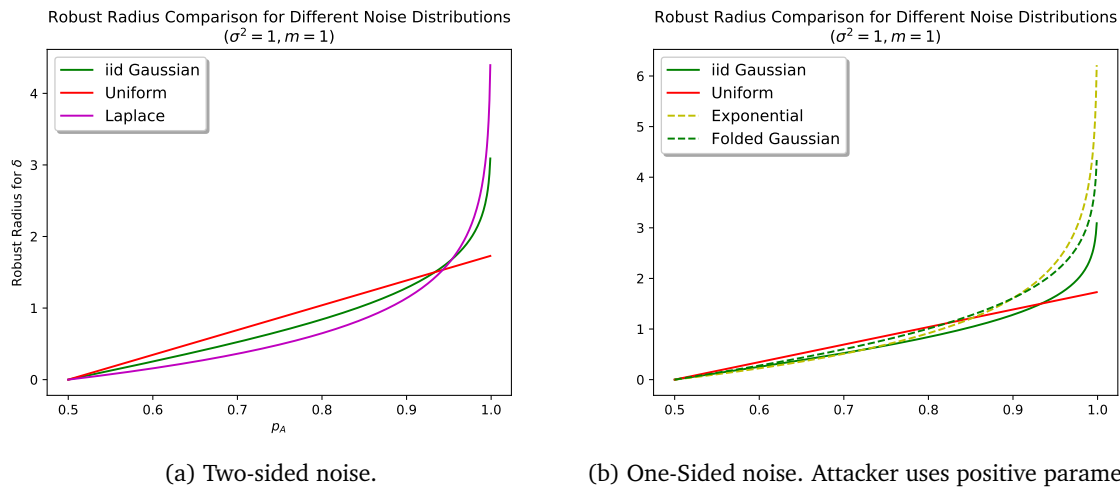


Figure 2: Robust radius comparison for different noise distributions. Additional knowledge on attack model leads to higher radii.

D Transformation Details for Rotation and Scaling

In this section we explain rotation and scaling transformations in greater detail. Due to bilinear interpolation, a more in-depth analysis is required. For the sequel, we define images to be real-valued tensors $x \in \mathbb{R}^{K \times W \times H}$. For a given image x , we use the notation $x(k, i, j) := x_{k,i,j}$ for the index function, retrieving the pixel value of x at position (k, i, j) . For a real number $y \in \mathbb{R}$ we denote by $\lfloor y \rfloor$ the nearest smaller and by $\lceil y \rceil$ the nearest larger integer.

D.1 Bilinear Interpolation

Let $\Omega_K := \{0, \dots, K-1\}$ and $\Omega := [0, W-1] \times [0, H-1]$. We define bilinear interpolation to be the map $Q: \mathbb{R}^{K \times W \times H} \rightarrow L^2(\Omega_K \times \mathbb{R}^2, \mathbb{R})$, $x \mapsto Q(x) =: Q_x$ where Q_x is given by

$$(k, i, j) \mapsto Q_x(k, i, j) := \begin{cases} 0 & (i, j) \notin \Omega \\ x_{k,i,j} & (i, j) \in \Omega \cap \mathbb{N}^2 \\ \tilde{x}_{k,i,j} & (i, j) \in \Omega \setminus \mathbb{N}^2. \end{cases} \quad (194)$$

where

$$\begin{aligned} \tilde{x}_{k,i,j} := & (1 - (i - \lfloor i \rfloor)) \cdot ((1 - (j - \lfloor j \rfloor)) \cdot x_{k,\lfloor i \rfloor,\lfloor j \rfloor} + (j - \lfloor j \rfloor) \cdot x_{k,\lfloor i \rfloor,\lfloor j \rfloor+1}) \\ & + (i - \lfloor i \rfloor) \cdot ((1 - (j - \lfloor j \rfloor)) \cdot x_{k,\lfloor i \rfloor+1,\lfloor j \rfloor} + (j - \lfloor j \rfloor) \cdot x_{k,\lfloor i \rfloor+1,\lfloor j \rfloor+1}). \end{aligned} \quad (195)$$

D.2 Rotation Transformation

The rotation transformation is denoted as $\phi_R: \mathbb{R}^{K \times W \times H} \times \mathbb{R} \rightarrow \mathbb{R}^{K \times W \times H}$ and acts on an image in three steps which we will highlight in greater detail. First, it rotates the image by α degrees counter-clockwise. After rotation, pixel values are determined using bilinear interpolation (194). Finally, we apply black-padding to all pixels (i, j) whose ℓ_2 -distance to the center pixel is larger than half of the length of the shorter side, and denote this operation by P . Let c_W and c_H be the center pixels

$$c_W := \frac{W-1}{2}, \quad c_H := \frac{H-1}{2}. \quad (196)$$

and

$$d_{i,j} = \sqrt{(i - c_W)^2 + (j - c_H)^2}, \quad g_{i,j} = \arctan 2(j - c_H, i - c_W). \quad (197)$$

We write $\tilde{\phi}_R$ for the rotation transform before black padding and decompose ϕ_R as $\phi_R = P \circ \tilde{\phi}_R$, where $\tilde{\phi}_R: \mathbb{R}^{K \times W \times H} \times \mathbb{R} \rightarrow \mathbb{R}^{K \times W \times H}$, $(x, \alpha) \mapsto \tilde{\phi}_R(x, \alpha)$ is defined by

$$\tilde{\phi}_R(x, \alpha)_{k,i,j} := Q_x(k, c_W + d_{i,j} \cos(g_{i,j} - \alpha), c_H + d_{i,j} \sin(g_{i,j} - \alpha)) \quad (198)$$

and $P: \mathbb{R}^{K \times W \times H} \rightarrow \mathbb{R}^{K \times W \times H}$ by

$$f \mapsto P(f)_{k,i,j} = \begin{cases} f(k, i, j) & d_{i,j} < \min\{c_W, c_H\} \\ 0 & \text{otherwise} \end{cases}. \quad (199)$$

D.3 Scaling Transformation

The scaling transformation is denoted as $\phi_S: \mathbb{R}^{K \times W \times H} \times \mathbb{R} \rightarrow \mathbb{R}^{K \times W \times H}$. Similar as for rotations, ϕ_S acts on an image in three steps. First, it stretches height and width by a fixed ratio $\alpha \in \mathbb{R}$. Secondly, we determine

missing pixel values with bilinear interpolation. Finally, we apply black-padding to regions with missing pixel values if the image is scaled by a factor smaller than 1. Let c_W and c_H be the center pixels

$$c_W := \frac{W-1}{2}, \quad c_H := \frac{H-1}{2}. \quad (200)$$

We notice that black padding is naturally applied during bilinear interpolation in cases where the scaling factor is smaller than 1 (that is, when we make images smaller). We can thus write the scaling operation as $\phi_S: \mathbb{R}^{K \times W \times H} \times \mathbb{R}_{>0} \rightarrow \mathbb{R}^{K \times W \times H}$, $(x, \alpha) \mapsto \phi(x, \alpha)$ where

$$\phi_S(x, \alpha)_{k,i,j} := Q_x \left(k, c_W + \frac{i - c_W}{\alpha}, c_H + \frac{j - c_H}{\alpha} \right). \quad (201)$$

E Adversarial Semantic Transforms: Proofs and Derivations

E.1 Gaussian Blur

Recall that Gaussian blur amounts to convolving an image with a Gaussian function

$$G_\alpha(k) = \frac{1}{\sqrt{2\pi\alpha}} \exp\left(-\frac{k^2}{2\alpha}\right) \quad (202)$$

where $\alpha > 0$ is a transformation parameter. The following Lemma shows that Gaussian blur is an additive transform.

Lemma 1 (restated). *Let $\phi: \mathcal{X} \times \mathbb{R}_{\geq 0} \rightarrow \mathbb{R}_{\geq 0}$ denote the Gaussian blur transform, $(x, \alpha) \mapsto \phi(x, \alpha) := (x * G_\alpha)$. Then, for any $\alpha, \beta \in \mathbb{R}_{\geq 0}$*

$$\phi(\phi(x, \alpha), \beta) = \phi(x, \alpha + \beta) \quad \forall x. \quad (203)$$

Proof. Note that associativity of the convolution operator implies that

$$\phi(\phi(x, \alpha), \beta) = (\phi(x, \alpha) * G_\beta) = ((x * G_\alpha) * G_\beta) = (x * (G_\alpha * G_\beta)). \quad (204)$$

The claim thus follows, if we can show that $(G_\alpha * G_\beta) = G_{\alpha+\beta}$. For that purpose let \mathcal{F} denote the Fourier transform and \mathcal{F}^{-1} the inverse Fourier transform and note that by the convolution Theorem $(G_\alpha * G_\beta) = \mathcal{F}^{-1}\{\mathcal{F}(G_\alpha) \cdot \mathcal{F}(G_\beta)\}$. Therefore we have to show that $\mathcal{F}(G_\alpha) \cdot \mathcal{F}(G_\beta) = \mathcal{F}(G_{\alpha+\beta})$. For that purpose, consider

$$\mathcal{F}(G_\alpha)(\omega) = \int_{-\infty}^{\infty} G_\alpha(y) \exp(-2\pi i \omega y) dy = \int_{-\infty}^{\infty} \frac{1}{\sqrt{2\pi\alpha}} \exp\left(-\frac{y^2}{2\alpha}\right) \exp(-2\pi i \omega y) dy \quad (205)$$

$$= \frac{1}{\sqrt{2\pi\alpha}} \int_{-\infty}^{\infty} \exp\left(-\frac{y^2}{2\alpha}\right) (\cos(2\pi\omega y) + i \sin(2\pi\omega y)) dy \quad (206)$$

$$\stackrel{(i)}{=} \frac{1}{\sqrt{2\pi\alpha}} \int_{-\infty}^{\infty} \exp\left(-\frac{y^2}{2\alpha}\right) \cos(2\pi\omega y) dy \stackrel{(ii)}{=} \exp(-\omega^2 \pi^2 2\alpha), \quad (207)$$

where (i) follows from the fact that the second term is an integral of an odd function over a symmetric range and (ii) follows from $\int_{-\infty}^{\infty} \exp(-ay^2) \cos(2\pi\omega y) dy = \sqrt{\frac{\pi}{a}} \exp\left(\frac{-(\pi\omega)^2}{a}\right)$ with $a = \frac{1}{2\alpha}$ (see p. 302, eq. 7.4.6 in (Abramowitz & Stegun, 1972)). This concludes our proof since

$$(\mathcal{F}(G_\alpha) \cdot \mathcal{F}(G_\beta))(\omega) = \exp(-\omega^2 \pi^2 2\alpha) \cdot \exp(-\omega^2 \pi^2 2\beta) = \exp(-\omega^2 \pi^2 2(\alpha + \beta)) = \mathcal{F}(G_{\alpha+\beta})(\omega) \quad (208)$$

and hence

$$(G_\alpha * G_\beta) = \mathcal{F}^{-1}\{\mathcal{F}(G_\alpha) \cdot \mathcal{F}(G_\beta)\} = \mathcal{F}^{-1}\{\mathcal{F}(G_{\alpha+\beta})\} = G_{\alpha+\beta}. \quad (209)$$

□

Remark 2. We notice that the above Theorem naturally extends to higher dimensional Gaussian kernels of the form

$$G_\alpha(k) = \frac{1}{(2\pi\alpha)^{\frac{m}{2}}} \exp\left(-\frac{\|k\|^2}{2\alpha}\right), \quad k \in \mathbb{R}^m. \quad (210)$$

Consider

$$\mathcal{F}(G_\alpha)(\omega) = \int_{\mathbb{R}^m} G_\alpha(y) \exp(-2\pi i \langle \omega, y \rangle) dy = \frac{1}{(2\pi\alpha)^{\frac{m}{2}}} \int_{\mathbb{R}^m} \exp\left(-\frac{\|y\|_2^2}{2\alpha} - 2\pi i \langle \omega, y \rangle\right) dy \quad (211)$$

$$= \prod_{j=1}^m \left(\frac{1}{\sqrt{2\pi\alpha}} \int_{\mathbb{R}} \exp\left(-\frac{y_j^2}{2\alpha} - 2\pi i \omega_j y_j\right) dy_j \right) = \exp\left(-\|\omega\|_2^2 \pi^2 2\alpha\right) \quad (212)$$

which leads to $(G_\alpha * G_\beta) = G_{\alpha+\beta}$, and hence additivity.

E.2 Brightness and contrast

Recall that the brightness and contrast transform is defined as

$$\begin{aligned} \phi_{BC}: \mathcal{X} \times \mathbb{R}^2 &\rightarrow \mathcal{X} \\ (x, \alpha) &\mapsto e^{\alpha_1}(x + \alpha_2). \end{aligned} \quad (213)$$

Lemma 2 (restated). *Let $\varepsilon \sim \mathcal{N}(0, \text{diag}(\sigma_1^2, \sigma_2^2))$, $\alpha = (k, b)^T \in \mathbb{R}^2$ and $\delta \sim \mathcal{N}(0, \text{diag}(\sigma_1^2, e^{-2k}\sigma_2^2))$. Then*

$$g_h^\varepsilon(\phi_{BC}(x, \alpha)) = g_h^{\alpha+\delta}(x) \quad \forall x. \quad (214)$$

Proof of Lemma 2. Let $x \in \mathcal{X}$, and note that

$$\phi_{BC}(\phi_{BC}(x, \alpha), \varepsilon) = e^{\varepsilon_1}(\phi_{BC}(x, \alpha) + \varepsilon_2) = e^{\varepsilon_1}(e^k(x + b) + \varepsilon_2) = e^{\varepsilon_1+k}(x + (b + e^{-k}\varepsilon_2)) \quad (215)$$

$$= \phi_{BC}(x, \alpha + \tilde{\varepsilon}) \quad (216)$$

where $\tilde{\varepsilon} = (\varepsilon_1, e^{-k}\varepsilon_2)^T$. Note that $\tilde{\varepsilon}$ follows a Gaussian distribution since

$$\tilde{\varepsilon} = A \cdot \varepsilon, \quad A = \begin{pmatrix} 1 & 0 \\ 0 & e^{-k} \end{pmatrix} \quad (217)$$

and hence

$$\mathbb{E}_{\tilde{\varepsilon}}[\tilde{\varepsilon}] = A \cdot \mathbb{E}_{\varepsilon}[\varepsilon] = 0 \quad (218)$$

$$\text{Cov}[\tilde{\varepsilon}] = \mathbb{E}_{\varepsilon}[\varepsilon A A^T \varepsilon^T] = A^2 \cdot \begin{pmatrix} \sigma_1^2 & 0 \\ 0 & \sigma_2^2 \end{pmatrix} = \begin{pmatrix} \sigma_1^2 & 0 \\ 0 & e^{-2k}\sigma_2^2 \end{pmatrix}. \quad (219)$$

Hence $\tilde{\varepsilon} \stackrel{d.}{=} \delta$ where $\delta \sim \mathcal{N}(0, \text{diag}(\sigma_1^2, e^{-2k}\sigma_2^2))$ and thus

$$g_h^\varepsilon(\phi_{BC}(x, \alpha)) = \mathbb{E}_{\tilde{\varepsilon}}[\phi(\phi(x, \alpha), \varepsilon)] = \mathbb{E}_{\delta}[\phi(x, \alpha + \delta)] = g_h^{\alpha+\delta}(x) \quad (220)$$

which is what needed to be shown. \square

Lemma 3 (restated). *Let $x_0 \in \mathcal{X}$, $k \in \mathbb{R}$, $\varepsilon \sim \mathcal{N}(0, \Sigma)$ and $\delta \sim \mathcal{N}(0, \text{diag}(\sigma_1^2, e^{-2k}\sigma_2^2))$. Suppose that $g_h^\varepsilon(x_0)_c \geq p$ for some $p \in [0, 1]$ and $c \in \mathcal{Y}$. Then*

$$g_h^\delta(x)_c \geq \begin{cases} 2\Phi(e^k \Phi^{-1}(\frac{1+p}{2})) - 1 & k < 0 \\ p & k = 0 \\ 2(1 - \Phi(e^k \Phi^{-1}(1 - \frac{p}{2}))) & k > 0. \end{cases} \quad (221)$$

Proof of Lemma 3. Note that $\varepsilon \sim \mathcal{N}(0, \Sigma)$ and $\delta = A\varepsilon \sim \mathcal{N}(0, A^2\Sigma)$ where

$$A = \begin{pmatrix} 1 & 0 \\ 0 & e^{-k} \end{pmatrix}, \quad \Sigma = \begin{pmatrix} \sigma_1^2 & 0 \\ 0 & \sigma_2^2 \end{pmatrix}. \quad (222)$$

Recall Definition 3, i.e. for $t \geq 0$, (strict) lower level sets are defined as

$$\underline{S}_t := \left\{ z \in \mathcal{Z} \mid \frac{\mu_\delta(z)}{\mu_\varepsilon(z)} < t \right\}, \quad \overline{S}_t := \left\{ z \in \mathcal{Z} \mid \frac{\mu_\delta(z)}{\mu_\varepsilon(z)} \leq t \right\} \quad (223)$$

By assumption $\mathbb{E}_\varepsilon[h(\phi(x, \varepsilon))_c] = g_h^\varepsilon(x)_c \geq p$. Let $\zeta(t) = \mathbb{P}_\varepsilon[\overline{S}_t]$ be defined as in Theorem 1 and note that by Lemma 7, for any $p \in [0, 1]$ we have $\mathbb{P}_\varepsilon[\underline{S}_{\zeta^{-1}(p)}] \leq p$. Let $\underline{S}_{\zeta^{-1}(p)} \subseteq S \subseteq \overline{S}_{\zeta^{-1}(p)}$ be such that $\mathbb{P}_\varepsilon[S] \leq p$. Then, from part 1 of Lemma 5, it follows that $\mathbb{E}_\delta[h(\phi(x, \delta))_c] = g_h^\delta(x)_c \geq \mathbb{P}_\delta[S]$. Note that

$$\frac{\mu_\delta(z)}{\mu_\varepsilon(z)} = \frac{((2\pi)^2|A^2\Sigma|)^{-\frac{1}{2}} \exp(-\frac{1}{2}(z^T(A^2\Sigma)^{-1}z))}{((2\pi)^2|\Sigma|)^{-\frac{1}{2}} \exp(-\frac{1}{2}(z^T(\Sigma)^{-1}z))} = \frac{1}{|A|} \exp\left(-\frac{1}{2}z^T((A^2\Sigma)^{-1} - \Sigma^{-1})z\right) \quad (224)$$

$$= \exp\left(k - \frac{z_2^2}{2\sigma_2^2}(e^{2k} - 1)\right). \quad (225)$$

Note that, if $k = 0$, then $\delta = \varepsilon$. Thus, suppose that $k \neq 0$ because otherwise the Lemma is satisfied trivially. Now suppose that $k > 0$ and consider

$$\zeta(t) = \mathbb{P}_\varepsilon[\overline{S}_t] = \mathbb{P}_{\varepsilon_2}\left[\exp\left(k - \frac{\varepsilon_2^2}{2\sigma_2^2}(e^{2k} - 1)\right) \leq t\right] = 1 - \mathbb{P}_{\varepsilon_2}\left[\left(\frac{\varepsilon_2}{\sigma_2}\right)^2 \leq (k - \log(t))\frac{2}{e^{2k} - 1}\right] \quad (226)$$

$$= 1 - F_{\chi^2}\left((k - \log(t))\frac{2}{e^{2k} - 1}\right) = \begin{cases} 0 & t = 0 \\ 1 - F_{\chi^2}\left((k - \log(t))\frac{2}{e^{2k} - 1}\right) & 0 < t < e^k \\ 1 & t \geq e^k, \end{cases} \quad (227)$$

where F_{χ^2} denotes the CDF of the χ^2 -distribution with one degree of freedom. Note that for any $t \geq 0$

$$\mathbb{P}_\varepsilon[\partial_t] = \mathbb{P}_\varepsilon[\overline{S}_t \setminus \underline{S}_t] = \mathbb{P}_\varepsilon\left[\left(\frac{\varepsilon_2}{\sigma_2}\right)^2 = (k - \log(t))\frac{2}{e^{2k} - 1}\right] = 0 \quad (228)$$

and hence $\mathbb{P}_\varepsilon[\overline{S}_t] = \mathbb{P}_\varepsilon[\underline{S}_t]$. The inverse $\zeta^{-1}(p) = \inf\{t \mid \zeta(t) \geq p\}$ is then given by

$$\zeta^{-1}(p) = \begin{cases} 0 & p = 0 \\ \exp\left(k - \frac{e^{2k} - 1}{2}F_{\chi^2}^{-1}(1-p)\right) & 0 < p < 1 \\ e^k & p = 1. \end{cases} \quad (229)$$

Thus, for any $p \in [0, 1]$, we find that $\mathbb{P}_\varepsilon[\overline{S}_{\zeta^{-1}(p)}] = \mathbb{P}_\varepsilon[\underline{S}_{\zeta^{-1}(p)}] = \zeta(\zeta^{-1}(p)) = p$. Then, $\mathbb{E}_\varepsilon[h(\phi(x, \varepsilon))_c] = g_h^\varepsilon(x)_c \geq p = \mathbb{P}_\varepsilon[\overline{S}_{\zeta^{-1}(p)}]$ and part 1 of Lemma 5 implies that $g_h^\delta(x)_c \geq \mathbb{P}_\delta[\overline{S}_{\zeta^{-1}(p)}]$. Computing $\mathbb{P}_\delta[\overline{S}_{\zeta^{-1}(p)}]$

yields

$$g_h^\delta(x)_c \geq \mathbb{P}_\delta[\bar{S}_{\zeta^{-1}(p)}] = 1 - \mathbb{P}_\delta \left[\left(\frac{\delta_2}{\sigma_2} \right)^2 \leq (k - \log(\zeta^{-1}(p))) \frac{2}{e^{2k} - 1} \right] \quad (230)$$

$$= 1 - \mathbb{P}_\varepsilon \left[\left(\frac{\varepsilon_2}{\sigma_2} \right)^2 \leq (k - \log(\zeta^{-1}(p))) \frac{2e^{2k}}{e^{2k} - 1} \right] \quad (231)$$

$$= 1 - F_{\chi^2} \left((k - \log(\zeta^{-1}(p))) \frac{2e^{2k}}{e^{2k} - 1} \right) \quad (232)$$

$$= 1 - F_{\chi^2} \left(\left(k - \left(k - \frac{e^{2k} - 1}{2} F_{\chi^2}^{-1}(1 - p) \right) \right) \frac{2e^{2k}}{e^{2k} - 1} \right) \quad (233)$$

$$= 1 - F_{\chi^2} \left(e^{2k} F_{\chi^2}^{-1}(1 - p) \right) \quad (234)$$

If, on the other hand, $k < 0$, then

$$\zeta(t) = \mathbb{P}_\varepsilon[\bar{S}_t] = \mathbb{P}_{\varepsilon_2} \left[\exp \left(k + \frac{\varepsilon_2^2}{2\sigma_2^2} |e^{2k} - 1| \right) \leq t \right] = \mathbb{P}_{\varepsilon_2} \left[\left(\frac{\varepsilon_2}{\sigma_2} \right)^2 \leq (\log(t) - k) \frac{2}{|e^{2k} - 1|} \right] \quad (235)$$

$$= F_{\chi^2} \left((\log(t) - k) \frac{2}{|e^{2k} - 1|} \right) = \begin{cases} 0 & t \leq e^k \\ F_{\chi^2} \left((\log(t) - k) \frac{2}{|e^{2k} - 1|} \right) & t > e^k, \end{cases} \quad (236)$$

A similar computation as in the case where $k > 0$ leads to $\mathbb{P}_\varepsilon[\bar{S}_t] = \mathbb{P}_\varepsilon[\underline{S}_t]$. The inverse $\zeta^{-1}(p) = \inf\{t \mid \zeta(t) \geq p\}$ is then given by

$$\zeta^{-1}(p) = \begin{cases} 0 & p = 0 \\ \exp \left(k + F_{\chi^2}^{-1}(p) \frac{|e^{2k} - 1|}{2} \right) & p > 0 \end{cases} \quad (237)$$

Thus, for any $p \in [0, 1]$, we find that $\mathbb{P}_\varepsilon[\bar{S}_{\zeta^{-1}(p)}] = \mathbb{P}_\varepsilon[\underline{S}_{\zeta^{-1}(p)}] = \zeta(\zeta^{-1}(p)) = p$. Then, $\mathbb{E}_\varepsilon[h(\phi(x, \varepsilon))_c] = g_h^\varepsilon(x)_c \geq p = \mathbb{P}_\varepsilon[\bar{S}_{\zeta^{-1}(p)}]$ and part 1 of Lemma 5 implies that $g_h^\delta(x)_c \geq \mathbb{P}_\delta[\bar{S}_{\zeta^{-1}(p)}]$. Computing $\mathbb{P}_\delta[\bar{S}_{\zeta^{-1}(p)}]$ yields

$$g_h^\delta(x)_c \geq \mathbb{P}_\delta[\bar{S}_{\zeta^{-1}(p)}] = \mathbb{P}_\delta \left[\left(\frac{\delta_2}{\sigma_2} \right)^2 \leq (\log(\zeta^{-1}(p)) - k) \frac{2}{|e^{2k} - 1|} \right] \quad (238)$$

$$= \mathbb{P}_\varepsilon \left[\left(\frac{\varepsilon_2}{\sigma_2} \right)^2 \leq (\log(\zeta^{-1}(p)) - k) \frac{2e^{2k}}{|e^{2k} - 1|} \right] \quad (239)$$

$$= F_{\chi^2} \left(\left(\left(k + F_{\chi^2}^{-1}(p) \frac{|e^{2k} - 1|}{2} \right) - k \right) \frac{2e^{2k}}{|e^{2k} - 1|} \right) \quad (240)$$

$$= F_{\chi^2} \left(e^{2k} F_{\chi^2}^{-1}(p) \right). \quad (241)$$

Finally, consider the following relation between $\chi^2(1)$ distribution and the standard normal distribution. Let $Z \sim \mathcal{N}(0, 1)$ and denote by Φ its CDF. Then, for any $z \geq 0$, $F_{\chi^2}(z) = \mathbb{P}[Z^2 \leq z] = \mathbb{P}[-\sqrt{z} \leq Z \leq \sqrt{z}] = \Phi(\sqrt{z}) - \Phi(-\sqrt{z}) = 2\Phi(\sqrt{z}) - 1$ and the inverse is thus given by $F_{\chi^2}^{-1}(p) = (\Phi^{-1}(\frac{1+p}{2}))^2$. Thus

$$g_h^\delta(x)_c \geq \begin{cases} 2\Phi(e^k \Phi^{-1}(\frac{1+p}{2})) - 1 & k < 0 \\ p & k = 0 \\ 2(1 - \Phi(e^k \Phi^{-1}(1 - \frac{p}{2}))) & k > 0 \end{cases} \quad (242)$$

□

E.3 Rotation and Scaling

In this section we state the proofs for the Theorems that justify our approach to certifying rotations and scaling transformations using randomized smoothing. In addition, we provide the details on computing the maximum ℓ_2 -sampling error for both rotation and scaling transforms. The following is used to compute Lipschitz constants for rotation and scaling transformations. Recall the definitions of the coordinate sets

$$\Omega_K = \{0, \dots, K-1\} \quad \text{and} \quad \Omega = [0, W-1] \times [0, H-1]. \quad (243)$$

Definition 6. For pixels $(i, j) \in \Omega$, we define the grid pixel generator G_{ij} as

$$G_{ij} := \{(i, j), (i+1, j), (i, j+1), (i+1, j+1)\}. \quad (244)$$

Definition 7 (max-color extractor). We define the operator which extracts the channel-wise maximum pixel wise on a grid $S \subseteq \Omega$ as

$$\begin{aligned} \bar{m}: \mathbb{R}^{K \times W \times H} \times \Omega_K \times 2^\Omega &\rightarrow \mathbb{R} \\ (x, k, S) &\mapsto \max_{(i,j) \in S} \left(\max_{(r,s) \in G_{ij}} x_{k,r,s} \right) \end{aligned} \quad (245)$$

Definition 8 (max-color difference extractor). We define the operator which extracts the channel-wise maximum change in color on a grid $S \subseteq \Omega$ as

$$\begin{aligned} m_\Delta: \mathbb{R}^{K \times W \times H} \times \Omega_K \times 2^\Omega &\rightarrow \mathbb{R} \\ (x, k, S) &\mapsto \max_{(i,j) \in S} \left(\max_{(r,s) \in G_{ij}} x_{k,r,s} - \min_{(r,s) \in G_{ij}} x_{k,r,s} \right) \end{aligned} \quad (246)$$

Lemma 9. Let $x \in \mathbb{R}^{K \times W \times H}$, $-\infty < t_1 < t_2 < \infty$ and suppose $\rho: [t_1, t_2] \rightarrow [0, W-1] \times [0, H-1]$ is a curve of class C^1 . Let

$$\psi_k: [t_1, t_2] \rightarrow \mathbb{R}, \quad \psi_k(t) := Q_x(k, \rho_1(t), \rho_2(t)) \quad (247)$$

where $k \in \Omega_K$ and Q_x denotes bilinear interpolation. Then ψ_k is L_k -Lipschitz continuous with constant

$$L_k = \max_{t \in [t_1, t_2]} \left(\sqrt{2} \|\dot{\rho}(t)\|_2 \cdot m_\Delta(x, k, \lfloor \rho(t) \rfloor) \right) \quad (248)$$

Proof of Lemma 9. Note that the function $t \mapsto \lfloor \rho(t) \rfloor$ is piecewise constant and let $t_1 =: u_1 < u_2 < \dots < u_{N_0} := t_2$ such that $\lfloor \rho(t) \rfloor$ is constant on $[u_i, u_{i+1})$ for all $1 \leq i \leq N_0 - 1$ and $\dot{\cup}_{i=1}^{N_0} [u_i, u_{i+1}) = [t_1, t_2]$. We notice that ψ_k is a continuous real-valued function since it is the composition of the continuous Q_x and C^1 -curve ρ . L_k -Lipschitz continuity on $[t_1, t_2]$ thus follows if we show that ψ_k is L_k -Lipschitz on each interval in the partition. For that purpose, let $1 \leq i \leq N_0$ be arbitrary and fix some $t \in [u_i, u_{i+1})$. Let $(w, h) := \lfloor \rho(t) \rfloor$ and $\gamma(t) := \rho(t) - \lfloor \rho(t) \rfloor$ and notice that $\gamma(t) \in [0, 1)^2$. Let

$$V_1 := x_{k,w,h}, \quad V_2 := x_{k,w,h+1}, \quad V_3 := x_{k,w+1,h}, \quad V_4 := x_{k,w+1,h+1}, \quad (249)$$

Then, for any $u \in [u_i, u_{i+1})$

$$\psi_k(u) = Q_x(k, \rho_1(u), \rho_2(u)) \quad (250)$$

$$= (1 - \gamma_1(u)) \cdot ((1 - \gamma_2(u)) \cdot V_1 + \gamma_2(u) \cdot V_2) + \gamma_1(u) \cdot ((1 - \gamma_2(u)) \cdot V_3 + \gamma_2(u) \cdot V_4). \quad (251)$$

Let $m_\Delta := m_\Delta(x, k, \lfloor \rho(t) \rfloor)$ and notice that by definition

$$m_\Delta = \max_i V_i - \min_i V_i \quad (252)$$

and in particular

$$|V_i - V_j| \leq m_\Delta \quad \forall i, j. \quad (253)$$

Since V_i is constant for each i and γ is differentiable, ψ_k is differentiable on $[u_i, u_{i+1})$ and hence

$$\dot{\psi}_k(u) = (\dot{\gamma}_1(u)\gamma_2(u) + \gamma_1(u)\dot{\gamma}_2(u))(V_1 - V_2 - V_3 + V_4) + \dot{\gamma}_1(u)(V_3 - V_1) + \dot{\gamma}_2(u)(V_2 - V_1). \quad (254)$$

Note that the derivative $\dot{\psi}_k$ is linear in γ_1 and γ_2 and hence its extreme values are bounded when evaluated at extreme values of γ , that is $(\gamma_1, \gamma_2) \in \{0, 1\}^2$. We treat each case separately:

- $\gamma_1 = \gamma_2 = 0$. Then,

$$\left| \dot{\psi}_k \right| \leq |\dot{\gamma}_1(V_3 - V_1) + \dot{\gamma}_2(V_2 - V_1)| \leq |\dot{\gamma}_1| \cdot |V_3 - V_1| + |\dot{\gamma}_2| \cdot |V_2 - V_1| \leq m_\Delta (|\dot{\gamma}_1| + |\dot{\gamma}_2|) \quad (255)$$

- $\gamma_1 = \gamma_2 = 1$. Then,

$$\left| \dot{\psi}_k \right| \leq |\dot{\gamma}_1(V_4 - V_2) + \dot{\gamma}_2(V_4 - V_3)| \leq |\dot{\gamma}_1| \cdot |V_4 - V_2| + |\dot{\gamma}_2| \cdot |V_4 - V_3| \leq m_\Delta (|\dot{\gamma}_1| + |\dot{\gamma}_2|) \quad (256)$$

- $\gamma_1 = 0, \gamma_2 = 1$. Then,

$$\left| \dot{\psi}_k \right| \leq |\dot{\gamma}_1(V_4 - V_2) + \dot{\gamma}_2(V_2 - V_1)| \leq |\dot{\gamma}_1| \cdot |V_4 - V_2| + |\dot{\gamma}_2| \cdot |V_2 - V_1| \leq m_\Delta (|\dot{\gamma}_1| + |\dot{\gamma}_2|) \quad (257)$$

- $\gamma_1 = 1, \gamma_2 = 0$. Then,

$$\left| \dot{\psi}_k \right| \leq |\dot{\gamma}_1(V_3 - V_1) + \dot{\gamma}_2(V_4 - V_3)| \leq |\dot{\gamma}_1| \cdot |V_3 - V_1| + |\dot{\gamma}_2| \cdot |V_4 - V_3| \leq m_\Delta (|\dot{\gamma}_1| + |\dot{\gamma}_2|) \quad (258)$$

Hence, for any $u \in [u_i, u_{i+1})$, the modulus of the derivative is bounded by $m_\Delta (|\dot{\gamma}_1| + |\dot{\gamma}_2|)$. We can further bound this by observing the following connection between ℓ_1 and ℓ_2 distance

$$\forall x \in \mathbb{R}^n : \quad \|x\|_1 = |\langle x, \mathbf{1} \rangle| \leq \|x\|_2 \|\mathbf{1}\|_2 = \sqrt{n} \|x\|_2 \quad (259)$$

and hence $\forall u \in [u_i, u_{i+1})$

$$|\dot{\psi}_k(u)| \leq m_\Delta \|\dot{\gamma}(u)\|_1 \leq m_\Delta \sqrt{2} \|\dot{\gamma}(u)\|_2 = m_\Delta \sqrt{2} \|\dot{\rho}(u)\|_2. \quad (260)$$

Since ψ_k is differentiable on $[u_i, u_{i+1})$, its Lipschitz constant is bounded by the maximum absolute value of its derivative. Hence

$$\max_{u \in [u_i, u_{i+1})} m_\Delta \sqrt{2} \|\dot{\rho}(u)\|_2 = \max_{u \in [u_i, u_{i+1})} m_\Delta(x, k, \lfloor \rho(u) \rfloor) \sqrt{2} \|\dot{\rho}(u)\|_2 \quad (261)$$

$$\leq \max_{u \in [t_1, t_2)} m_\Delta(x, k, \lfloor \rho(u) \rfloor) \sqrt{2} \|\dot{\rho}(u)\|_2 = L_k \quad (262)$$

is a Lipschitz constant for ψ_k on $[u_i, u_{i+1})$. Note that L_k does not depend on i . Furthermore, i was chosen arbitrarily and hence L_k is a Lipschitz constant for ψ_k on $[t_1, t_2)$ and due to continuity on $[t_1, t_2]$, concluding the proof. \square

Definition 4 (restated). Let $x \in \mathcal{X}$, $\phi: \mathcal{X} \times \mathcal{Z} \rightarrow \mathcal{X}$ be a transform, $a < b$ real numbers, $N \in \mathbb{N}$ and suppose $\{\alpha_i\}_{i=1}^N \subseteq [a, b]$. We define the maximum ℓ_2 sampling error as

$$M_{a,b} := \max_{a \leq \alpha \leq b} \min_{1 \leq i \leq N} \|\phi(x, \alpha) - \phi(x, \alpha_i)\|_2 \quad (263)$$

Theorem 2 (restated). Let $a < b$ be real numbers, $N \in \mathbb{N}$ and suppose $\{\alpha_i\}_{i=1}^N \subseteq [a, b]$. Furthermore, let $\phi: \mathcal{X} \times \mathcal{Z} \rightarrow \mathcal{X}$ be a transform, $x_0 \in \mathcal{X}$, $c_A \in \mathcal{Y}$, $\varepsilon \sim \mathcal{N}(0, \sigma^2 \mathbb{1})$ isotropic Gaussian noise and suppose that the ε -smoothed classifier

$$\begin{aligned} g_h^\varepsilon: \mathcal{X} &\rightarrow \mathcal{S}_C, \\ x &\mapsto \mathbb{E}_\varepsilon[h(x + \varepsilon)] \end{aligned} \quad (264)$$

is (p_A, p_B) -confident at x_0 for some $p_A, p_B \in [0, 1]$. If

$$M_{a,b} < \sigma \min_{1 \leq i \leq N} \Phi^{-1}(g_h^\varepsilon(\phi(x_0, \alpha_i))_{c_A}) =: r, \quad (265)$$

then for any $\alpha \in [a, b]$, the ε -smoothed classifies $\phi(x_0, \alpha)$ to be of class c_A , that is

$$g_h^\varepsilon(\phi(x_0, \alpha))_{c_A} > \max_{c \neq c_A} g_h^\varepsilon(\phi(x_0, \alpha))_c. \quad (266)$$

Proof. Suppose that for $x \in \mathcal{X}$ there exists $1 \leq i \leq N$ such that $\|x - \phi(x_0, \alpha_i)\|_2 < r$. Then, by Corollary 1, we know that $g_h^\varepsilon(x)_{c_A} > \max_{c \neq c_A} g_h^\varepsilon(x)_c$. Since $M_{a,b} = \max_{a \leq \alpha \leq b} \min_{1 \leq i \leq N} \|\phi(x_0, \alpha) - \phi(x_0, \alpha_i)\|_2 < r$, we find that for any $\alpha \in [a, b] \exists i$ such that $\|\phi(x_0, \alpha) - \phi(x_0, \alpha_i)\|_2 < r$. Hence

$$g_h^\varepsilon(\phi(x_0, \alpha))_{c_A} > \max_{c \neq c_A} g_h^\varepsilon(\phi(x_0, \alpha))_c, \quad (267)$$

concluding the proof. \square

In order to apply Theorem 2 we have to compute the maximum ℓ_2 -sampling error (23). In the next sections, we provide detailed explanations on how we can upper bound this quantity for scaling and rotations transforms.

E.3.1 Computing an upper bound on $M_{a,b}$ for rotations

Recall Definition 4 of the maximum ℓ_2 -sampling error for some $a < b$, and $\{\alpha_i\}_{i=1}^N$

$$M_{a,b} := \max_{a \leq \alpha \leq b} \min_{1 \leq i \leq N} \|\phi_R(x, \alpha) - \phi_R(x, \alpha_i)\|_2. \quad (268)$$

In order to compute an upper bound on (268) for rotations, we are interested in finding $M \geq 0$ such that

$$M_{a,b}^2 \leq M \quad (269)$$

in which case we can replace condition (265) by $\sqrt{M} < r$. For that purpose, consider sampling the α_i equally spaced from the interval $[a, b]$, that is

$$\alpha_i := a + (b - a) \frac{i - 1}{N - 1} \quad (270)$$

and note that $a = \alpha_1 < \alpha_2 < \dots < \alpha_N = b$. Furthermore, let g_i be the set of functions

$$\begin{aligned} g_i: [a, b] &\rightarrow \mathbb{R}_{\geq 0} \\ \alpha &\mapsto g_i(\alpha) := \|\phi_R(x, \alpha) - \phi_R(x, \alpha_i)\|_2^2 \end{aligned} \quad (271)$$

where $1 \leq i \leq N$. Note that $\forall \alpha \in [a, b] \exists i$ such that $\alpha \in [\alpha_i, \alpha_{i+1}]$ and let

$$M_i := \max_{\alpha_i \leq \alpha \leq \alpha_{i+1}} \min\{g_i(\alpha), g_{i+1}(\alpha)\}. \quad (272)$$

Note that

$$\max_{\alpha_i \leq \alpha \leq \alpha_{i+1}} \left(\min_{1 \leq j \leq N} g_j(\alpha) \right) \leq \max_{\alpha_i \leq \alpha \leq \alpha_{i+1}} (\min\{g_i(\alpha), g_{i+1}(\alpha)\}) \quad \forall 1 \leq i \leq N - 1 \quad (273)$$

and thus

$$M_{a,b}^2 = \max_{a \leq \alpha \leq b} \left(\min_{1 \leq j \leq N} g_j(\alpha) \right) = \max_{1 \leq i \leq N-1} \left(\max_{\alpha_i \leq \alpha \leq \alpha_{i+1}} \left(\min_{1 \leq j \leq N} g_j(\alpha) \right) \right) \quad (274)$$

$$\leq \max_{1 \leq i \leq N-1} \left(\max_{\alpha_i \leq \alpha \leq \alpha_{i+1}} (\min \{g_i(\alpha), g_{i+1}(\alpha)\}) \right) = \max_{1 \leq i \leq N-1} M_i \quad (275)$$

We now further divide each interval $[\alpha_i, \alpha_{i+1}]$ by sampling $R \in \mathbb{N}$ equally spaced points $\{\gamma_{i,j}\}_{j=1}^R$ given by

$$\gamma_{i,j} := \alpha_i + (\alpha_{i+1} - \alpha_i) \frac{j-1}{R-1} \quad (276)$$

and define

$$m_{i,j} := \max_{\gamma_{i,j} \leq \gamma \leq \gamma_{i,j+1}} \min \{g_i(\gamma), g_{i+1}(\gamma)\} \quad (277)$$

and thus

$$M_i \leq \max_{1 \leq j \leq R-1} m_{i,j}. \quad (278)$$

Once we can compute an upper bound on each $m_{i,j}$, we have found an upper bound on $M_{a,b}^2$. Now, suppose $\exists L \geq 0$ such that

$$\max \left\{ \max_{c, d \in [\alpha_i, \alpha_{i+1}]} \left| \frac{g_i(c) - g_i(d)}{c - d} \right|, \max_{c, d \in [\alpha_i, \alpha_{i+1}]} \left| \frac{g_{i+1}(c) - g_{i+1}(d)}{c - d} \right| \right\} \leq L \quad \forall i. \quad (279)$$

Then, for any $c, d \in [\alpha_i, \alpha_{i+1}]$ we know that

$$g_i(d) \leq g_i(c) + L \cdot |d - c|, \quad (280)$$

$$g_{i+1}(d) \leq g_{i+1}(c) + L \cdot |d - c| \quad (281)$$

and hence for any $\gamma \in [\gamma_{i,j}, \gamma_{i,j+1}]$

$$g_i(\gamma) \leq g_i(\gamma_{i,j}) + L \cdot |\gamma - \gamma_{i,j}|, \quad (282)$$

$$g_i(\gamma) \leq g_i(\gamma_{i,j+1}) + L \cdot |\gamma - \gamma_{i,j+1}|, \quad (283)$$

$$g_{i+1}(\gamma) \leq g_{i+1}(\gamma_{i,j}) + L \cdot |\gamma - \gamma_{i,j}|, \quad (284)$$

$$g_{i+1}(\gamma) \leq g_{i+1}(\gamma_{i,j+1}) + L \cdot |\gamma - \gamma_{i,j+1}|. \quad (285)$$

We can thus bound each g_i on the intervals $[\gamma_{i,j}, \gamma_{i,j+1}]$

$$\max_{\gamma_{i,j} \leq \gamma \leq \gamma_{i,j+1}} g_i(\gamma) \leq \max_{\gamma_{i,j} \leq \gamma \leq \gamma_{i,j+1}} (\min \{g_i(\gamma_{i,j}) + L \cdot |\gamma - \gamma_{i,j}|, g_i(\gamma_{i,j+1}) + L \cdot |\gamma - \gamma_{i,j+1}|\}) \quad (286)$$

$$\leq \max_{\gamma_{i,j} \leq \gamma \leq \gamma_{i,j+1}} \left(\frac{g_i(\gamma_{i,j}) + g_i(\gamma_{i,j+1})}{2} + L \cdot \frac{|\gamma - \gamma_{i,j}| + |\gamma - \gamma_{i,j+1}|}{2} \right) \quad (287)$$

$$= \frac{g_i(\gamma_{i,j}) + g_i(\gamma_{i,j+1})}{2} + L \cdot \frac{\gamma_{i,j+1} - \gamma_{i,j}}{2} \quad (288)$$

$$= \frac{g_i(\gamma_{i,j}) + g_i(\gamma_{i,j+1})}{2} + L \cdot \frac{\alpha_{i+1} - \alpha_i}{2(R-1)}. \quad (289)$$

Similarly, bounding g_{i+1} on the interval $[\gamma_{i,j}, \gamma_{i,j+1}]$ yields

$$\max_{\gamma_{i,j} \leq \gamma \leq \gamma_{i,j+1}} g_{i+1}(\gamma) \leq \max_{\gamma_{i,j} \leq \gamma \leq \gamma_{i,j+1}} (\min \{g_{i+1}(\gamma_{i,j+1}) + L \cdot |\gamma - \gamma_{i,j+1}|, g_{i+1}(\gamma_{i,j}) + L \cdot |\gamma - \gamma_{i,j}|\}) \quad (290)$$

$$\leq \max_{\gamma_{i,j} \leq \gamma \leq \gamma_{i,j+1}} \left(\frac{g_{i+1}(\gamma_{i,j}) + g_{i+1}(\gamma_{i,j+1})}{2} + L \cdot \frac{|\gamma - \gamma_{i,j}| + |\gamma - \gamma_{i,j+1}|}{2} \right) \quad (291)$$

$$= \frac{g_{i+1}(\gamma_{i,j}) + g_{i+1}(\gamma_{i,j+1})}{2} + L \cdot \frac{\gamma_{i,j+1} - \gamma_{i,j}}{2} \quad (292)$$

$$= \frac{g_{i+1}(\gamma_{i,j}) + g_{i+1}(\gamma_{i,j+1})}{2} + L \cdot \frac{\alpha_{i+1} - \alpha_i}{2(R-1)}. \quad (293)$$

We can thus bound $m_{i,j}$ for each i and j

$$m_{i,j} = \max_{\gamma_{i,j} \leq \gamma \leq \gamma_{i,j+1}} \min\{g_i(\gamma), g_{i+1}(\gamma)\} \quad (294)$$

$$\leq \min \left\{ \frac{g_i(\gamma_{i,j}) + g_i(\gamma_{i,j+1})}{2} + L \cdot \frac{\alpha_{i+1} - \alpha_i}{2(R-1)}, \frac{g_{i+1}(\gamma_{i,j}) + g_{i+1}(\gamma_{i,j+1})}{2} + L \cdot \frac{\alpha_{i+1} - \alpha_i}{2(R-1)} \right\} \quad (295)$$

$$= \frac{1}{2} \left(\min\{g_i(\gamma_{i,j}) + g_i(\gamma_{i,j+1}), g_{i+1}(\gamma_{i,j}) + g_{i+1}(\gamma_{i,j+1})\} + L \cdot \frac{\alpha_{i+1} - \alpha_i}{(R-1)} \right) \quad (296)$$

and note that $\alpha_{i+1} - \alpha_i = \frac{b-a}{N-1}$. Then

$$m_{i,j} \leq \frac{1}{2} \left(\min\{g_i(\gamma_{i,j}) + g_i(\gamma_{i,j+1}), g_{i+1}(\gamma_{i,j}) + g_{i+1}(\gamma_{i,j+1})\} + L \cdot \frac{b-a}{(N-1)(R-1)} \right) \quad (297)$$

leading to an expression for an upper bound on M_i

$$M_i \leq \max_{1 \leq j \leq R-1} m_{i,j} \quad (298)$$

$$\leq \max_{1 \leq j \leq R-1} \frac{1}{2} \left(\min\{g_i(\gamma_{i,j}) + g_i(\gamma_{i,j+1}), g_{i+1}(\gamma_{i,j}) + g_{i+1}(\gamma_{i,j+1})\} + L \cdot \frac{b-a}{(N-1)(R-1)} \right) \quad (299)$$

and hence setting

$$M := \max_{1 \leq i \leq N-1} \left(\max_{1 \leq j \leq R-1} \frac{1}{2} \left(\min\{g_i(\gamma_{i,j}) + g_i(\gamma_{i,j+1}), g_{i+1}(\gamma_{i,j}) + g_{i+1}(\gamma_{i,j+1})\} \right) + L \cdot \frac{b-a}{(N-1)(R-1)} \right) \quad (300)$$

yields $\max_{1 \leq i \leq N-1} M_i \leq M$. Equation (300) thus provides us with a computable upper bound of the maximum ℓ_2 -sampling error.

Computing the Lipschitz bound L We now need to find the Lipschitz bound L satisfying (279), which is defined to be the maximum of the Lipschitz bound for g_i and g_{i+1} . Recall that ϕ_R acts on images $x \in \mathbb{R}^{K \times W \times H}$ and that g_i is defined as

$$g_i(\alpha) = \|\phi_R(x, \alpha) - \phi_R(x, \alpha_i)\|_2^2 = \sum_{k=0}^{K-1} \sum_{r=0}^{W-1} \sum_{s=0}^{H-1} (\phi_R(x, \alpha)_{k,r,s} - \phi_R(x, \alpha_i)_{k,r,s})^2 \quad (301)$$

Let c_W and c_H denote the center pixels

$$c_W := \frac{W-1}{2}, \quad c_H := \frac{H-1}{2}. \quad (302)$$

and recall the following quantities from the definition of ϕ_R (see Section D.2):

$$d_{r,s} = \sqrt{(r - c_W)^2 + (s - c_H)^2}, \quad g_{r,s} = \arctan 2(s - c_H, r - c_W) \quad (303)$$

Note that

$$d_{r,s} \geq \min\{c_W, c_H\} \Rightarrow \phi_R(x, \alpha)_{k,r,s} = 0. \quad (304)$$

We thus only need to consider pixels which lie inside the centered disk. We call the collection of such pixels *valid pixels*, denoted by V :

$$V := \{(r, s) \in \mathbb{N}^2 \mid d_{r,s} < \min\{c_W, c_H\}\}. \quad (305)$$

Let $f_1^{r,s} : \mathbb{R} \rightarrow \mathbb{R}$ and $f_2^{r,s} : \mathbb{R} \rightarrow \mathbb{R}$ be functions defined as

$$f_1^{r,s}(\alpha) := c_W + d_{r,s} \cos(g_{r,s} - \alpha), \quad f_2^{r,s}(\alpha) := c_H + d_{r,s} \sin(g_{r,s} - \alpha). \quad (306)$$

Then for any valid pixel (r, s) , the value of the rotated image $\phi_R(x, \alpha)$ is given by

$$\phi_R(x, \alpha)_{k,r,s} = Q_x(k, f_1^{r,s}(\alpha), f_2^{r,s}(\alpha)) \quad (307)$$

where Q_x denotes bilinear interpolation. We define the shorthand

$$g_i^{k,r,s}(\alpha) := (\phi_R(x, \alpha)_{k,r,s} - \phi_R(x, \alpha_i)_{k,r,s})^2 \quad (308)$$

and denote by $L_i^{k,r,s}$ and $L_{i+1}^{k,r,s}$ the Lipschitz constants of $g_i^{k,r,s}$ and $g_{i+1}^{k,r,s}$ on $[\alpha_i, \alpha_{i+1}]$. We can write (301) as

$$g_i(\alpha) = \sum_{k=0}^{K-1} \sum_{(r,s) \in V} g_i^{k,r,s}(\alpha), \quad g_{i+1}(\alpha) = \sum_{k=0}^{K-1} \sum_{(r,s) \in V} g_{i+1}^{k,r,s}(\alpha) \quad (309)$$

and note that Lipschitz constants of g_i and g_{i+1} on $[\alpha_i, \alpha_{i+1}]$ are given by

$$\max_{c, d \in [\alpha_i, \alpha_{i+1}]} \frac{|g_i(c) - g_i(d)|}{|c - d|} \leq \left(\sum_{k=0}^{K-1} \sum_{(r,s) \in V} L_i^{k,r,s} \right) =: L_i \quad (310)$$

$$\max_{c, d \in [\alpha_i, \alpha_{i+1}]} \frac{|g_{i+1}(c) - g_{i+1}(d)|}{|c - d|} \leq \left(\sum_{k=0}^{K-1} \sum_{(r,s) \in V} L_{i+1}^{k,r,s} \right) =: L_{i+1} \quad (311)$$

We can hence determine L according to equation (279) as

$$L = \max_i \{ \max \{ L_i, L_{i+1} \} \}. \quad (312)$$

Without loss of generality, consider $L_i^{k,r,s}$ and note that

$$\max_{c, d \in [\alpha_i, \alpha_{i+1}]} \left| \frac{g_i^{k,r,s}(c) - g_i^{k,r,s}(d)}{c - d} \right| \quad (313)$$

$$= \max_{c, d \in [\alpha_i, \alpha_{i+1}]} \left| \frac{\phi_R(x, c)_{k,r,s} - \phi_R(x, d)_{k,r,s}}{c - d} \right| \cdot |\phi_R(x, c)_{k,r,s} + \phi_R(x, d)_{k,r,s} - 2\phi_R(x, \alpha_i)_{k,r,s}| \quad (314)$$

$$\leq \underbrace{\max_{c, d \in [\alpha_i, \alpha_{i+1}]} \left| \frac{\phi_R(x, c)_{k,r,s} - \phi_R(x, d)_{k,r,s}}{c - d} \right|}_{(I)} \cdot 2 \cdot \underbrace{\max_{\theta \in [\alpha_i, \alpha_{i+1}]} |\phi_R(x, \theta)_{k,r,s} - \phi_R(x, \alpha_i)_{k,r,s}|}_{(II)}. \quad (315)$$

In order to compute a Lipschitz constant for $g_i^{k,r,s}$ on the interval $[\alpha_i, \alpha_{i+1}]$ we thus only need to compute a Lipschitz constant for $\phi_R(x, \cdot)$ on $[\alpha_i, \alpha_{i+1}]$ and an upper bound on (II). For that purpose, note that ϕ_R takes only positive values and consider

$$(II) \leq \max_{\theta \in [\alpha_i, \alpha_{i+1}]} \{ \phi_R(x, \theta)_{k,r,s}, \phi_R(x, \alpha_i)_{k,r,s} \} = \max_{\theta \in [\alpha_i, \alpha_{i+1}]} \phi_R(x, \theta)_{k,r,s} \quad (316)$$

Notice that now both $L_i^{k,r,s}$ and $L_{i+1}^{k,r,s}$ share the same upper bound. Recall (307), that is

$$\phi_R(x, \theta)_{k,r,s} = Q_x(k, f_1^{r,s}(\theta), f_2^{r,s}(\theta)). \quad (317)$$

Now, we upper bound (316) by finding all integer grid pixels that are covered by the trajectory $(f_1^{r,s}(\theta), f_2^{r,s}(\theta))$. Specifically, let

$$\mathcal{P}_{r,s} := \bigcup_{\theta \in [\alpha_i, \alpha_{i+1}]} (\lfloor f_1^{r,s}(\theta) \rfloor, \lfloor f_2^{r,s}(\theta) \rfloor). \quad (318)$$

Since ϕ_R is interpolated from integer pixels, we can consider the maximum over $\mathcal{P}_{r,s}$ in order to upper bound (316):

$$\max_{\theta \in [\alpha_i, \alpha_{i+1}]} \phi_R(x, \theta)_{k,r,s} = \max_{\theta \in [\alpha_i, \alpha_{i+1}]} Q_x(k, f_1^{r,s}(\theta), f_2^{r,s}(\theta)) \quad (319)$$

$$\leq \max_{(i,j) \in \mathcal{P}_{r,s}} \max \{x(k, i, j), x(k, i+1, j), x(k, i, j+1), x(k, i+1, j+1)\} \quad (320)$$

$$= \bar{m}(x, k, \mathcal{P}_{r,s}). \quad (321)$$

We now have to find an upper bound of (I), that is, a Lipschitz constant of $\phi_R(x, \cdot)_{k,r,s}$ on the interval $[\alpha_i, \alpha_{i+1}]$. For that purpose, consider the following. Note that the curve $\rho: [\alpha_i, \alpha_{i+1}] \rightarrow \mathbb{R}^2$, $\rho(t) := (f_1^{r,s}(t), f_2^{r,s}(t))$ is of class C^1 and

$$\frac{df_1^{r,s}(t)}{dt} = \frac{d}{dt} (c_W + d_{r,s} \cos(g_{r,s} - t)) = d_{r,s} \sin(g_{r,s} - t) \quad (322)$$

$$\frac{df_2^{r,s}(t)}{dt} = \frac{d}{dt} (c_H + d_{r,s} \sin(g_{r,s} - t)) = -d_{r,s} \cos(g_{r,s} - t) \quad (323)$$

and hence

$$\|\dot{\rho}(t)\|_2 = \sqrt{\left(\frac{df_1^{r,s}(t)}{dt}\right)^2 + \left(\frac{df_2^{r,s}(t)}{dt}\right)^2} = \sqrt{2} d_{r,s}. \quad (324)$$

By Lemma 9 a Lipschitz constant for the function $\phi_R(x, \cdot)_{k,r,s}$ is thus given by

$$\max_{c,d \in [\alpha_i, \alpha_{i+1}]} \left| \frac{\phi_R(x, c)_{k,r,s} - \phi_R(x, d)_{k,r,s}}{c - d} \right| \leq 2 d_{r,s} \cdot m_\Delta(x, k, \mathcal{P}_{r,s}). \quad (325)$$

We can thus upper bound (I) and (II) in (315) yielding a Lipschitz constant for $g_i^{k,r,s}$ and $g_{i+1}^{k,r,s}$ on $[\alpha_i, \alpha_{i+1}]$

$$\max_{c,d \in [\alpha_i, \alpha_{i+1}]} \left| \frac{g_i^{k,r,s}(c) - g_i^{k,r,s}(d)}{c - d} \right| \leq 2 d_{r,s} \cdot m_\Delta(x, k, \mathcal{P}_{r,s}) \cdot \bar{m}(x, k, \mathcal{P}_{r,s}) = L_i^{k,r,s} = L_{i+1}^{k,r,s}. \quad (326)$$

Finally, we can compute L in (279) as

$$L = \max_i \sum_{k=0}^{K-1} \sum_{(r,s) \in V} L_i^{k,r,s} \quad (327)$$

E.3.2 Computing an upper bound on $M_{a,b}$ for scaling

Recall the Definition of the Scaling transformation $\phi_S: \mathbb{R}^{K \times W \times H} \times \mathbb{R} \rightarrow \mathbb{R}^{K \times W \times H}$, $(x, \alpha) \mapsto \phi_S(x, \alpha)$, where

$$\phi_S(x, \alpha)_{k,r,s} := Q_x \left(k, c_W + \frac{r - c_W}{s}, c_H + \frac{s - c_H}{s} \right). \quad (328)$$

Recall that the set Ω is given by $\Omega = [0, W-1] \times [0, H-1] = \{1, \dots, K\}$ and let

$$\Omega_{\mathbb{N}} := \Omega \cap \mathbb{N}^2 \quad (329)$$

be the set of integers in Ω . Let $f_1^r: [a, b] \rightarrow \mathbb{R}$ and $f_2^{r,s}: [a, b] \rightarrow \mathbb{R}$ be functions defined as

$$f_1^r(\alpha) := c_W + \frac{r - c_W}{\alpha}, \quad f_2^{r,s}(\alpha) = c_H + \frac{s - c_H}{\alpha}. \quad (330)$$

Then, the value of the scaled image $\phi_S(x, \alpha)$ is given by

$$\phi_S(x, \alpha)_{k,r,s} = Q_x(k, f_1^r(\alpha), f_2^s(\alpha)) \quad (331)$$

where Q_x denotes bilinear interpolation. Let

$$\psi_k: [a, b] \rightarrow \mathbb{R} \quad (332)$$

$$\alpha \mapsto Q_x(k, f_1^r(\alpha), f_2^s(\alpha)). \quad (333)$$

We notice that – in contrast to rotations – ψ_k is *not* continuous at every $\alpha \in \mathbb{R}_{>0}$. Namely, when considering scaling factors in $(0, 1)$, bilinear interpolation applies black padding to some $(r, s) \in \Omega$ resulting in discontinuities of ψ_k . To see this, consider the following. The interval $[\alpha_{i+1}, \alpha_i]$ contains a discontinuity of ψ_k , if

$$\begin{cases} \alpha_{i+1} < \frac{r - c_W}{c_W} < \alpha_i & r > c_W, \\ \alpha_{i+1} < \frac{c_W - r}{c_W} < \alpha_i & r < c_W \end{cases} \quad (334)$$

because then $\exists \alpha_0 \in [\alpha_{i+1}, \alpha_i]$ such that $f_1^r(\alpha_0) \in \{0, W - 1\} \subseteq \Omega$ and hence

$$\phi_S(x, \alpha_0)_{k,r,s} \neq 0 \quad (335)$$

but, for $r > c_W$,

$$\phi_S(x, \alpha_0 + \varepsilon)_{k,r,s} = 0 \quad \forall \varepsilon > 0 \quad (336)$$

or, when $r < c_W$,

$$\phi_S(x, \alpha_0 - \varepsilon)_{k,r,s} = 0 \quad \forall \varepsilon > 0. \quad (337)$$

A similar reasoning leads to a discontinuity in the s -coordinates. We can thus define the set of discontinuities of ψ_k as

$$\mathcal{D} := \left(\bigcup_{r=0}^{W-1} \mathcal{D}^r \right) \cup \left(\bigcup_{s=0}^{H-1} \mathcal{D}^s \right) \quad (338)$$

where

$$\mathcal{D}^r := \{\alpha_0 \in [a, b] \mid f_1^r(\alpha_0) \in \{0, W - 1\}\} \quad (339)$$

$$\mathcal{D}^s := \{\alpha_0 \in [a, b] \mid f_2^s(\alpha_0) \in \{0, H - 1\}\}. \quad (340)$$

We notice that $|\mathcal{D}| \leq H + W$ and hence for large enough N , each interval $[\alpha_i, \alpha_{i+1}]$ contains at most 1 discontinuity.

We now derive an upper bound on $M_{a,b}^2$. For that purpose, recall Definition 4: for some $a < b$, and $\{\alpha_i\}_{i=1}^N$

$$M_{a,b} := \max_{a \leq \alpha \leq b} \min_{1 \leq i \leq N} \|\phi_S(x, \alpha) - \phi_S(x, \alpha_i)\|_2. \quad (341)$$

In order to compute an upper bound on (341) for scaling, we are interested in finding $M \geq 0$ such that

$$M_{a,b}^2 \leq M \quad (342)$$

in which case we can replace condition (265) by $\sqrt{M} < r$. For scaling, we sample the α_i according to

$$\alpha_i = \frac{ab}{a + (b - a) \frac{i-1}{N-1}} \quad (343)$$

and note that $\alpha_1 = b$ and $\alpha_N = a$. For $1 \leq i \leq N$ Let g_i be the functions defined by

$$g_i : [a, b] \rightarrow \mathbb{R}_{\geq 0} \quad (344)$$

$$\alpha \mapsto g_i(\alpha) := \|\phi_S(x, \alpha) - \phi_S(x, \alpha_i)\|_2^2. \quad (345)$$

Note that $\forall \alpha \in [a, b]$, $\exists i$ such that $\alpha \in [\alpha_{i+1}, \alpha_i]$. Suppose that N is large enough such that $\forall i: |\mathcal{D} \cap [\alpha_{i+1}, \alpha_i]| \leq 1$ and denote the discontinuity in interval $[\alpha_{i+1}, \alpha_i]$ by t_i if it exists. Let

$$M_i := \begin{cases} \max_{\alpha_{i+1} \leq \alpha \leq \alpha_i} \min\{g_i(\alpha), g_{i+1}(\alpha)\} & [\alpha_{i+1}, \alpha_i] \cap \mathcal{D} = \emptyset \\ \max \left\{ \max_{\alpha_{i+1} \leq \alpha \leq t_i} g_{i+1}(\alpha), \max_{t_i \leq \alpha \leq \alpha_i} g_i(\alpha) \right\} & [\alpha_{i+1}, \alpha_i] \cap \mathcal{D} = \{t_i\} \end{cases} \quad (346)$$

Similarly as in the case for rotations, we find

$$M_{a,b}^2 \leq \max_{1 \leq i \leq N-1} M_i. \quad (347)$$

For simplicity, we assume for the sequel that $\mathcal{D} = \emptyset$. The case where discontinuities exist can be treated analogously. We further divide each interval $[\alpha_{i+1}, \alpha_i]$ by sampling $R \in \mathbb{N}$ points $\{\gamma_{i,j}\}_{j=1}^R$ according to

$$\gamma_{i,j} := \frac{\alpha_i \alpha_{i+1}}{\alpha_i + (\alpha_{i+1} - \alpha_i) \frac{j-1}{R-1}} \quad (348)$$

and define

$$m_{i,j} := \max_{\gamma_{i,j+1} \leq \gamma \leq \gamma_{i,j}} \min\{g_i(\gamma), g_{i+1}(\gamma)\}. \quad (349)$$

We can thus upper bound each M_i by

$$M_i \leq \max_{1 \leq j \leq R-1} m_{i,j}. \quad (350)$$

In order to find an upper bound on $M_{a,b}^2$, we thus need to find upper bound on $m_{i,j}$ and can proceed analogously to rotations. Namely, setting

$$M := \max_{1 \leq i \leq N-1} \left(\max_{1 \leq j \leq R-1} \left(\frac{1}{2} \cdot (\min\{g_i(\gamma_{i,j}) + g_i(\gamma_{i,j+1}), g_{i+1}(\gamma_{i,j}) + g_{i+1}(\gamma_{i,j+1})\}) + L \cdot \frac{\gamma_{i,j} - \gamma_{i,j+1}}{2} \right) \right) \quad (351)$$

yields a computable upper bound of the maximum ℓ_2 sampling error. Computing a Lipschitz constant for g_i and g_{i+1} is also analogous to rotations. The only difference lies in computing a Lipschitz constant for ϕ_S what we will explain in greater detail.

Recall that Lemma 9 provides us with a way to compute a Lipschitz constant for the function $t \mapsto \psi_k(t) := Q_x(k, \rho_1(t), \rho_2(t))$ where ρ is a differentiable curve with values in \mathbb{R}^2 . Namely, a Lipschitz constant for ψ_k is given by

$$L_k = \max_{t \in [t_1, t_2]} \left(\sqrt{2} \|\dot{\rho}(t)\|_2 \cdot m_{\Delta}(x, k, \lfloor \rho(t) \rfloor) \right). \quad (352)$$

Consider the curve

$$\rho(t) := (f_1^r(t), f_2^s(t)), \quad t > 0 \quad (353)$$

and note that it is differentiable with derivatives

$$\frac{df_1^r(t)}{dt} = \frac{d}{dt} \left(c_W + \frac{r - c_W}{t} \right) = \frac{c_W - r}{t^2} \quad (354)$$

$$\frac{df_2^s(t)}{dt} = \frac{d}{dt} \left(c_H + \frac{s - c_H}{t} \right) = \frac{c_H - s}{t^2} \quad (355)$$

and

$$\|\dot{\rho}(t)\|_2 = \frac{1}{t^2} \sqrt{(c_W - r)^2 + (c_H - s)^2}. \quad (356)$$

A Lipschitz constant for $\phi_S(x, \cdot)_{k,r,s}$ is thus given by

$$L_k^{r,s} = \max_{t \in [t_1, t_2]} \left(\frac{\sqrt{(c_W - r)^2 + (c_H - s)^2}}{t^2} \cdot \sqrt{2} m_\Delta(x, k, \lfloor \rho(t) \rfloor) \right) \quad (357)$$

$$\leq \frac{\sqrt{(c_W - r)^2 + (c_H - s)^2}}{t_1^2} \cdot \sqrt{2} \cdot m_\Delta(x, k, \mathcal{P}_{r,s}) \quad (358)$$

where

$$\mathcal{P}_{r,s} = \bigcup_{\alpha \in [t_1, t_2]} \{(\lfloor f_1^r(t) \rfloor), \lfloor f_2^s(t) \rfloor)\}. \quad (359)$$

Finally, setting

$$L_i^{k,r,s} := L_k^{r,s} \cdot \bar{m}(x, k, \mathcal{P}_{r,s}) \quad (360)$$

and

$$L := \sum_{k=0}^{K-1} \sum_{(r,s) \in \Omega_{\mathbb{N}}} L_i^{k,r,s} \quad (361)$$

yields a Lipschitz constant for g_i and g_{i+1} on $[\alpha_{i+1}, \alpha_i]$.

F Proofs of Theoretical Barriers

In this section we show the proof for Lemma 4. Recall that we look at smoothed classifiers with additive Gaussian noise

$$g_h^\varepsilon(x) = \mathbb{E}_\varepsilon [h(x + \varepsilon)], \quad \varepsilon \sim \mathcal{N}(0, \sigma^2 \mathbb{1}_d) \quad (362)$$

and the following families of classifiers:

$$\mathcal{G}_0 := \mathcal{H}, \quad \mathcal{G}_\sigma := \{g_h^\varepsilon \mid \varepsilon \sim \mathcal{N}(0, \sigma^2 \mathbb{1}), h \in \mathcal{H}\}. \quad (363)$$

Lemma 4 (restated). *If $\sigma_1 < \sigma_2$, then $\mathcal{G}_{\sigma_2} \subsetneq \mathcal{G}_{\sigma_1}$.*

Proof. We first show that $\mathcal{G}_{\sigma_2} \subseteq \mathcal{G}_{\sigma_1}$ and then construct a smoothed classifier that belongs to \mathcal{G}_{σ_1} but not to \mathcal{G}_{σ_2} . Let

$$\varepsilon_1 \sim \mathcal{N}(0, \sigma_1^2 \mathbb{1}), \quad \varepsilon_2 \sim \mathcal{N}(0, \sigma_2^2 \mathbb{1}) \quad (364)$$

and suppose that $g_h^{\varepsilon_2} \in \mathcal{G}_{\sigma_2}$ for some $h \in \mathcal{H}$. Inclusion follows if we show that $g_h^{\varepsilon_2} \in \mathcal{G}_{\sigma_1}$. For that purpose, consider

$$h_0 := g_h^{\varepsilon_0}, \quad \varepsilon_0 \sim \mathcal{N}(0, (\sigma_2^2 - \sigma_1^2) \mathbb{1}) \quad (365)$$

and note that h_0 is a classifier. Indeed, for any $x \in \mathcal{X}$

$$\sum_{i=1}^C h_0(x)_i = \sum_{i=1}^C \mathbb{E}_{\varepsilon_0} [h(x + \varepsilon_0)_i] = \mathbb{E}_{\varepsilon_0} \left[\sum_{i=1}^C h(x + \varepsilon_0)_i \right] = 1 \quad (366)$$

and hence $h \in \mathcal{H}$. Note that $\varepsilon_0 + \varepsilon_1 \sim \mathcal{N}(0, \sigma_2^2 \mathbb{1})$. Hence $\varepsilon_0 + \varepsilon_1 \stackrel{d}{=} \varepsilon_2$ and

$$\mathcal{G}_{\sigma_1} \ni g_{h_0}^{\varepsilon_1}(x) = \mathbb{E}_{\varepsilon_1} [h_0(x + \varepsilon_1)] = \mathbb{E}_{\varepsilon_1} [\mathbb{E}_{\varepsilon_0} [h(x + \varepsilon_1 + \varepsilon_0)]] = \mathbb{E}_{\varepsilon_2} [h(x + \varepsilon_2)] = g_h^{\varepsilon_2}(x) \quad (367)$$

yielding $g_h^{\varepsilon_2} = g_{h_0}^{\varepsilon_1} \in \mathcal{G}_{\sigma_1}$ and hence

$$\mathcal{G}_{\sigma_2} \subseteq \mathcal{G}_{\sigma_1}. \quad (368)$$

We now construct a classifier $g_1 \in \mathcal{G}_{\sigma_1}$ such that $g_1 \notin \mathcal{G}_{\sigma_2}$. Without loss of generality, assume that $C = 1$ because otherwise we can apply the following to each component. Let h_1 be the classifier defined as $h_1(x) := \mathbb{1}[x_1 \geq 0]$ and

$$g_1(x) := \mathbb{E}_{\varepsilon_1} [h_1(x + \varepsilon_1)]. \quad (369)$$

where we dropped the sub- and superscripts to simplify notation. Note that $g_1 \in \mathcal{G}_{\sigma_1}$. Let $e_1 = (1, 0, \dots, 0)^T \in \mathbb{R}^d$, μ_{ε_1} be the density function of ε and $\langle \cdot, \cdot \rangle$ denote the standard scalar product in \mathbb{R}^d . Consider

$$\langle e_1, \nabla_x g_1(x) \rangle = \left\langle e_1, \nabla_x \int_{\mathbb{R}^d} h_1(x + s) \mu_\varepsilon(s) ds \right\rangle = \left\langle e_1, \nabla_x \int_{\mathbb{R}^d} h_1(t) \mu_\varepsilon(t - x) dt \right\rangle \quad (370)$$

$$= \left\langle e_1, \int_{\mathbb{R}^d} h_1(t) \nabla_x (\mu_\varepsilon(t - x)) dt \right\rangle \quad (371)$$

$$= \left\langle e_1, \frac{1}{(2\pi\sigma_1^2)^{\frac{d}{2}}} \int_{\mathbb{R}^d} h_1(t) \nabla_x \left(\exp \left(-\frac{\|t - x\|_2^2}{2\sigma_1^2} \right) \right) dt \right\rangle \quad (372)$$

$$= \frac{1}{(2\pi\sigma_1^2)^{\frac{d}{2}}} \int_{\mathbb{R}^d} h_1(t) \left\langle e_1, \nabla_x \left(\exp \left(-\frac{\|t - x\|_2^2}{2\sigma_1^2} \right) \right) \right\rangle dt \quad (373)$$

$$= \frac{1}{(2\pi\sigma_1^2)^{\frac{d}{2}}} \int_{\mathbb{R}^d} h_1(t) \exp \left(-\frac{\|t - x\|_2^2}{2\sigma_1^2} \right) \frac{t_1 - x_1}{\sigma_1^2} dt \quad (374)$$

$$= \frac{1}{(2\pi\sigma_1^2)^{\frac{1}{2}}} \int_0^\infty \exp \left(-\frac{(t_1 - x_1)^2}{2\sigma_1^2} \right) \frac{t_1 - x_1}{\sigma_1^2} dt_1. \quad (375)$$

Thus, evaluating $\langle e_1, \nabla_x g_1(x) \rangle$ at $x = 0$ yields

$$\langle e_1, \nabla_x |_{x=0} g_1(x) \rangle = \frac{1}{\sqrt{2\pi\sigma_1^2}}. \quad (376)$$

Let $\tau := \sqrt{\sigma_2^2 - \sigma_1^2}$. Note that, by (367), for any $g_2 \in \mathcal{G}_{\sigma_2}$ there exists a smoothed classifier $g_0 \in \mathcal{G}_\tau$ such that

$$g_2(x) = \mathbb{E}_{\varepsilon_1} [g_0(x + \varepsilon_1)]. \quad (377)$$

We now show that for any $\sigma > 0$ and $g \in \mathcal{G}_\sigma$, the gradient of g exists and is bounded. For that purpose, let $v \in \mathbb{R}^d$ be a unit vector and consider

$$\langle v, \nabla_x g(x) \rangle = \frac{1}{(2\pi\sigma^2)^{\frac{d}{2}}} \int_{\mathbb{R}^d} h_1(t) \left\langle v, \nabla_x \left(\exp \left(-\frac{\|t-x\|_2^2}{2\sigma^2} \right) \right) \right\rangle dt \quad (378)$$

$$= \frac{1}{(2\pi\sigma^2)^{\frac{d}{2}}} \frac{1}{\sigma^2} \int_{\mathbb{R}^d} h_1(t) \langle v, t-x \rangle \exp \left(-\frac{\|t-x\|_2^2}{2\sigma^2} \right) dt \quad (379)$$

$$\stackrel{(i)}{\leq} \frac{1}{(2\pi\sigma^2)^{\frac{d}{2}}} \frac{1}{\sigma^2} \int_{\mathbb{R}^d} |\langle v, t-x \rangle| \exp \left(-\frac{\|t-x\|_2^2}{2\sigma^2} \right) dt \quad (380)$$

$$\stackrel{(ii)}{=} \frac{1}{(2\pi)^{\frac{d}{2}}} \frac{1}{\sigma} \int_{\mathbb{R}^d} |\langle v, s \rangle| \exp \left(-\frac{1}{2} \|s\|_2^2 \right) ds =: I_v \quad (381)$$

where (i) follows from $|h_1(t)| \leq 1$ and in (ii) we substitute $s = \frac{t-x}{\sigma}$. Now let $\mathcal{B}_v = \{v_1, v_2, \dots, v_d\}$ be an orthonormal basis of \mathbb{R}^d with $v_1 = v$ and denote by P_v its transformation matrix with columns v_1, \dots, v_d . Then

$$I_v = \frac{1}{(2\pi)^{\frac{d}{2}}} \frac{1}{\sigma} \int_{\mathbb{R}^d} |\langle P_v^T v, P_v^T s \rangle| \exp \left(-\frac{1}{2} \|P_v^T s\|_2^2 \right) ds \stackrel{(iii)}{=} \frac{1}{(2\pi)^{\frac{d}{2}}} \frac{1}{\sigma} \int_{\mathbb{R}^d} |\langle e_1, u \rangle| \exp \left(-\frac{1}{2} \|u\|_2^2 \right) du \quad (382)$$

$$= \frac{1}{\sqrt{2\pi}} \frac{1}{\sigma} \left(\int_{\mathbb{R}} |u_1| \exp \left(-\frac{1}{2} u_1^2 \right) du_1 \right) \cdot \left(\frac{1}{\sqrt{2\pi}} \int_{\mathbb{R}} \exp \left(-\frac{1}{2} z^2 \right) dz \right)^{d-1} \quad (383)$$

$$= \frac{1}{\sqrt{2\pi}} \frac{1}{\sigma} \cdot 2 \cdot \int_0^\infty u_1 \exp \left(-\frac{1}{2} u_1^2 \right) du_1 = \frac{1}{\sigma} \sqrt{\frac{2}{\pi}}. \quad (384)$$

where (iii) follows from the change of variables $u = P_v^T s$. Since the choice of v was arbitrary, we get

$$\|\nabla_x g(x)\|_2 = \left\langle \frac{\nabla_x g(x)}{\|\nabla_x g(x)\|_2}, \nabla_x g(x) \right\rangle \leq \frac{1}{\sigma} \sqrt{\frac{2}{\pi}}. \quad (385)$$

Recall that $g_0 \in \mathcal{G}_\tau$ and hence

$$\|\nabla_x g_0(x)\|_2 \leq \frac{1}{\tau} \sqrt{\frac{2}{\pi}} =: \kappa. \quad (386)$$

Let $p := g_0(0)$. Then, for any $x \in \mathbb{R}^d$

$$p - g_0(x) \leq |g_0(x) - g_0(0)| \leq \kappa \cdot \|x\|_2 \quad (387)$$

and thus

$$\|x\|_2 \leq \frac{p}{2\kappa} \Rightarrow g_0(x) \geq \frac{p}{2} \quad (388)$$

$$\|x\|_2 \leq \frac{1-p}{2\kappa} \Rightarrow g_0(x) \leq \frac{1+p}{2}. \quad (389)$$

Now consider

$$\langle e_1, \nabla_x|_{x=0} g_2(x) \rangle = \left\langle e_1, \frac{1}{(2\pi\sigma_1^2)^{\frac{d}{2}}} \int_{\mathbb{R}^d} g_0(t) \cdot \nabla_x|_{x=0} \left(\exp\left(-\frac{\|t-x\|_2^2}{2\sigma_1^2}\right) \right) dt \right\rangle \quad (390)$$

$$= \frac{1}{(2\pi\sigma_1^2)^{\frac{d}{2}}} \int_{\mathbb{R}^d} g_0(t) \cdot \exp\left(-\frac{\|t\|_2^2}{2\sigma_1^2}\right) \frac{t_1}{\sigma_1^2} dt =: I \quad (391)$$

and

$$I_1 := \frac{1}{(2\pi\sigma_1^2)^{\frac{d}{2}}} \left(\int_{\mathbb{R}^d \cap \{t_1 \geq 0\}} \frac{t_1}{\sigma_1^2} \exp\left(-\frac{\|t\|_2^2}{2\sigma_1^2}\right) dt \right) \quad (392)$$

$$I_2 := \frac{1}{(2\pi\sigma_1^2)^{\frac{d}{2}}} \left(\int_{\mathbb{R}^d \cap \{t_1 \geq 0\}} (1 - g_0(t)) \frac{t_1}{\sigma_1^2} \cdot \exp\left(-\frac{\|t\|_2^2}{2\sigma_1^2}\right) dt \right) \quad (393)$$

$$I_3 := \frac{1}{(2\pi\sigma_1^2)^{\frac{d}{2}}} \left(\int_{\mathbb{R}^d \cap \{t_1 < 0\}} g_0(t) \frac{t_1}{\sigma_1^2} \cdot \exp\left(-\frac{\|t\|_2^2}{2\sigma_1^2}\right) dt \right). \quad (394)$$

Note that $I = I_1 - I_2 + I_3$ and

$$I_1 = \frac{1}{\sqrt{2\pi\sigma_1^2}}. \quad (395)$$

Now, we compute a lower and upper bounds on I_2 and I_3 . For that purpose, let

$$S_+^2 := \{t \in \mathbb{R}^d \mid \|t\|_2 \leq \frac{1-p}{2\kappa} \wedge t_1 \geq 0\}, \quad S_+^\infty := \{t \in \mathbb{R}^d \mid \|t\|_\infty \leq \frac{1-p}{2\kappa\sqrt{d}} \wedge t_1 \geq 0\} \quad (396)$$

$$S_-^2 := \{t \in \mathbb{R}^d \mid \|t\|_2 \leq \frac{p}{2\kappa} \wedge t_1 < 0\}, \quad S_-^\infty := \{t \in \mathbb{R}^d \mid \|t\|_\infty \leq \frac{p}{2\kappa\sqrt{d}} \wedge t_1 < 0\} \quad (397)$$

and note that $S_+^\infty \subseteq S_+^2$ and $S_-^\infty \subseteq S_-^2$. Then

$$I_2 \geq \frac{1}{(2\pi\sigma_1^2)^{\frac{d}{2}}} \int_{S_+^2} (1 - g_0(t)) \frac{t_1}{\sigma_1^2} \cdot \exp\left(-\frac{\|t\|_2^2}{2\sigma_1^2}\right) dt \stackrel{(389)}{\geq} \frac{1}{(2\pi\sigma_1^2)^{\frac{d}{2}}} \int_{S_+^\infty} \frac{1-p}{2} \frac{t_1}{\sigma_1^2} \cdot \exp\left(-\frac{\|t\|_2^2}{2\sigma_1^2}\right) dt \quad (398)$$

$$\geq \frac{1-p}{2} \frac{1}{\sigma_1} \frac{1}{(2\pi\sigma_1^2)^{\frac{d}{2}}} \int_{S_+^\infty} \frac{t_1}{\sigma_1} \cdot \exp\left(-\frac{\|t\|_2^2}{2\sigma_1^2}\right) dt \quad (399)$$

$$= \frac{1-p}{2} \frac{1}{\sigma_1} \left(\frac{1}{\sqrt{2\pi}} \int_0^{\frac{1-p}{2\kappa\sqrt{d}\sigma_1}} s_1 \exp\left(-\frac{1}{2}s_1^2\right) ds_1 \right) \cdot \left(\frac{1}{\sqrt{2\pi}} \int_{-\frac{1-p}{2\kappa\sqrt{d}\sigma_1}}^{\frac{1-p}{2\kappa\sqrt{d}\sigma_1}} \exp\left(-\frac{1}{2}z^2\right) dz \right)^{d-1} \quad (400)$$

$$= \frac{1-p}{2\sigma_1} \frac{1}{\sqrt{2\pi}} \left(1 - \exp\left(-\frac{(1-p)^2}{8d\kappa^2\sigma_1^2}\right) \right) \cdot \left(2\Phi\left(\frac{1-p}{2\kappa\sqrt{d}\sigma_1}\right) - 1 \right)^{d-1}. \quad (401)$$

Similarly, we upper bound I_3

$$I_3 \leq \frac{1}{(2\pi\sigma_1^2)^{\frac{d}{2}}} \int_{S_-^2} g_0(t) \frac{t_1}{\sigma_1^2} \cdot \exp\left(-\frac{\|t\|_2^2}{2\sigma_1^2}\right) dt \stackrel{(388)}{\leq} \frac{1}{(2\pi\sigma_1^2)^{\frac{d}{2}}} \int_{S_-^2} \frac{p}{2} \frac{t_1}{\sigma_1^2} \cdot \exp\left(-\frac{\|t\|_2^2}{2\sigma_1^2}\right) dt \quad (402)$$

$$\leq \frac{p}{2} \frac{1}{\sigma_1} \frac{1}{(2\pi\sigma_1^2)^{\frac{d}{2}}} \int_{S_-^\infty} \frac{t_1}{\sigma_1} \cdot \exp\left(-\frac{\|t\|_2^2}{2\sigma_1^2}\right) dt \quad (403)$$

$$= \frac{p}{2} \frac{1}{\sigma_1} \left(\frac{1}{\sqrt{2\pi}} \int_{-\frac{p}{2\kappa\sqrt{d}\sigma_1}}^0 s_1 \exp\left(-\frac{1}{2}s_1^2\right) ds_1 \right) \cdot \left(\frac{1}{\sqrt{2\pi}} \int_{-\frac{p}{2\kappa\sqrt{d}\sigma_1}}^{\frac{p}{2\kappa\sqrt{d}\sigma_1}} \exp\left(-\frac{1}{2}z^2\right) dz \right)^{d-1} \quad (404)$$

$$= \frac{p}{2\sigma_1} \frac{1}{\sqrt{2\pi}} \left(\exp\left(\frac{p^2}{8d\kappa^2\sigma_1^2}\right) - 1 \right) \cdot \left(2\Phi\left(\frac{p}{2\kappa\sqrt{d}\sigma_1}\right) - 1 \right)^{d-1}. \quad (405)$$

Note that

$$I_2 \begin{cases} > 0 & p \in [0, 1) \\ = 1 & p = 1 \end{cases} \quad \text{and} \quad I_3 \begin{cases} < 0 & p \in (0, 1] \\ = 0 & p = 0 \end{cases} \quad (406)$$

and hence $I_3 - I_2 < 0$ for $p \in [0, 1]$. Thus, we can upper bound (391) by

$$\langle e_1, \nabla_x|_{x=0} g_2(x) \rangle = I_1 - I_2 + I_3 < \frac{1}{\sqrt{2\pi\sigma_1^2}} \stackrel{(376)}{=} \langle e_1, \nabla_x|_{x=0} g_1(x) \rangle \quad (407)$$

Since the choice of g_2 was arbitrary, we find that $g_1 \notin \mathcal{G}_{\sigma_2}$ and hence together with (368)

$$\mathcal{G}_{\sigma_2} \subsetneq \mathcal{G}_{\sigma_1}. \quad (408)$$

□

G Robustness Certificates

When we focus on general transformations, instead of additive noises as in previous work, there is a subtle difference. In this paper, given a data example x , our algorithm tries to certify the following property

(C1) $g_h^\varepsilon(\phi(x, \alpha))$ predicts the same as $g_h^\varepsilon(x)$.

But what if we are given a data point $\phi(x, \beta)$ with an unknown β ? Directly applying our algorithm would lead to

(C2) $g_h^\varepsilon(\phi(\phi(x, \beta), \alpha))$ predicts the same as $g_h^\varepsilon(\phi(x, \beta))$

The meaning of this can be confusing. However, for transformations that are *reversible*:

$$\forall \beta \in A. \forall x \in \mathcal{X}. \exists \alpha \in A. \phi(\phi(x, \beta), \alpha) = x$$

the system can also guarantee

(C3) $g_h^\varepsilon(\phi(x, \beta))$ predicts the same as $g_h^\varepsilon(x)$.

In the existing work on certifying robustness against ℓ_p norm bounded perturbation, both C1 and C3 are automatically satisfied since the additive noise is reversible. Moreover, for many transformations that we focused on in this paper, namely brightness, contrast, and translation, they are also reversible and thus can also certify both C1 and C3. However, for other transformations such as Gaussian blur, rotation, and scaling, the function smoothing-based technique can only certify C1. This illustrates one important difference between function smoothing over general transformations and specific additive noises, and we believe it is exciting future work to fully understand the differences, and application scenarios, of these three different types of certificates. Moreover, this would also shed light on future research on understanding the gap between $g_h^\varepsilon(x)$ and the ground truth as the utility depends on whether $g_h^\varepsilon(x)$ agrees with the ground truth. Some recent endeavors by other researchers already start to touch this question (Jacobsen et al., 2019), which we believe will become increasingly important.

H Experiment Details

In this section, we provide our experimental setup, dataset specifications and analysis for each transformation in detail.

H.1 Datasets and Certification

H.1.1 Datasets

We run experiments on the three publicly available MNIST (LeCun et al., 1998), CIFAR-10 (Krizhevsky et al., 2009) and ImageNet-1k datasets (Deng et al., 2009).

- **MNIST** contains 60,000 training and 10,000 testing images of handwritten digits from 0 to 9 corresponding to 10 classes. Each image is a gray scale 28×28 image normalized to $[0, 1]$. Before feeding the images to the models, we follow common practice and scale the pixel values to $[-1, 1]$.
- **CIFAR-10** contains natural images of 10 classes with 50,000 training and 10,000 testing samples. Each image is a RGB-image of resolution 32×32 pixels. We normalize each image to $[0, 1]$ and then scale each image by subtracting $(0.485, 0.456, 0.406)$ from each channel and divide by $(0.229, 0.224, 0.225)$ (also per channel).
- **ImageNet-1k**¹ contains over 10^6 training and 50,000 validation images from 1,000 classes. Since the image resolutions vary, we firstly scale each image so that the short edge is 256-pixel long, then apply center cropping to get 224×224 -sized 3-channel colored images. Similarly, the pixel colors are normalized to range $[0, 1]$. We then scale each image by subtracting $(0.4914, 0.4822, 0.4465)$ from each channel and divide by $(0.2023, 0.1994, 0.2010)$ (also per channel).

Note that preprocessing does not affect the measurement of perturbation - we report perturbation magnitude with respect to the original image.

H.1.2 Robustness Certification

For all randomized-smoothing based robust certification, we follow common practice and adopt $\alpha = 0.001$, such that the certified radii hold true with probability at least $1 - \alpha = 99.9\%$ (per sample).

The number of samples, N , is another important hyperparameter for randomized-smoothing. Larger N results in better robust radii but consumes longer running time as shown in (Cohen et al., 2019). In previous works, the common choice is $N = 10^5$. We also adopt $N = 10^5$ for MNIST and CIFAR-10 models, while for ImageNet, we use $N = 10^4$. Note that for rotation and scaling transformation, we adopt early-stop strategy once we get enough samples to certify robustness, so the actual N is much smaller than the setting. For predicted class guessing, we adopt $N_0 = 100$ throughout all experiments which is in line with previous works.

The reported robust accuracy is actually the *approximate robust accuracy* as mentioned in the main part of this paper. We compute this metric on a subset of the test set. Following common practice, we construct the subset as follows:

- On MNIST, pick one sample in every 20 samples. In total 500 samples.
- On CIFAR-10, pick one sample in every 20 samples. In total 500 samples.
- On ImageNet-1k, pick one sample in every 500 samples. In total 100 samples.

¹<http://image-net.org/challenges/LSVRC/2012/>

For each setting, we run the certification process 5 times. Due to the large number of N , the robust accuracies are mostly the same and always differ within 0.2% on MNIST and CIFAR-10, and within 1% on ImageNet-1k. When there are multiple numbers among repeated runs, we report the mode.

H.1.3 Rotation and Scaling: Progressive Certification

According to Theorem 2, once we have computed $M_{a,b}$, we need to certify that for every sampled parameter α_i , its robust radius satisfies $r > M$. Comparing with the normal usage, where we need to compute the exact r , here we just need to know $r > M$. We exploit this and adopt a progressive certification strategy in order to speed up certification. We first determine the batch size B . Then, we sample B noisy inputs in order to derive the current r_0 with confidence $1 - \alpha$. Once we have $r_0 > M$, we early-stop the process, since in this case we already know that $r > M$. Otherwise, we continue sampling another batch of size B until termination or failing to certify after N inputs. In practice, we set $B = 400$. We find that usually r is much larger than $M_{a,b}$, and hence we can obtain that $r > M_{a,b}$ after a relatively small number of batches. Comparing with generating and computing all N samples, this progressive certification strategy significantly improves speed.

H.2 Classification Models

H.2.1 Model Architectures

For each dataset, we use one neural network architecture, aligning with models used in the literature such as (Wong et al., 2018; Cohen et al., 2019; Salman et al., 2019b; Fischer et al., 2020).

- **MNIST.** Table 4 shows the architecture used in greater detail. The model is the identical with the one used in (Wong et al., 2018).
- **CIFAR-10.** Here we use ResNet-110, a 110-layer ResNet model which is the same as (Cohen et al., 2019; Salman et al., 2019a).
- **ImageNet-1k.** Here, we use ResNet-50 (He et al., 2016) aligning with the model chosen in (Cohen et al., 2019; Salman et al., 2019b; Fischer et al., 2020).

On ImageNet we initialize our models with weights obtained from pretrained classifiers. Namely, for training with rotation and scaling transformations, we initialize the model with weights from the best trained models in (Salman et al., 2019b). For training with Gaussian blur, translation, and contrast and brightness transformations, we initialize the model weights from (He et al., 2016). We then retrain the model with corresponding data augmentation. On both MNIST and CIFAR-10 we train each model from scratch.

Table 4: MNIST model architecture. “Conv2d” stands for 2-dimensional convolutional layer. All convolutional layers use 1-pixel padding for both sides of each dimension. “FC” stands for a fully-connected layer.

Layer	Activation	in-channels	out-channels	kernel size	stride
Conv 2d	ReLU	1	32	3	1
Conv 2d	ReLU	32	32	4	2
Conv 2d	ReLU	32	64	3	1
Conv 2d	ReLU	64	64	4	2
Flatten	-	64	64×7×7	-	-
FC	ReLU	64×7×7	512	-	-
FC	ReLU	512	512	-	-
FC	Softmax	512	10	-	-

H.2.2 Training

We implement all models in Python using the PyTorch² Library and train them on a single NVIDIA GTX 1080Ti GPU.

Hyperparameters On *MNIST*, we train each model using SGD with weight decay 10^{-4} , batch size 400, and learning rate 0.1 for 20 epochs. On *CIFAR-10*, for the Gaussian blur transformation we use the Adam optimizer with the learning rate set to 0.1, while for other transformations we use SGD with learning rate 0.1 and weight decay 10^{-4} . The learning rate is multiplied by 0.1 for every 30 epochs. and we train each model for 90 epochs. On *ImageNet-1k*, we use SGD optimizer with a small learning rate set to 0.001 and weight decay 10^{-4} . We train the models only for 3 epochs, since the accuracy on the training set stabilizes after 3 epochs. On MNIST and CIFAR-10 we set the batch size to 400 and on ImageNet-1k to 80 due to the larger image resolution.

Data Augmentation During training, we first do random flipping (except on MNIST), then data augmentation by sampling transformation parameters from the corresponding noise distribution and apply the resulting transformation to the image. The specific distributions vary for different transformations.

H.3 Detailed Experimental Results for Noise Distribution Tuning

We explore smoothing using exponential, uniform and Gaussian distributions for a fixed variance level for Gaussian blur transformation on CIFAR-10. The results are shown in Table 5. The “Robust Acc. for Radius $\alpha \leq$ ” stands for the robust accuracy permitting any Gaussian blur with parameter α smaller or equal than the corresponding threshold. For the case $\sigma_{\text{train}}^2 = 100$, we show robust accuracy curves corresponding to different noise distributions in Figure 3.

Table 5: Comparison of different noise distributions for *Gaussian Blur* on CIFAR-10. σ_{train}^2 stands for the variance of distribution from which we sample noise in training data augmentation. We highlight best numbers in **bold** for the experiments with the same variance.

Variance	Setting	Clean	Robust Acc. for radius $\alpha \leq$							
		Acc.	1.0	4.0	9.0	16.0	25.0	36.0	49.0	64.0
$\sigma_{\text{train}}^2 = 4.0$	Exp(1/2)	88.2%	84.6%	76.6%	58.4%	0.0%	0.0%	0.0%	0.0%	0.0%
	$\mathcal{U}(0, \alpha = 4\sqrt{3})$	83.2%	80.8%	0.0%	0.0%	0.0%	0.0%	0.0%	0.0%	0.0%
	$\mathcal{N}(0, \sigma^2 = \frac{4\pi}{\pi-2})$	81.4%	77.6%	69.6%	47.0%	0.0%	0.0%	0.0%	0.0%	0.0%
$\sigma_{\text{train}}^2 = 100.0$	Exp(1/10)	76.4%	74.2%	70.0%	62.8%	55.4%	47.8%	40.8%	31.2%	20.2%
	$\mathcal{U}(0, \alpha = 20\sqrt{3})$	66.8%	65.2%	60.4%	55.8%	45.6%	0.0%	0.0%	0.0%	0.0%
	$\mathcal{N}(0, \sigma^2 = \frac{100\pi}{\pi-2})$	69.8%	68.2%	64.2%	57.4%	50.6%	42.4%	35.4%	0.0%	0.0%
$\sigma_{\text{train}}^2 = 400.0$	Exp(1/20)	70.4%	69.8%	67.0%	63.4%	57.0%	49.4%	43.2%	37.4%	32.6%
	$\mathcal{U}([0, 40\sqrt{3}])$	57.0%	56.8%	54.8%	51.0%	47.8%	40.8%	0.0%	0.0%	0.0%
	$\mathcal{N}(0, \frac{400\pi}{\pi-2})$	64.8%	63.6%	61.0%	56.6%	50.4%	43.6%	37.0%	32.4%	27.4%

From both the table and figure, we find that smoothing using exponential noise is much better than using uniform noise or normal distribution noise, when the noise variance is the same, which confirms our theoretical analysis.

²<https://pytorch.org/>

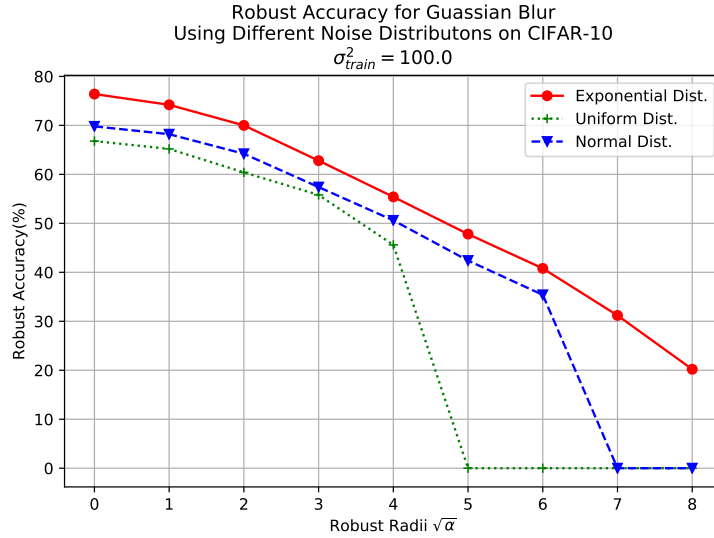


Figure 3: Comparison of different noise distributions for Gaussian blur on CIFAR-10 with $\sigma_{\text{train}}^2 = 100$.

H.4 Detailed Experimental Results for specific Semantic Transformations

H.4.1 Gaussian Blur

Table 6 presents the robust accuracy for different kernel radii α for Gaussian blur transformation. We adopt exponential noise $\text{Exp}([0, 1/\lambda])$ for both training data augmentation and robust certification and in each setting, we use the same λ for training and certifying.

To compare the effect of noise variance, in Figure 4 we compare different λ on CIFAR-10. From both the table and figure, we observe that larger λ , i.e., larger variance brings better robust accuracy for large perturbation, but on the other hand hurts robust accuracy for small perturbations and clean accuracy. Previous works on ℓ_2 robustness (Cohen et al., 2019) and our theoretical analysis (Corollary 6) also indicate a similar phenomenon.

Table 6: Clean and robust accuracy for different kernel radii for *Gaussian Blur*. Smoothing and data augmentation are performed with exponential noise $\text{Exp}(1/\lambda)$.

Dataset	Exp($1/\lambda$)	Clean Acc.	Robust Acc. for radius $\alpha \leq$							
			1.0	4.0	9.0	16.0	25.0	36.0	49.0	64.0
MNIST	$\lambda = 2.0$	97.8%	97.6%	95.8%	90.4%	70.4%	0.0%			
	$\lambda = 10.0$	93.8%	93.6%	91.2%	89.2%	85.8%	80.8%	73.2%	62.8%	44.8%
CIFAR-10	$\lambda = 2.0$	88.2%	84.6%	76.6%	58.4%	0.0%				
	$\lambda = 10.0$	76.4%	74.2%	70.0%	62.8%	55.4%	47.8%	40.8%	31.2%	20.2%
	$\lambda = 20.0$	70.4%	69.8%	67.0%	63.4%	57.0%	49.4%	43.2%	37.4%	32.6%
ImageNet	$\lambda = 10.0$	60.0%	58.0%	58.0%	55.0%	51.0%	42.0%	37.0%	24.0%	20.0%

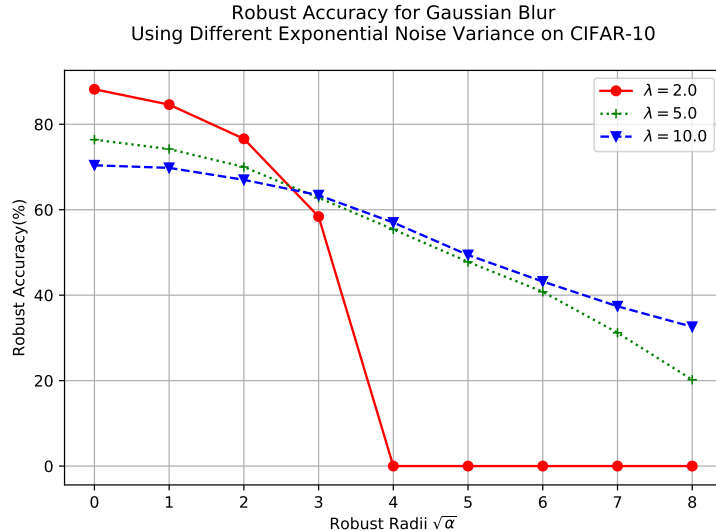


Figure 4: Comparison of different λ used in noise distribution $\text{Exp}(1/\lambda)$ for Gaussian blur on CIFAR-10.

H.4.2 Brightness and Contrast

We present the clean and robust accuracy against brightness change, contrast change and the composition of brightness and contrast change in Tables 7, 8 and 9. The parameter b stands for the brightness change, which adds b uniformly to every pixel value. Note that the pixel value is normalized to the range $[0, 1]$ so $b = +0.1$ stands for brightness change $+25.5/255$. The parameter k determines the change in contrast and is applied by uniformly multiplying all pixel values with e^k . For example, $e^k - 1 = -10\%$ means -10% contrast adjustment and multiplying all pixel values by 0.9. The training and certification settings are specified by σ_b and σ_s , which are the standard deviation of the Gaussian noise applied on brightness and contrast dimension respectively. We use the same noise magnitude during training and certification.

Table 7: Clean and robust accuracy for *Brightness*. During inference with the smoothed classifier, we set $\sigma_s = 0$ to disable contrast changes which improves robust accuracy.

Dataset	Setting	Clean Acc.	Robust Acc. for $ b \leq$					
			0.1	0.2	0.3	0.4	0.5	0.6
MNIST	$\sigma_b = \sigma_s = 0.3$	98.6%	98.6%	98.6%	98.6%	98.6%	98.6%	98.6%
CIFAR-10	$\sigma_b = \sigma_s = 0.2$	84.8%	84.2%	83.6%	83.0%	82.6%	82.0%	81.2%
ImageNet	$\sigma_b = \sigma_s = 0.2$	68.0%	64.0%	63.0%	61.0%	60.0%	60.0%	59.0%

H.4.3 Translation

The robust accuracy against translation with reflection-padding and black-padding is shown in Tables 10 and 11. We report the robust accuracy obtained from two methods: randomized smoothing and enumeration. Note that when we consider translation with black-padding, we can only use the enumeration approach. The models are trained with data augmentation using displacement parameters sampled from Gaussian noise. The same variance σ is used for both x - and y - axis. We use the same distribution when certifying with

Table 8: Clean and robust accuracy for *Contrast*.

Dataset	Setting	Clean Acc.	Robust Acc. for $ e^k - 1 \leq$				
			10%	20%	30%	40%	50%
MNIST	$\sigma_b = \sigma_s = 0.3$	98.6%	98.6%	98.6%	98.6%	97.8%	0.0%
CIFAR-10	$\sigma_b = \sigma_s = 0.2$	85.0%	82.8%	80.6%	76.8%	0.0%	
ImageNet	$\sigma_b = \sigma_s = 0.2$	67.0%	62.0%	60.0%	56.0%	0.0%	

Table 9: Clean and robust accuracy for *Contrast and Brightness Composition*.

Dataset	Setting	Clean Acc.	Robust Acc. for $ e^k - 1 \leq 20\% \wedge b \leq$					
			0.0	0.1	0.2	0.3	0.4	0.5
MNIST	$\sigma_b = \sigma_s = 0.3$	98.6%	98.6%	98.6%	98.6%	98.6%	98.2%	97.8%
CIFAR-10	$\sigma_b = \sigma_s = 0.2$	85.0%	80.0%	78.4%	77.4%	75.8%	72.0%	0.0%
ImageNet	$\sigma_b = \sigma_s = 0.2$	67.0%	60.0%	60.0%	57.0%	56.0%	54.0%	0.0%

randomized smoothing. The quantity $\sqrt{\Delta x^2 + \Delta y^2}$ in the tables specifies the displacement magnitude, where Δx corresponds to the x axis displacement and Δy to the y axis displacement.

Table 10: Clean and robust accuracy for *Translation with reflection-padding*.

Dataset	$\mathcal{N}(0, \sigma^2)$	Method	Clean Acc.	Robust Acc. for $\sqrt{\Delta x^2 + \Delta y^2} \leq$								
				1.0	2.0	5.0	7.5	10.0	12.5	15.0	17.5	20.0
MNIST	$\sigma = 3.0$	Rand. Smooth	99.0%	99.0%	98.6%	96.0%	92.2%	59.0%	0.0%			
		Enumeration	99.4%	99.4%	98.2%	96.8%	91.8%	74.8%	23.2%	2.8%	0.2%	0.0%
	$\sigma = 10.0$	Rand. Smooth	99.4%	99.4%	99.2%	99.2%	98.6%	97.8%	97.2%	96.2%	94.6%	93.2%
		Enumeration	99.0%	99.0%	98.6%	96.4%	93.0%	90.0%	85.6%	84.2%	82.4%	81.8%
CIFAR-10	$\sigma = 3.0$	Rand. Smooth	90.4%	88.8%	86.6%	76.0%	64.6%	49.6%	0.0%			
		Enumeration	89.4%	89.4%	84.6%	74.4%	62.6%	51.6%	35.2%	25.6%	19.6%	16.0%
	$\sigma = 10.0$	Rand. Smooth	88.0%	87.2%	86.4%	84.8%	82.0%	79.8%	76.0%	71.2%	67.0%	63.8%
		Enumeration	87.6%	87.6%	82.0%	74.4%	68.2%	64.6%	57.4%	51.8%	49.2%	47.2%
ImageNet	$\sigma = 3.0$	Rand. Smooth	63.0%	63.0%	62.0%	56.0%	54.0%	0.0%				
		Enumeration	63.0%	63.0%	58.0%	56.0%	54.0%	53.0%	53.0%	50.0%	48%	47.0%
	$\sigma = 10.0$	Rand. Smooth	66.0%	66.0%	66.0%	63.0%	61.0%	60.0%	57.0%	54.0%	54.0%	53.0%
		Enumeration	69.0%	69.0%	59.0%	54.0%	53.0%	53.0%	53.0%	53.0%	52.0%	52.0%

Table 11: Clean and robust accuracy for *Translation with black-padding*.

Dataset	$\mathcal{N}(0, \sigma^2)$	Clean Acc.	Robust Acc. for $\sqrt{\Delta x^2 + \Delta y^2} \leq$								
			1.0	2.0	5.0	7.5	10.0	12.5	15.0	17.5	20.0
MNIST	$\sigma = 3.0$	99.2%	99.2%	98.8%	93.6%	80.4%	45.8%	8.6%	3.2%	2.6%	2.6%
	$\sigma = 10.0$	99.0%	99.0%	97.6%	94.8%	88.4%	75.2%	42.4%	12.4%	0.8%	0.2%
CIFAR-10	$\sigma = 3.0$	88.6%	88.6%	84.2%	77.0%	64.6%	54.2%	37.0%	19.8%	6.0%	0.6%
	$\sigma = 10.0$	86.2%	86.2%	80.8%	74.6%	67.6%	60.8%	47.4%	33.2%	21.2%	11.4%
ImageNet	$\sigma = 3.0$	71.0%	71.0%	66.0%	58.0%	51.0%	50.0%	49.0%	48.0%	48.0%	47.0%
	$\sigma = 10.0$	67.0%	67.0%	66.0%	61.0%	58.0%	57.0%	55.0%	53.0%	52.0%	50.0%

Randomized Smoothing vs. Enumeration. To compare the performance of randomized smoothing and

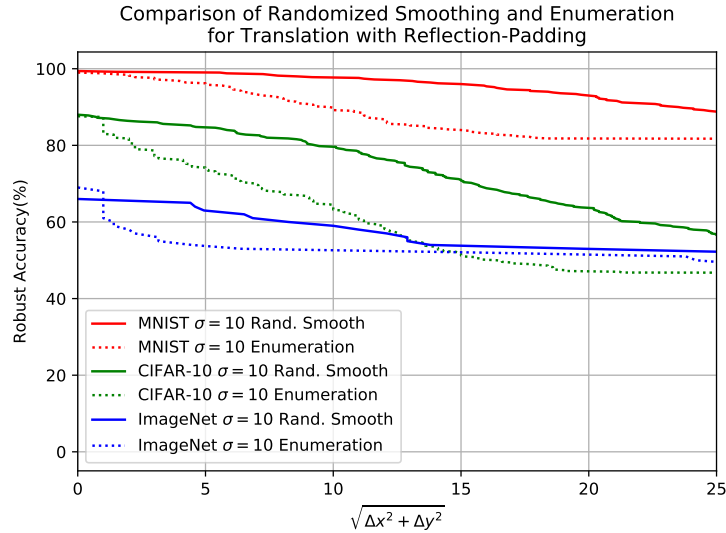


Figure 5: Comparison of Randomized Smoothing and Enumeration for Translation with Reflection-Padding. The models are trained using $\sigma = 10$ Gaussian noise data augmentation. Randomized smoothing results are shown by solid lines, and enumeration results are shown by dotted lines.

enumeration, we plot the robust accuracy curve with respect to the displacement $\sqrt{\Delta x^2 + \Delta y^2}$ for all $\sigma = 10$ models in Fig. 5. The randomized smoothing results are shown by solid lines, while enumeration results are shown by dotted lines. We observe that in most cases, randomized smoothing outperforms the enumeration approach in terms of robust accuracy. We attribute this to the power of smoothing, which flattens the extreme points of single-point prediction.

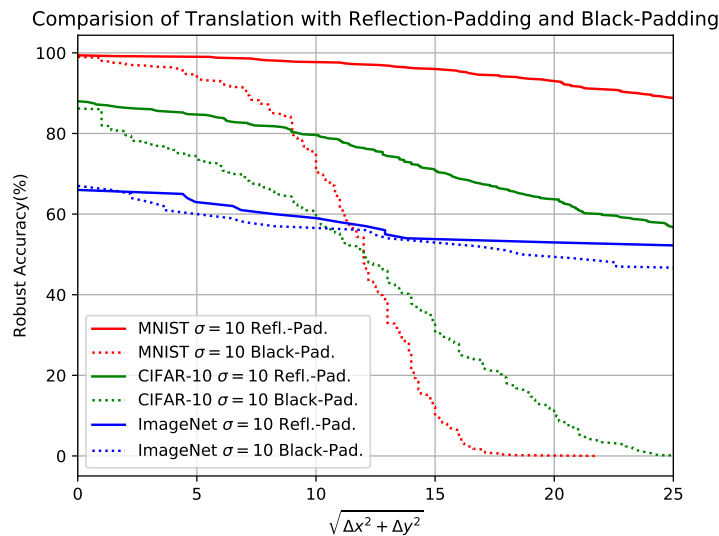


Figure 6: Comparison of Best Achieved Robust Accuracy of Reflection-Padding and Black-Padding. The models are trained using $\sigma = 10$ Gaussian noise data augmentation. Reflection-padding results are shown by solid lines, and enumeration results are shown by dotted lines.

Reflection-Padding vs. Black Padding. In Figure 6 we compare the best achieved robust accuracy of

reflection-padding and black-padding on all three datasets with models trained using $\sigma = 10$. We observe that the robust accuracy of reflection-padding is much higher than that of black-padding. We attribute this observation to two causes: 1) For reflection-padding, randomized smoothing can be used, which usually results in higher robust accuracy than enumeration; and 2) For reflection-padding, the out-of-margin pixels reappear at the opposite side, while for black-padding, they are replaced by black pixels, resulting in information loss.

H.4.4 Rotation

We present the clean and robust accuracy for rotations in Table 12. During training, we first apply rotations with angles sampled uniformly at random from the interval $[\pm\alpha_{\text{train}}]$, then add additive Gaussian noise with variance σ_{train}^2 . During certification, we do randomized smoothing with additive Gaussian noise with variance σ_{test}^2 , and certify the rotation robustness against angles from the interval $[\pm\alpha_{\text{test}}]$ using our sampling-based approach. For certification, in our sampling-based approach, we use $N = 10,000$ and $R = 1,000$. In other words, we partition the whole rotation angle interval $[-180^\circ, 180^\circ]$ to $N = 10,000$ small intervals. We then further sample $R = 1,000$ points for the local max aliasing computation. Note that since we only certify $|\alpha_{\text{test}}| \leq 30^\circ$, in our implementation we only consider $10,000 \times \frac{30}{180} \leq 2,000$ intervals. This selection of hyperparameters balances the efficiency and precision as shown in Section H.5. From the table, we find that the training and certification noise variance σ_{train}^2 and σ_{test}^2 does not play an important role in general. However, we find that not applying noise (see CIFAR-10 $\sigma_{\text{train}} = 0.00$ row) harms robust accuracy considerably.

Table 12: Clean and robust accuracy for *rotations*. During training, data augmentation is applied with angles sampled uniformly at random from the interval $[\pm\alpha_{\text{train}}]$. In addition we use additive Gaussian noise with variance σ_{train}^2 .

Dataset	$ \alpha_{\text{train}} \leq$	σ_{train}	σ_{test}	Clean Acc.	$ \alpha_{\text{test}} \leq$	Robust Acc.
MNIST	35.0°	0.10	0.10	99.4%	30.0°	92.8%
	35.0°	0.25	0.25	99.2%	30.0°	94.6%
	35.0°	0.50	0.50	98.6%	30.0°	95.6%
CIFAR-10	12.5°	0.00	0.05	63.6%	10.0°	16.0%
	12.5°	0.05	0.05	84.2%	10.0°	63.8%
	12.5°	0.10	0.10	78.4%	10.0°	63.2%
	12.5°	0.15	0.15	77.4%	10.0°	60.8%
ImageNet	12.5°	0.25	0.25	64.0%	10.0°	19.0%
	12.5°	0.50	0.50	56.0%	10.0°	33.0%

H.4.5 Scaling

We present the clean and robust accuracy for scaling in Table 13. Similar as for rotation transformations, during training we first apply scaling with a factor s_{train} sampled uniformly at random, then add additive Gaussian noise with variance σ^2 . During certification, we do randomized smoothing with additive Gaussian noise with variance σ^2 and certify the scaling robustness against factor s using our sampling-based approach. For certification, in our sampling-based approach, we use $N = 1,000$ and $R = 250$. In other words, we partition the whole scaling factor interval to 1,000 small intervals and then further sample 250 points for the local max aliasing computation. This selection of hyperparameters balances the efficiency and precision as shown in Section H.5. Similar as rotation, the noise variance σ^2 has a small effect on the robust accuracy.

Table 13: Clean and robust accuracy for *scaling transformations*. During training, data augmentation is applied with scaling factors sampled uniformly at random from the interval $[1 \pm s_{\text{train}}]$. In addition we use additive Gaussian noise with variance σ^2 .

Dataset	$ s_{\text{train}} - 1 \leq$	σ	Clean Acc.	$ s - 1 \leq$	Robust Acc.
MNIST	25.0%	0.10	98.8%	20.0%	96.8%
	25.0%	0.25	98.8%	20.0%	95.6%
	25.0%	0.50	98.6%	20.0%	95.8%
CIFAR-10	25.0%	0.05	86.8%	20.0%	57.2%
	25.0%	0.10	81.4%	20.0%	57.8%
	25.0%	0.15	82.0%	20.0%	58.4%
	25.0%	0.20	75.0%	20.0%	53.4%
	25.0%	0.25	78.6%	20.0%	58.2%
	25.0%	0.30	74.6%	20.0%	54.0%
ImageNet	15.0%	0.50	58.0%	15.0%	31.0%

H.5 For Sampling-Based Certification: Effects of Number of Samples

In Table 14 we compare the effect of different sampling numbers. We find that the time needed to compute the sampling error M is roughly linearly proportional to $N \times R$. Increasing N and R significantly reduces the maximum sampling error upper bound M . For fixed $N \times R$, increasing N (and decreasing R) reduces M more effectively, opposed to increasing R and decreasing N . Furthermore, we observe that the robust accuracy is directly related with M . We observe that when M is smaller, a smaller ℓ_2 robustness margin is required to certify a sample. We furthermore find that models with larger σ usually have larger ℓ_2 robustness margin, and thus tolerate larger M (compare $\sigma = 0.05$ column and $\sigma = 0.15$ column). We also find that certification time does not scale linearly with N , while the running time to compute M does.

Table 14: Effect of the number of samples for sampling-based certification for rotation transformation. The rotation angle interval $[\pm 180^\circ]$ is uniformly divided into N subintervals, then each interval is further divided R times in order to estimate the upper bound of the maximum ℓ_2 sampling error M . Note that we only certify $[\pm 10^\circ]$ while the outer intervals are skipped. The time needed to compute M for each sample is reported in the column ‘‘Computing Time’’. The robust accuracy and certification time of each model (specified by the noise std σ) is shown in the corresponding columns. The results are computed from 100 random samples from the CIFAR-10 test set.

Sampling Numbers	Sampling Err. M	Computing Time	$\sigma = 0.05$		$\sigma = 0.10$		$\sigma = 0.15$	
			Rob. Acc.	Certify Time	Rob. Acc.	Certify Time	Rob. Acc.	Certify Time
$N = 100, R = 100$	11.0	1.069 s	0%	13.5 s	0%	25.7 s	0%	11.9 s
$N = 100, R = 1000$	8.17	5.701 s	0%	13.2 s	0%	25.7 s	0%	11.3 s
$N = 1000, R = 100$	0.414	7.58 s	0%	14.0 s	0%	21.6 s	4%	13.9 s
$N = 1000, R = 1000$	0.122	80.35 s	2%	14.1 s	22%	73.9 s	28%	13.8 s
$N = 1000, R = 10000$	0.0932	660.2 s	3%	23.0 s	30%	56.2 s	32%	14.3 s
$N = 10000, R = 1000$	0.00417	669.1 s	59%	28.7 s	63%	37.5 s	59%	63.3 s

H.6 Running Time

Table 15 records the certification time per sample in seconds. Our certification procedure uses one NVIDIA GTX 1080Ti GPU with a single core Intel Xeon E5-2650 CPU. Note that for most settings and most methods, the average time is less than 60 s, even for the large ImageNet ResNet-50 model, indicating that the approach is scalable.

Moreover, from the table we find that enumeration method runs the fastest, taking less than 1 s even for the

slowest sample. Randomized smoothing method running time is very stable, mostly in the range from 10 s to 30 s. Note that randomized smoothing running time on ImageNet is comparable to those on MNIST and CIFAR-10 mainly because we set $N = 10,000$ on ImageNet and $N = 100,000$ on other datasets. Sampling randomized smoothing running time is on average the slowest on CIFAR-10 and ImageNet. We notice that the running time varies largely from sample to sample. For example, for rotations on ImageNet, the fastest sample takes only 0.152 s and the slowest sample takes 14 880 s. We attribute this to the effect of progressive certification, which significantly accelerates the certification process of easy-to-verify samples.

Table 15: Certification time per sample for all types for transformations on all datasets.

Dataset	Transformation	Setting	Method	Avg.(s)	Min.(s)	Max.(s)
MNIST	Gaussian Blur	$\lambda = 2.0$	Rand. Smooth	16.9	14.7	20.5
		$\lambda = 10.0$	Rand. Smooth	17.3	14.0	21.7
	Brightness	$\sigma_b = \sigma_s = 0.3$	Rand. Smooth	10.3	9.33	11.9
	Contrast	$\sigma_b = \sigma_s = 0.3$	Rand. Smooth	10.5	9.25	12.7
	Contrast and Brightness	$\sigma_b = \sigma_s = 0.3$	Rand. Smooth	11.6	9.18	13.7
	Translation w/ Reflection-Pad.	$\sigma = 3$	Rand. Smooth	17.1	14.5	19.6
		$\sigma = 10$	Rand. Smooth	18.6	16.7	22.2
		$\sigma = 3$	Enumeration	0.132	0.108	0.496
		$\sigma = 10$	Enumeration	0.378	0.11	0.995
	Translation w/ Black-Pad.	$\sigma = 3$	Enumeration	0.0735	0.0506	0.632
		$\sigma = 10$	Enumeration	0.0676	0.0491	0.595
	Rotation	$\sigma_{\text{test}} = 0.10$	Sampling Rand. Smooth	4.59	0.00155	143
		$\sigma_{\text{test}} = 0.25$	Sampling Rand. Smooth	0.942	0.0016	2.63
		$\sigma_{\text{test}} = 0.50$	Sampling Rand. Smooth	0.851	0.00147	3.84
	Scaling	$\sigma = 0.10$	Sampling Rand. Smooth	4.78	0.00145	6.44
		$\sigma = 0.25$	Sampling Rand. Smooth	5.05	0.00151	24.3
		$\sigma = 0.50$	Sampling Rand. Smooth	5.32	0.00144	29.2
	CIFAR-10	Gaussian Blur	$\lambda = 2.0$	Rand. Smooth	28.4	26.9
$\lambda = 10.0$			Rand. Smooth	30.8	29.5	33.7
$\lambda = 50.0$			Rand. Smooth	36.9	34.9	40.4
Brightness		$\sigma_b = \sigma_s = 0.2$	Rand. Smooth	23.9	22.6	26.5
Contrast		$\sigma_b = \sigma_s = 0.2$	Rand. Smooth	26.2	23.3	29.8
Contrast and Brightness		$\sigma_b = \sigma_s = 0.2$	Rand. Smooth	27.6	22.7	42.4
Translation w/ Reflection-Pad.		$\sigma = 3$	Rand. Smooth	26.8	25.0	28.8
		$\sigma = 10$	Rand. Smooth	28.2	25.6	29.7
		$\sigma = 3$	Enumeration	0.389	0.245	1.15
		$\sigma = 10$	Enumeration	0.591	0.222	1.21
Translation w/ Black-Pad.		$\sigma = 3$	Enumeration	0.186	0.172	0.462
		$\sigma = 10$	Enumeration	0.213	0.172	0.526
Rotation		$\sigma_{\text{train}} = 0.00, \sigma_{\text{test}} = 0.05$	Sampling Rand. Smooth	304	0.021	2852
		$\sigma_{\text{test}} = 0.05$	Sampling Rand. Smooth	431	0.0593	2633
		$\sigma_{\text{test}} = 0.10$	Sampling Rand. Smooth	413	0.0243	2300
		$\sigma_{\text{test}} = 0.15$	Sampling Rand. Smooth	353	0.0834	3501
Scaling		$\sigma = 0.05$	Sampling Rand. Smooth	987	0.0381	13423
		$\sigma = 0.10$	Sampling Rand. Smooth	693	0.0184	3438
	$\sigma = 0.15$	Sampling Rand. Smooth	743	0.0188	3720	
	$\sigma = 0.20$	Sampling Rand. Smooth	638	0.0533	2798	
	$\sigma = 0.25$	Sampling Rand. Smooth	747	0.0367	4940	
	$\sigma = 0.30$	Sampling Rand. Smooth	693	0.0189	6809	
ImageNet	Gaussian Blur	$\lambda = 10.0$	Rand. Smooth	60.2	56.8	63.8
	Brightness	$\sigma_b = \sigma_s = 0.2$	Rand. Smooth	21.2	19.6	25.0
	Contrast	$\sigma_b = \sigma_s = 0.2$	Rand. Smooth	21.2	19.8	25.0
	Contrast and Brightness	$\sigma_b = \sigma_s = 0.2$	Rand. Smooth	21.9	21.2	26.7
	Translation w/ Reflection-Pad.	$\sigma = 3$	Rand. Smooth	20.1	19.6	25.0
		$\sigma = 10$	Rand. Smooth	20.2	19.6	25.4
		$\sigma = 3$	Enumeration	121	0.723	450
		$\sigma = 10$	Enumeration	134	0.719	460
	Translation w/ Black-Pad.	$\sigma = 3$	Enumeration	22.9	0.685	194
		$\sigma = 10$	Enumeration	25.9	0.685	211
	Rotation	$\sigma_{\text{test}} = 0.25$	Sampling Rand. Smooth	767	0.152	14880
		$\sigma_{\text{test}} = 0.50$	Sampling Rand. Smooth	336	0.153	2947
Scaling	$\sigma = 0.50$	Sampling Rand. Smooth	280	0.152	1828	

I Comparison to Other Semantic Transformation Certification Approaches

We compare our semantic transformation certification approaches with recent works (Singh et al., 2019; Balunovic et al., 2019; Fischer et al., 2020).

(Singh et al., 2019). Within our knowledge, (Singh et al., 2019) propose the first approach to certify neural network robustness against rotation transformations. In order to certify robustness against rotations, they split the interval of rotation angles to small sub-intervals and subsequently compute each pixel’s color range and perform interval bound propagation to derive the final output range. However, the certification is relatively loose and does not scale to larger datasets such as ImageNet. Our sampling-based approach for rotation and scaling is similar in that we also split the rotation angle or scaling factor interval. However, we do a rigorous analysis on the ℓ_2 aliasing and bound the maximum ℓ_2 sampling error instead. This allows us to circumvent the looseness of interval bound propagation and effectively exploit the strong ℓ_2 -certification of randomized smoothing.

(Balunovic et al., 2019). (Balunovic et al., 2019) improves on (Singh et al., 2019) by alternating the interval bound for per pixel value by linear constraints. Similar to our method, they also first split the transformation parameter interval. After this, they optimize the per pixel linear constraints via sampling and optimizing from general Lipschitz optimization. The approach obtains substantially better robust accuracy compared to previous works. In our sampling-based approach for rotation and scaling, we analyze the concrete form of the Lipschitz upper bound and, rather than expressing the aliasing bounds using linear constraints, we use the ℓ_2 norm which significantly improves efficiency and scalability. Note that (Balunovic et al., 2019) also cover the composition of geometric transformations such as composition of scaling and shearing. Our sampling-based approach can also be extended to support those types of transformations but requires additional Lipschitz bound analysis.

(Fischer et al., 2020) (Fischer et al., 2020) are the first to generalize randomized smoothing to semantic transformations and certify rotations and translation for ImageNet classification. They furthermore cover volume changes and pitch shifts on audio data and robustness to floating-point soundness. Their theoretical results generalize randomized smoothing to a richer class of transformations and go beyond isotropic Gaussian noise. However their result is limited to additive transformations while our theoretical result generalizes to a broader class of noise distributions and to transforms which are resolvable. In addition, we provide theoretical barriers on the randomized smoothing approach enabling a deeper understanding.

Since rotations are by nature non-additive transforms, Fischer et al. overcome the limitation to additive transforms by computing the maximum ℓ_2 -error induced from random sampling and use a statistical upper bound. However, an attacker can deterministically select the transformation parameter with maximum ℓ_2 -error in order to break the certification. Our sampling-based approach on the other hand provides us with a rigorous upper bound resulting in stronger certification.